

Ninevah University

College of Electronics Engineering

Communication Engineering Department



## **An Investigation into Multi-Band Fractal Antennas**

**Submitted by:**

**Dalia Ahmed Ibraheem AL-Khafaf**

**M.Sc. Dissertation**

**in**

**Communication Engineering**

**Supervised by:**

**Prof. Dr. Jafar Ramadhan Mohammed**

2024 A.D.

1445 A.H.

# **An Investigation into Multi-Band Fractal Antennas**

**Dissertation Submitted by**

**Dalia Ahmed Ibraheem AL-Khafaf**

**To**

**The Council of College of Electronics Engineering**

**Ninevah University**

**In Partial Fulfillment of the Requirements**

**For the Degree of Master of Sciences**

**In**

**Communication Engineering**

**Supervised by:**

**Prof. Dr. Jafar Ramadhan Mohammed**

2024 A.D.

1445 A.H

بِسْمِ اللَّهِ الرَّحْمَنِ الرَّحِيمِ

"نرفع درجات من نشاء وفوق كل ذي علم عليم"

صدق الله العظيم

يوسف من الآية 76

## ***Supervisor's Certification***

I certify that the Thesis entitled (**An Investing into Multi-Band Fractal Antennas**) was prepared by **Dalia Ahmed Ibraheem** under my supervision at the Department of Communication Engineering, Ninevah University, as a partial requirement for the Master of Science Degree in Communication Engineering.

Signature:

**Name: Prof. Dr. Jaafar R. Muhammad**

Department of Communication Engineering

**Date:     /     /2024**

## **Report of Linguistic Reviewer**

I certify that the linguistic reviewer of this Thesis was carried out by me and it is accepted linguistically and in expression.

Signature:

**Name: Mohammed N. Mahmoud**

**Date:     /     /2024**

## **Report of the Head of Department**

I certify that this Thesis was carried out in the Department of Communication Engineering. I nominate it to be forwarded to discussion.

Signature:

**Name: Dr. Mahmoud A. Mahmoud**

**Date:     /     /2024**

## **Report of the Head of Postgraduate Studies Committee**

According to the recommendations presented by the supervisor of this Thesis and the linguistic reviewer, I nominate this Thesis to be forwarded to discussion.

Signature:

**Name: Dr. Mahmoud A. Mahmoud**

**Date:     /     /2024**

## **Committee Certification**

We the examining committee, certify that we have read this Thesis entitled  
**(An Investigation into Multi-Band Fractal Antennas)**

and have examined the postgraduate student (Dalia Ahmed Ibraheem) in its contents and that in our opinion; it meets the standards of a dissertation for the degree of Master of Science in Communication Engineering.

**Signature:**

**Name: Prof. Dr. Khalil**

**H. Sayidmarie**

**Head of committee**

**Date:     /     /2024**

**Signature:**

**Name: Dr. Adham Maan**

**Salih**

**Member**

**Date:     /     /2024**

**Signature**

**Name: Prof. Dr. Jaafar**

**R. muhammad**

**Member and Supervisor**

**Date:     /     /2024**

**Signature:**

**Name: Dr. Yasser Ahmed**

**Fadhil**

**Member**

**Date:     /     /2024**

**The college council, in it ..... meeting on     /     /2024, has decided to award the degree of Master of Science in Communication Engineering to the candidate.**

**Signature:**

**Name: Prof. Dr. Khalid**

**K. Mohammad**

**Dean of the College**

**Date:     /     /2024**

**Signature:**

**Name: Assist. Prof. Dr. Bilal**

**A. Jebur**

**Council registrar**

**Date:     /     /2024**

## **Acknowledgements**

First and foremost, praises and thanks to Allah, the Almighty, for His showers of blessings throughout my research work to complete the dissertation successfully.

I would like to express my sincere gratitude and special thanks to my supervisor Dr. Jafar Ramadhan for his ongoing support, scientific supervision and encouragement during the composition of my dissertation. His candid comments have really sharpened my viewpoint and enhanced my comprehension.

I also, would like to express my appreciation to the teaching staff of the department of Communication Engineering, in particular the head of the department Dr Mahmod A. Mahmod. I also must mention my respected professors who taught me lectures throughout my academic study, as well as those who have provided me with a hope of support.

I want to express my sincere gratitude to my great mother and brother for their support and inspiration during the entirety of my academic study, without their help and prayers, I would not have been able to complete it. I attribute my accomplishment to them. I ask Allah to grant them a blessed life and good health.

Last but not the least, my sincere thanks also must go to my husband Ali Alany and his family who encouraged me and prayed for me throughout the time of my research and gave me as much support and assistance as they could, may the Almighty Allah richly bless all of them.

## **Abstract**

In many applications, it is desirable to use a single antenna that has a capability to operate at several tuned frequencies instead of using multiple separate single-resonance antennas. Fractal antennas have many advantages and they are capable of fulfilling these requirements. In this dissertation, three different types of antennas were designed and their performances were analyzed. The first type was a simple narrowband dipole antenna that operates at a single frequency; the second type was a broadband bowtie antenna that has a capability to operate at a wide band of frequencies and the third one is a Sierpinski fractal multiband bowtie antenna. This fractal bowtie antenna is an improved version of the original broadband bowtie antenna with self-similarity fractal geometries at different scale sizes. The performances of these three designed antennas in terms of reflection coefficient, radiated power, gain and the directivity, are extensively studied and compared. Computer simulation showed that the designed narrowband dipole antenna has a single resonant frequency at 2.4 GHz as well as other resonance values that appear at multiple integer frequencies. The second designed antenna has a relatively wideband resonance frequency at 2.4 GHz, while the third designed fractal bowtie that constructed at the second-stage of growth (or iteration) has multiple resonant frequency at different scale copies of the structure at 2.4, 9.2 and 17.4 GHz. The performances of two types of antennas are verified using both MATLAB simulation as well as the CST full-wave modeling software.

The method of moment was used to design these antennas in MATLAB which involves dividing the antenna's surface into a number of small triangular segments. For each segment, the electric and magnetic fields have been solved. Then, the antenna impedance and the current distribution on the overall antenna's surface is solved which is used to find the antenna's radiation pattern.

For CST software, the design mechanism of these three antennas were much easier because it deals with blocks rather than MATLAB codes or scripts.

It was shown that the proposed fractal bowtie antenna structure is capable of providing a significant improvement in the radiation performance compared to its counterpart original bowtie antenna without fractal structure. The improvements include reflection coefficient, radiated power .

## **Published Research**

Some of the results obtained in this work were submitted for publication in the following:

**[1] Dalia Ahmed Ibrahim and Jafar Ramadhan Mohammed, " Performance comparison investigation of the narrowband, Wideband and fractal multiband antennas** accepted in Journal of Engineering Science and Technology.

## **TABLE OF CONTENTS**

Subject	Page
---------	------

Acknowledgments		I
Abstract		II
Published Research		V
Table of Contents		V
List of Tables		X
List of Figures		XI
List of Abbreviations		XV
List of Symbols		XVI
<b>CHAPTER ONE – INTRODUCTION</b>		1
<b>1.1</b>	Introduction	1
<b>1.2</b>	Literature Survey	4
<b>1.3</b>	Objectives and Aims of the Thesis	9
<b>1.4</b>	Organization of the Thesis	10
<b>CHAPTER TWO – BACKGROUND THEORY</b>		11
<b>2.1</b>	Overview	11
<b>2.2</b>	Principle of Radiation	11
<b>2.3</b>	Wire Antenna	11
<b>2.4</b>	Dipole Antenna	12
<b>2.4.1</b>	Half-Wave Length Dipole	13
<b>2.4.2</b>	Electric and Magnetic Field Component	14
<b>2.4.3</b>	Radiation Pattern	15
<b>2.4.4</b>	Radiation Resistance	18
<b>2.4.5</b>	Dipole Uses	20
<b>2.5</b>	Bowtie antenna	21
<b>2.5.1</b>	Unipolar Bowtie Antenna	22
<b>2.5.2</b>	Geometry of the Bowtie	22

2.5.3	Feed Point	22
2.5.4	Broadband Performance	22
2.5.6	Bowtie Applications	23
2.5.7	Types of Bowtie Antenna	23
2.5.8	Different Types of Bowties	27
2.5.9	The Significance of Coplanar Wave Guide (CPW-Fed) Slot Antennas	28
2.6	Fractal Antenna	29
2.6.1	Concept of Fractal	30
2.6.2	Fractal Antenna Advantage	31
2.6.3	Fractal Antenna Disadvantage	31
2.6.4	Fractal Antenna Application	31
2.6.5	Some Useful Geometries for Fractal Antenna Engineering	34
2.6.5.1	Koch Curve	34
2.6.5.2	The Koch snowflake	34
2.6.5.3	Hilbert Curve	35
2.6.5.4	Cantor Set	36
2.6.5.4.1	The Cantor Ternary set	36
2.6.5.5	Sierpinski Carpet	38
2.6.5.6	Hexagonal Fractals	38
2.6.5.7	Minkowski Geometry	39
2.6.5.8	Sierpinski Gasket	39
2.6.5.9	Antenna Hybrid Fractal	40
<b>CHAPTER THREE – DESIGN OF NARROWBAND DIPOLE AND WIDEBAND BOWTIE</b>		42
3.1	Software Tools	42

3.1.1	MATLAB Simulation	42
3.1.2	CST Full-Wave Modeling Software	42
3.2	Antenna Design and Simulation	42
3.2.1	Half Wave Length Dipole	43
3.2.2	Designing Antenna Parameters	43
3.2.3	The discrepancy between the half wavelength dipole's physical and electrical lengths	44
3.2.4	Simulated Performance of Narrowband Dipole Antenna using MATLAB	48
3.2.5	Dipole Input Impedance and Power Resonance	49
3.2.6	Dipole Radiated Power and Reflection Coefficient and Gain	51
3.3	Wideband Bowtie Antenna	53
3.3.1	Planar Bowtie Antenna with Thick Dielectric Substrate	54
3.3.2	Wideband Bowtie Antenna Using CST	55
3.3.3	Simulation Result for Wideband Bowtie Using CST	56
3.3.4	Wideband Bowtie Antenna Design and Simulation Using MATLAB	57
3.3.5	MATLAB Mesh for Bowtie Antenna	58
3.3.6	Bowtie Radiation Power, Reflection Coefficient and Gain	61
3.3.7	Bowtie Radiation Pattern	63
3.3.8	Bow-tie Applications	66
<b>CHAPTER FOUR DESIGN AND ANALYSIS OF BOWTIE FRACTAL ANTENNA BY SIERPINISKI</b>		67
	Introduction	67

4.1	Bowtie Fractal Antenna by Sierpiniski	67
4.2	Sierpiniski Triangle / Gasket	67
4.3	Affine Transformations	69
4.4	Collection of Transformations	69
4.5	Iterative Process	69
4.6	Weights	69
4.7	Contraction Property	69
4.8	Flare Angle and its Effect on Antenna Performance	72
4.9	Fractal Sierpiniski Antenna Design Using MATLAB	74
4.9.1	Sierpiniski Fractal's Reflection Coefficient and radiated Power.	75
4.10	Fractal Sierpiniski Antenna Design and Simulation Using CST Software.	78
<b>CHAPTER FIVE – CONCLUSIONS AND FUTURE WORK</b>		84
5.1	Conclusions	84
5.2	Future Works	85
<b>REFERENCES</b>		86

## LIST OF TABLES

<b>CHAPTER TWO– BACK GROUND THEORY</b>		
<b>Table</b>	<b>Title</b>	<b>Page</b>
<b>2.1</b>	<b>Summary of Dipole Directivity, Gain and Realized Gain (Resonant <math>X_A = 0</math>; <math>f = 100</math> MHz; <math>\sigma = 5.7 \times 10^7</math> S/m; <math>Z_c = 50</math>; <math>b = 3 \times 10^{-4}\lambda</math>)</b>	<b>20</b>
<b>CHAPTER THREE- ANTENNA DESIGN (NARROWBAND DIPOLE, WIDEBAND BOWTIE AND MULTIBAND FRACTAL)</b>		
<b>3.1</b>	<b>Design parameter of half wave length dipole at (<math>f = 2.4</math> GHz).</b>	<b>46</b>
<b>CHAPTER FOUR- RESULTS AND DISCUSSION</b>		
<b>Table</b>	<b>Title</b>	<b>Page</b>
<b>4.1</b>	<b>Summarizes and Compares between the Performances of the Three Designed Antennas Under Study.</b>	<b>84</b>

## LIST OF FIGURES

<b>Chapter Two – Background Theory</b>		
<b>Figure</b>	<b>Title</b>	<b>Page</b>
<b>2.1</b>	<b>The basic half-wavelength dipole antenna with center feed point</b>	<b>12</b>
<b>2.2</b>	<b>Geometry of the half wavelength Dipole Antenna.</b>	<b>14</b>
<b>2.3</b>	<b>Two and three-dimensional patterns of a <math>\lambda/2</math> dipole</b>	<b>17</b>
<b>2.4</b>	<b>Radiation resistance and reactance, input resistance and directivity of a thin dipole with sinusoidal current distribution.</b>	<b>19</b>
<b>2.5</b>	<b>Geometry of Bowtie Antenna in Cartesian (x, y, z) and radial Coordinates (r, b), and the corresponding oblique coordinates (s, t) with unit vectors, n1, n2.</b>	<b>21</b>
<b>2.6</b>	<b>Three types of bowtie antennas in the same height.</b>	<b>24</b>
<b>2.7</b>	<b>The layout of the bowtie slot antenna and its dimensions.</b>	<b>25</b>
<b>2.8</b>	<b>Geometry of the self-complementary bowtie antenna</b>	<b>26</b>
<b>2.9</b>	<b>Geometry of the fractal self-complementary bowtie antenna (FSCBT-antenna)</b>	<b>27</b>
<b>2.10</b>	<b>Return loss versus frequency for SCBT and FSCBT</b>	<b>27</b>
<b>2.11</b>	<b>Different design of bowtie antenna</b>	<b>28</b>
<b>2.12</b>	<b>Fractals used to represent plants in nature.</b>	<b>30</b>
<b>2.13</b>	<b>Iterative generation process of fractal</b>	<b>33</b>

<b>2.14</b>	<b>Classification of fractal antenna.</b>	<b>34</b>
<b>2.15</b>	<b>Koch Snowflakes and Koch islands</b>	<b>35</b>
<b>2.16</b>	<b>Hilbert curve's initial stages of creation</b>	<b>36</b>
<b>2.17</b>	<b>The first stages towards creating the Cantor ternary set</b>	<b>37</b>
<b>2.18</b>	<b>Sierpinski carpets, used in multiband antennas</b>	<b>38</b>
<b>2.19</b>	<b>The hexagonal fractal's first three iterations</b>	<b>38</b>
<b>2.20</b>	<b>(a) Initiator geometry, (b) Generator geometry and (c) Proposed Minkowski curve.</b>	<b>39</b>
<b>2.21</b>	<b>a) Sierpinski Gasket - Approach to Multiple Copy Generation, b) Sierpinski Gasket - Decomposition Generation Approach.</b>	<b>40</b>
<b>2.22</b>	<b>Hybrid fractal slot - (a) Koch- Koch and (b) Koch-Minkowski</b>	<b>41</b>
<b>2.23</b>	<b>a) Minkowski Curve, (b) Sierpinski Carpet geometry and (c) Hybrid fractal structure.</b>	<b>41</b>
<b>Chapter Three – Design and Simulation of Narrowband Dipole and Wideband Bow-tie Antennas</b>		
<b>Figure</b>	<b>Title</b>	<b>Page</b>
<b>3.1</b>	<b>Factor "A" of multiplication is used to determine the length of a dipole.</b>	<b>45</b>
<b>3.2</b>	<b>Narrow band dipole antenna at 2.4 GHz using CST software</b>	<b>46</b>
<b>3.3</b>	<b>Dipole reflection coefficient with frequency</b>	<b>47</b>

3.4	<b>Dipole radiated power.</b>	<b>47</b>
3.5	<b>Bandwidth curve for the half-wavelength dipole antenna</b>	<b>48</b>
3.6	<b>Genral construction of half-wavelength dipole (A 62.5mm length)</b>	<b>49</b>
3.7	<b>Dipole input impedance as a function of frequency. A 62.5mm length and 0.625mm diameter of wire</b>	<b>50</b>
3.8	<b>(a) Dipole radiated power, (b) Reflection coefficient and (c) Gain as a function of frequency</b>	<b>52-53</b>
3.9	<b>Front view Wide- Band Bow-tie Antenna at 2.4GHz using CST Software</b>	<b>56</b>
3.10	<b>(a) Reflection coefficient 2.4GHz. (b) Radiated power with respect to frequency at 2.4GHz. (c) Bandwidth curve for bowtie antenna.</b>	<b>56-57</b>
3.11	<b>Broadband Bow-tie design using MATLAB in XY-plane</b>	<b>58</b>
3.12	<b>Bowtie input impedance as a function of frequency. The flare angle is <math>67.38^{\circ}</math>.</b>	<b>59</b>
3.13	<b>Performance of the constructed bowtie antenna using MATLAB (a) Reflection coefficient, (b) Radiated power, (c) Gain</b>	<b>62-63</b>
3.14	<b>Radiation Pattern of the Bowtie Antenna at four different frequencies in the xz-plane</b>	<b>66</b>
<b>Chapter Four –</b>		

<b>Figure</b>	<b>Title</b>	<b>Page</b>
<b>4.1</b>	<b>Sierpinski's monopoly. A scaled-down representation of the entire structure may be seen in each sub gasket (circled)</b>	<b>69</b>
<b>4.2</b>	<b>The code for an iterated function system for a Sierpinski gasket</b>	<b>72</b>
<b>4.3</b>	<b>Computed reflection coefficients of the adaptive wire bow-tie antenna as functions of antenna elevation for the eight possible effective flare angles</b>	<b>74</b>
<b>4.4</b>	<b>Designed Fractal multiband bowtie at second iterations antennas using MATLAB simulation</b>	<b>75</b>
<b>4.5</b>	<b>Geometry of the Bowtie Fractal Antenna</b>	<b>76</b>
<b>4.6</b>	<b>Reflection Coefficient and Radiated Power of multiband fractal antenna</b>	<b>78</b>
<b>4.7</b>	<b>Fractal Multiband Bowtie at various iteration using CST software in xy-plane.</b>	<b>79</b>
<b>4.8</b>	<b>Performance of designed Sierpiniski Fractal Antenna.</b>	<b>80</b>
<b>4.9</b>	<b>The B.W curve at first and second iteration of Sierpiniski fractal antenna.</b>	<b>81</b>
<b>4.10</b>	<b>Reflection Coefficient of Three Designed Antennas under study using CST.</b>	<b>82</b>
<b>4.11</b>	<b>Radiated powers of the designed three antennas using CST</b>	<b>82</b>

## LIST OF ABBREVIATIONS

<b>Abbreviation</b>	<b>Name</b>
<b>CPW</b>	<b>Conventional Coplanar Waveguide</b>
<b>FSCBT</b>	<b>Fractal Self-Complementary Bow-tie Antenna</b>
<b>GHz</b>	<b>GIGA Hertz</b>
<b>GSM</b>	<b>Global System Mobile</b>
<b>IEEE</b>	<b>Institute of Electrical and Electronics Engineers</b>
<b>IFS</b>	<b>Iterated Function Systems</b>
<b>LO</b>	<b>Local Oscillator</b>
<b>MRCM</b>	<b>Multiple Reduction Copy Machine</b>
<b>PCB</b>	<b>Printed Circuit Board</b>
<b>RFID</b>	<b>Radio Frequency Identification</b>
<b>RF</b>	<b>Radio Frequency</b>
<b>SMA</b>	<b>Sub Miniature Version A (connectors)</b>
<b>SWB</b>	<b>Super Wide Band</b>
<b>STJ</b>	<b>Superconducting Tunnel Junctions</b>
<b>SCBT</b>	<b>Self-complementary Bow-tie Antenna</b>
<b>UWB</b>	<b>Ultra-Wide Band</b>
<b>UHF</b>	<b>Ultra-High Frequency</b>
<b>WLAN</b>	<b>Wide Local Area Network</b>

## LIST OF SYMBOLS

Symbols	Name
$A_{em}$	Maximum Effective Area
$A$	Multiplication Factor
<b>B.W</b>	Band Width
$C_{in}$	Input capacitance
$D$	Diameter of the Dipole
$D_0$	Directivity
$e_{cd}$	Efficiency at Transmitter
$E_{\theta}$	Electric Field
$e_r$	Receiver Efficiency
$\epsilon_{eff}$	Effective Dielectric Constant
$\epsilon_r$	Dielectric Constant
$f_r$	Resonant Frequency
$f_L$	Lower Frequency
$f_H$	Higher Frequency
$G$	Gap between two Strips of Dipole
$G_0$	Gain
$G_{re0}$	Realized Gain
$H$	Height of the Substrate

$I_0$	<b>Current Density</b>
$I_1$	<b>Initial State</b>
$I_2$	<b>Second State</b>
$K$	<b>Constant</b>
$L_n$	<b>New Length</b>
$L$	<b>Length of the Dipole</b>
$L$	<b>Length of Substrate</b>
$L_{BT}$	<b>Length of the Bowtie Arm</b>
$L_m$	<b>Slot Length</b>
$L_{eff}$	<b>Effective Length</b>
$\Delta L$	<b>Length Difference</b>
$P_{rad}$	<b>Radiated Power</b>
$R_r$	<b>Radiation Resistance</b>
$R$	<b>Radius of Dipole</b>
$R_{HF}$	<b>High Frequency Resistance</b>
$R_{in}$	<b>Input Resistance</b>
$R_l$	<b>Load Resistance</b>
$s$	<b>Spacing between Feed Line Slots</b>
$S$	<b>Fractal Growth Stages</b>
$S_{11}, \Gamma$	<b>Reflection Coefficient</b>
$U$	<b>Power Intensity</b>

$U_{\max}$	<b>Maximum Power Intensity</b>
<b>VSWR</b>	<b>Voltage Standing Wave Ratio</b>
<b>W</b>	<b>Width of the Substrate.</b>
$W_{BT}$	<b>Bowtie Arm Width</b>
$W_m$	<b>Slot Width</b>
$Z_A$	<b>Antenna Input Impedance</b>
$\alpha$	<b>Flare Angle</b>
$\lambda_0$	<b>Wavelength in the Free Space</b>
$\Omega$	<b>Ohm</b>

# CHAPTER ONE

## INTRODUCTION AND LITERATURE SURVEY

### 1.1 Introduction

With the development of wireless technologies, antenna designers have been challenged to create small, effective antennas that are simple to produce and have great radiation efficiency in order to meet rising demands. Due to the rapid development of wireless applications, the size of the antenna is the key area of focus for low-profile communication systems. One of the techniques to decrease the shape of the antenna and to achieve multiband performance is by using fractal geometry [1].

In general, fractal geometries have two characteristics: self-similarity and space filling. Mandelbrot was the first to suggest these geometries. Fractals are self-similarity patterns that get their inspiration from natural occurrences including mountains, clouds, and coastlines. Antenna designs can use fractals to meet multiband, wideband, and size minimization objectives. Many fractal designs, including the Koch snowflake, Sierpinski gasket, and Hilbert curve, have been used in the construction of antennas[2]. Benoit Mandelbrot was the first to use the term "fractal" to describe a group of numerous structures whose dimensions were not integers in 1975. Characterizing these rare occurrences, which were challenging with Euclidean geometries, has demonstrated the benefits of fractal geometries [3].

Indeed, fractal antennas have gained attention and popularity in the field of antenna design for the very reasons. Fractal antennas are a unique and innovative approach to designing antennas that offer several advantages over traditional antenna designs. delve a bit deeper into these properties and advantages:

- 1- **Self-Similarity:** Fractals exhibit self-similarity, which means that they have similar patterns at various scales. This property allows fractal antennas to be designed with intricate structures that repeat themselves in a self-similar manner. This property can be leveraged to create antennas that work across a wide range of frequencies, making them suitable for wideband or multiband operations. This is particularly advantageous in modern communication systems where devices need to support a variety of wireless communication standards.
- 2- **Space-Filling:** Fractals possess space-filling properties. This characteristic can be used to design compact antennas that can efficiently utilize available space. Traditional antennas often require a certain amount of space to operate optimally based on the wavelength of the signal they are designed to receive or transmit. Fractal antennas can overcome this limitation and be designed to operate effectively even in confined spaces.
- 3- **Reduction in Size:** The space-filling property of fractal antennas allows for a reduction in size without sacrificing performance. This is a significant advantage, especially in applications where size constraints are critical, such as in small electronic devices like smartphones, wearables, and IoT devices. Fractal antennas enable these devices to maintain good connectivity without compromising on their compact form factor.
- 4- **Multiband and Wideband Operation:** Traditional antennas are often designed for a specific frequency or narrow frequency range. Fractal antennas, due to their self-similarity, can be designed to cover multiple frequency bands simultaneously. This is particularly useful in modern communication systems where devices need to support various wireless standards like Wi-Fi (wireless fidelity), Bluetooth, cellular, and more applications.

5- **Ease of Fabrication:** Fractal antennas can be manufactured using standard printed circuit board (PCB) fabrication techniques, which simplifies the manufacturing process. This contributes to their practicality and cost-effectiveness.

Despite their many advantages, fractal antennas also have some challenges, such as potential complexity in design and the need for careful tuning to achieve desired performance characteristics. Moreover, their performance can be affected by the specific fractal geometry chosen and the surrounding environment.

In summary, the self-similarity and space-filling properties of fractals make them attractive candidates for antenna design. They enable wideband and multiband operation, as well as the creation of compact antennas that can be efficiently used in space-constrained applications. These properties have contributed to the growing interest and research in the field of fractal antenna design [1].

Fractal geometry technology has recently been used to practically all areas of science and engineering. Fractal geometry is used in antenna engineering with significant qualities such self-similarity, frequency selectivity, conformality, and frequency independence.

Three different types of antennas were designed and compared in this work. The performance of dipole, bowtie and second iteration of Sierpiniski fractal antenna was compared.

A comparative study can help antenna designers and engineers make informed decisions about antenna selection for specific applications, taking into account the trade-offs between different antenna types.

## 1.2 Literature Survey

In 2003, Hall Peter S. and Ghafouri-Shiraz H. discussed overcoming the matching difficulties of a perturbed fractal Sierpinski gasket antenna based on the Sierpinski fractal pattern [4].

In 2008, Lin Shu and Yang introduced an original concept of a multi-band semi-circle fractal antenna, by manipulating specific design parameters. The successful realization of an antenna were covering frequencies of 900 MHz, 1.8 GHz, and 2.4 GHz [5]

In 2011, Sayidmarie, K. H. and Fadhel Y.A. applied the fractal notion to rectangular and triangular geometries for the design of monopole antennas using two iterations. The repetition of the shape produces a multi-resonance operation in which the bottom and upper monopoles merge to form a new monopole known as the fractal monopole antenna. When compared to single (traditional) monopole antennas, fractal monopole antennas of rectangular and triangular geometries performed better and had a larger impedance bandwidth [6].

In the same year Sayidmarie K. H. and Fadhel Y.A., used the self-complementary approach to create a planar triangular monopole antenna, with bended microstrip feed line. The antenna offers a larger frequency band than a standard bow-tie antenna which is ultra-wide band (UWB) compliant, and is directly matched to the sub miniature version A connectors (SMA) via a 50-microstrip feed line as well as another enhancement to this new bow-tie antenna is the fractal self-similarity repeating of the triangular shape on each patch and complementary slot [7].

In 2012, Daotie Li and Jun-fa Mao proposed an UWB bow-tie that modified with a Koch-like fractal curve, forming so called Koch-like sided

fractal bow-tie dipole. The antenna can operate in multiband as well as ultra-wideband depending on notch angle [8].

In 2013, Dorostkara M. Ali and Islam M. T. proposed  $\Gamma$ -shaped fractal antenna for wideband communication applications. The proposed antenna's design evolution and parametric research were offered to provide information for designing, optimizing, and understanding the fundamental operation and radiation process. The suggested antenna design was simple, easy to construct, and well suited for integration into microwave circuitry for cheap production costs. The results shown that the suggested antenna has 880 MHz to 2720 MHz and is adequate for a wide range of wireless communications [9].

In 2014, Jena Manas Ranjan, and Mangarajand B.B. through the use of circular forms, they created a unique sierpiniski fractal antenna array that offers higher performance with reduced SLL (side lobe level) The ratio usually expressed in decibels (dB), (the amplitude at the peak of the main lobe to the amplitude at the peak of a side lobe.). with resonance frequencies of 0.1936 GHz and 0.222 GHz ,the developed antenna offers multiband performance [3].

In 2014, Indhumathi V. described a modified bowtie antenna that incorporates a Koch-like fractal shape to achieve multiple resonances across different frequency bands within the lower microwave spectrum. This design approach allows a single antenna to cover a range of frequencies used in various wireless applications, including GSM upper (1.8 GHz), GSM lower (850 MHz), 3.5 GHz, and 5 GHz [10]

In the same year, Kumar N. Naresh and Behera S.K. proposed Sierpinski diamond antenna model with three iterations which is versatile and promising due to its volume reduction, multiband operation, approximately omnidirectional radiation pattern, and support for various wireless communication technologies. Its design characteristics cater to applications that demand low-profile, cost-effective, and adaptable antenna solutions [11].

In 2015, Srivastava S. and Mishra P. Singh explored the potential benefits of combining fractal-based antenna design with the reconfigurability offered by varactor diodes. This could lead to antennas with improved performance, adaptability, and compactness, making them highly relevant in modern wireless communication systems [12].

In 2016, Sharma Nitika and Kaur Simranjit proposed a novel triple-band hybrid fractal boundary antenna design with specific dimensions and fractal shapes. The proposed antenna incorporates a combination of the Koch and Minkowski curves to achieve its unique characteristics. The antenna was possible to utilize the suggested antenna as a triple band antenna, and has a high gain, at 2.45 GHz, 3.85 GHz, and 4.45 GHz. The suggested antenna has a number of uses, including MIMO systems [1].

In 2016, Bhatia S. S. and Sivia J. S. described wearable fractal antenna design which has been crafted to address the demands of modern wearable technology. The use of polyester fabric and the integration into clothing items indicate a focus on creating unobtrusive and user-friendly wearable devices that maintain reliable communication capabilities across a wide range of frequencies. The designed antenna's operating frequency range of 4.3 GHz to 29.6 GHz indicates that it is suitable for both Ultra-Wideband (UWB) and Super-Wideband (SWB) applications [13].

In 2017, Yu Zhen and Zhu Chenhua suggested a novel square-circle structure fractal Mult broadband planar antenna for second generation (2G), third generation (3G), fourth generation (4G), wide local area network (WLAN), and navigation wireless applications that is reminiscent of an antique Chinese coin. The system is built on the structural underpinnings and concepts of traditional monopole antenna elements, along with the benefits of microstrip antennas and fractal geometry [14].

In 2017, Mishraa G. Prasad and Maharanaa Madhu Sudan, designed a multiband Sierpinski fractal antenna with several patch shapes (rectangular, circular, and triangular). A 2x2 fractal antenna array was constructed and studied to validate the influence of fractal on microstrip array. Finally, for the whole single antenna and array scenarios, a qualitative comparison was conducted between fractal-based defected patch and defected ground plane designs. All antennas were developed with HFSS and optimized for 28 GHz operation with a FR-4 substrate [15].

In 2017, Madhav B. T. P. and Sarvani and et al. gave a periwinkle-shaped fractal antenna loaded with a split ring resonator with partial ground was proposed. The proposed antenna covers all radar frequency ranges, including 4.1GHz,4.5GHz,4.8GHz (S-band), 6.7GHz,6.75GHz (C-band), 9.4GHz (X-band), and 12.7GHz (ku) [16].

In 2017, Kumar Devesh and Tripathy M. R., designed a straightforward, small, and miniature Bow-tie-shaped fractal antenna for THz applications which has been discussed for frequency range extending from 1.1 THz to 1.8 THz. A bow-tie-shaped fractal antenna was constructed and modelled for the return loss having less than -10 dB [17].

In 2018, Mondal Tapas and Maity Sandip proposed a new approach to achieving circularly polarized radiating fields with wide beamwidth using a microstrip antenna and a Fern fractal-shaped patch. The combination of the aperture-coupled feed mechanism and the fractal patch design introduces innovative elements that contribute to the antenna's performance. This type of design could find applications in wireless communication systems where circular polarization and wide coverage are important requirements [18].

In 2020 Saharsh S B. and Sanoj Viswa Som and et al. described the use of various configurations of the Koch snowflake fractal for antenna design and simulation, focusing on the comparison of gain between linear and corporate

array configurations. The simulation results indicated a gain enhancement in the antenna arrays compared to a single element antenna and to achieve multiband and compactness [19]

In 2022, Zhen Yu et al., proposed a multiband printed planar antenna with cloud-like grooves. The antenna's outside contour is formed like a cloud, and the groove-like pattern is akin to the cloud-like design found in ancient China. It is capable of supporting 3G, 4G, 5G, WLAN, Bluetooth, WiMAX, and a variety of other applications. The antenna, which is based on the classic monopole antenna, combines the benefits of a coplanar waveguide. An Archimedes helix is used to generate grooves that imitate old Chinese cloud patterns, The antenna is possible to obtain effective frequency bands [20].

In 2021, Sultan Qusai Hadi and Sabaawi Ahmed M. A. discussed the use of fractal curves in the design of loop antennas for passive (UHF) RFID tags operating at 900 MHz Passive UHF (ultra-high frequency) RFID (Radio Frequency Identification) tags are commonly used for identification, tracking, and data collection in various applications. The use of fractal geometry in antenna design can help achieve specific performance characteristics and frequency response [21].

In 2022, the same authors Qusai and Ahmed pointed out that the focuses on the design, optimization, and implementation of multiband fractal slot antennas for RF energy harvesting applications. This type of research involves creating antennas that can efficiently capture and convert radio frequency (RF) energy from the surrounding environment into usable electrical power [22].

In 2022, El-Khamy Said E, EL-Sayed Huda F., and et. discussed a comprehensive methodology for designing a thinned Eisenstein fractal antenna array with advanced capabilities like adaptive beamforming and reduced SLL. This approach takes advantage of optimization techniques and

adaptive algorithms to create an antenna array with enhanced performance characteristics for specific applications [23].

In 2022 by Abdul Rahim and Praveen Kumar Malik and et al. shown a single patch and  $2 \times 2$  patch fractal geometry is chakra-shaped microstrip patch antenna for vehicular communications was investigated and discussed. The  $2 \times 2$  patch covers five operating bands in the range of 25GHz to 36GHz. The gain of the antenna reaches the maximum of 6.72dB at resonating frequency of 32.8GHz and 6.69dB at 28.5GHz respectively [24].

In 2024, Benkhadda Omaima, Saih Mohamed and et al. suggested a tri-wideband Sierpinski hexagonal fractal antenna with a modified ground plane for wireless communication applications. The frequency ranges where the examined antenna worked were 2.19-4.43 GHz, 4.8-7.76 GHz, and 8.04-11.32 GHz. Additionally, at the resonant frequencies, the gains and radiation efficiencies were 1.074, 4.19, and 4.01 dBi and 68.35%, 64.15%, and 62.7%, respectively [25].

### **1.3 Objectives and aims of the Dissertation**

- To design various types of antennas such as narrowband, wideband, and multiband fractal antennas.
- To compare the performances of these three types of antennas and find out their potential use in practice.
- To compare between two used methods of construction namely MATLAB and CST and provide a clear conclusion about their advantages and limitations in designing these types of antennas.
- To use a single antenna that capable to operate at different frequency bands as well as a wide band of frequencies with a simple modification in the original antenna structures.

- To highlight the performance of the multiband Sierpiniski fractal bowtie antenna with simplest construction steps.

## **1.4 Organization of the Dissertation**

This dissertation is organized as follows. The first chapter contains an introduction and discusses the previous research and the general analysis and latest literature techniques, which act as the inspiration for writing this dissertation. The second chapter gives the theoretical background of narrowband, multiband and wideband antenna proposed designs. In Chapter three, two types of antennas were designed (dipole and bow-tie) and presented simulation performance of these antennas. Chapter four presents design and simulation results of fractal bowtie antenna (second iteration Sierpiniski fractal), using the codes in MATLAB. The obtained results from MATLAB are also verified by using CST STUDIO SUITE software and clear comparison between these three antennas using CST software. Chapter Five presents conclusions of the dissertation and a list of future works.

# CHAPTER TWO

## BACKGROUND THEORY

### 2.1 Overview

An electronic device that transforms electronic power into radio waves and vice versa is known as antenna. The function of the antenna is the interface between space and circuitry, much like the electrical eyes and ears. It might be referred to as the foundation of the wireless communication system [26].

### 2.2 Principle of Radiation

Variation of current density  $J$  or charge density with time produced EM waves. The size of the radiating structures starts from a small number of  $\lambda$  up to few hundreds of  $\lambda$ [27].

### 2.3 Wire Antenna

Wire antennas are a type of antenna that uses a conductive wire or set of wires to transmit or receive radio frequency (RF) signals. They come in various shapes and sizes, and they are among the most basic and widely used types of antennas. Linear or curved wire antennas are among the most traditional, straightforward, affordable, and frequently the most adaptable for a wide range of applications. A very popular and useful wire antenna is the dipole. Dipole antennas come in a variety of designs, including Hertzian, half-wave, tiny, bowtie and more[27].

Wire antennas are widely used for applications ranging from amateur radio and shortwave broadcasting to wireless communication and RFID systems. Their versatility, ease of construction, and ability to be tailored to specific frequency bands make them a popular choice across various industries. However, it is important to consider factors such as antenna length, positioning, and environmental conditions to achieve optimal performance.

## 2.4 Dipole Antenna

This is the first kind of simplest antenna ever utilized, and it is seen in Figure (2.1). "A pair of equal and unlike electric charges or magnetic poles of opposite signs isolated by small distance" is how M.W. Diction defines a dipole [28]. It is divided into two categories like Short Dipole Antenna and Folded Dipole Antenna.

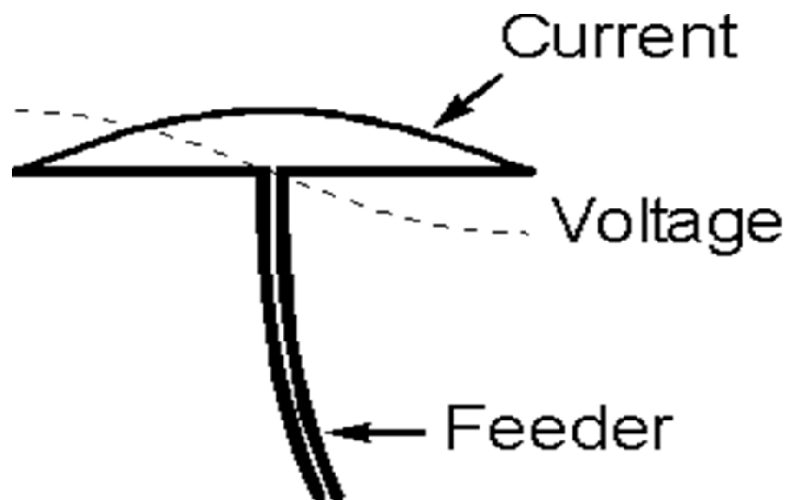


Figure (2.1) The basic half wave dipole antenna with Centre feed point [29].

Dipole antennas are widely used due to their simplicity and effectiveness in certain applications. They are a fundamental type of antenna and serve as the building blocks for more complex antenna designs. Dipole antennas are simple wire-based radio antennas having a center-fed driving element. It comprises of two conductors made of metal in line with each other, with a small space between them. In the middle, between the two conductors, the antenna receives the radio frequency voltage. As a cylindrical structure, this antenna's geometry is completely determined by five factors: length, radius, feeding gap, frequency, and wavelength [26].

In antenna engineering, the word "Short" is always associated with wavelength. In terms of frequency, the size of the wire, which is connected to wavelength, matters more than the size of the antenna. The gain of a dipole

antenna also increases with wavelength. The size of the dipole should be greater than the wavelength for maximum gain. Two parallel conductor wires that are looped together to make the folded dipole antenna [28].

The theory of transmission lines is where wired antennas first emerged. Electromagnetic waves can move from their source to their receiver through a transmission line. If the line's load end is left unconnected, power will radiate into space. But the radiation becomes considerable if the ends are gradually opened out. Radiation increases to its maximum as the two ends align such that they are across from one another. This turns into a cable antenna that radiates energy into space. After printing techniques were developed, this antenna arrangement became known as a dipole antenna or a wired dipole antenna [30].

### **2.4.1 Half-Wave Length Dipole**

The half-wavelength ( $l = \lambda/2$ ) dipole is one of the most widely used antennas. Its radiation resistance is 73 ohms, which is quite close to several transmission lines' characteristic impedances of 50 or 75 ohms. In particular at resonance, its matching to the line is made simpler. Its radiation characteristics in more detail because of how well accepted it is in practice.

The length of a half wave dipole should be half the wavelength, but in practice, the length of a half-wave dipole is often taken to be slightly less than half the wavelength of the target frequency. This is to account for factors such as end effects and the velocity factor of the medium through which the signal travels. The 0.45 factor mentioned is a common rule of thumb that takes these factors into consideration [26].

The half-wave, full-wave, and folding dipole antennas are all part of the finite length dipole antenna [30].

Figure (2.2) depicts a dipole antenna's general construction. Half-wave length dipole (Antenna) is the term used when the length of a dipole antenna  $L$  equals half-wave length. Half-wave dipole antennas have two arms, and there is a space between them for feeding ( $g$  is the feeding gap). Here,  $L$  stands for the antenna's overall length and  $D$  for the antenna arm's thickness or rod's diameter. The half-wave dipole's radiation resistance is 73 Ohm, matching the line impedance.

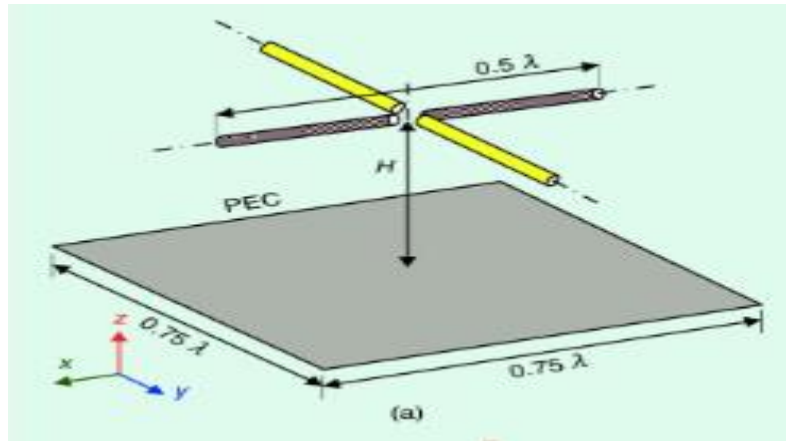


Figure 2.2 Geometry of the half wavelength dipole antenna [31].

## 2.4.2 Electric and Magnetic field component

One may determine a halfwave length dipole's electric and magnetic field components from equations (2.1) and (2.2) [32]:

$$\mathbf{E}_{\theta} = j\eta \frac{I_0 e^{-jkr}}{2\pi r} \left[ \frac{\cos\left(\frac{\pi}{2} \cos \theta\right)}{\sin \theta} \right] \quad (2.1)$$

$$\boxed{H_{\Phi} = j \frac{I_0 e^{-jkr}}{2\pi r} \left[ \frac{\cos\left(\frac{\pi}{2} \cos \theta\right)}{\sin \theta} \right]} \quad (2.2)$$

Where:

$E_{\theta}$  = the electric field,  $H_{\Phi}$  = magnetic field.

$I_0$ ,  $K$  = constant.

$r$  = radius of the dipole

The time-average power density and radiation intensity, meanwhile, can be expressed as [7]:

$$W_{av} = \eta \frac{|I_0|^2}{8\pi^2 r^2} \left[ \frac{\cos\left(\frac{\pi}{2} \cos \theta\right)}{\sin \theta} \right]^2 \cong \eta \frac{|I_0|^2}{8\pi^2 r^2} \sin^3 \theta . \quad (2.3)$$

$$U = r^2 W_{av} = \eta \frac{|I_0|^2}{8\pi^2} \left[ \frac{\cos\left(\frac{\pi}{2} \cos \theta\right)}{\sin \theta} \right]^2 \cong \eta \frac{|I_0|^2}{8\pi^2 r^2} \sin^3 \theta . \quad (2.4)$$

The total power radiated can be obtained as a special case [32] :

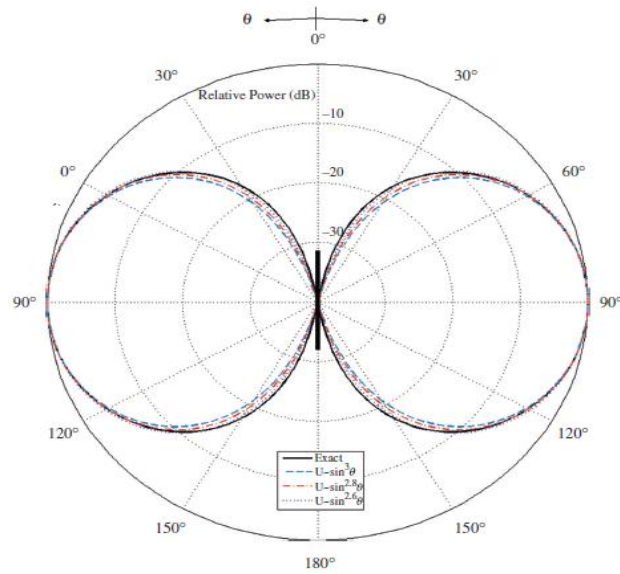
$$P_{rad} = \eta \frac{|I_0|^2}{4\pi} \int_0^{\pi} \frac{\cos^2\left(\frac{\pi}{2} \cos \theta\right)}{\sin \theta} d\theta . \quad (2.5)$$

### 2.4.3 Radiation Pattern

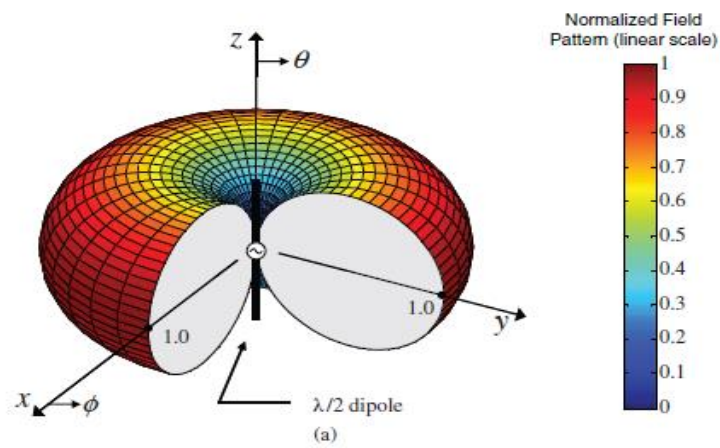
The radiation pattern of a half-wave dipole antenna is an important characteristic that describes how the antenna radiates electromagnetic energy into space. The radiation pattern indicates the intensity of the radiated electromagnetic field at different angles relative to the antenna's orientation. For a half-wave dipole antenna, the radiation pattern is influenced by its geometry and the length of the antenna compared to the wavelength of the signal it is transmitting or receiving.

- **Omnidirectional in the Horizontal Plane:** The radiation pattern of a half-wave dipole antenna is nearly omnidirectional in the horizontal plane. This means that the antenna radiates energy fairly evenly in all directions around the antenna when viewed from the side.
- **Maximum Radiation Perpendicular to the Dipole:** The strongest radiation from a half-wave dipole occurs perpendicular to the plane of the dipole itself. In other words, the antenna radiates most strongly in directions that are broadside to the orientation of the dipole elements.
- **Nulls Along the Axis:** In the plane of the dipole (end-on view), the radiation pattern of a half-wave dipole has nulls, or regions of reduced radiation. These nulls occur along the axis of the dipole, meaning that there is little to no radiation directly off the ends of the dipole.
- **Polarization:** The radiation from a half-wave dipole antenna is linearly polarized, and the polarization direction is aligned with the orientation of the dipole's elements. If the elements of the dipole are oriented vertically, the Polarization will be vertical; if the elements are horizontal, the polarization will be horizontal.

And the two-dimensional pattern is shown plotted in Figure (2.3) a) while the three-dimensional pattern 3D is depicted in Figure (2.3) b)



a)



b)

Figure (2.3) (a) two dimensional and (b) three-dimensional patterns of a  $\lambda/2$  dipole [32].

The maximum directivity of the half-wavelength dipole is [7]:

$$D_0 = 4\pi \frac{U_{max}}{P_{rad}} = 4\pi \frac{U|\theta=\pi/2}{P_{rad}} = \frac{4}{C_{in}(2\pi)} = \frac{4}{2.435} \cong 1.643. \quad (2.6)$$

Where:

$U_{max}$  = maximum intensity

$P_{rad}$  = radiated power.

maximum effective area is equal to [7]:

$$A_{em} = \frac{\lambda^2}{4\pi} D_0 = \frac{\lambda^2}{4\pi} (1.643) \cong 0.13\lambda^2 . \quad (2.7)$$

## 2.4.4 Radiation Resistance

The characteristic impedance of a half-wave dipole antenna is typically around 73 ohms. In practical applications, a balun (balanced-to-unbalanced transformer) is often used to match the impedance of the antenna to the impedance of the transmission line (usually 50 ohms for coaxial cable).

and the radiation resistance, for a free-space medium is [7]:

$$R_r = \frac{2P_{rad}}{|I_0|^2} = \frac{\eta}{4\pi} C_{in}(2\pi) = 30(2.435) \cong 73 . \quad (2.8)$$

Thus, the total input impedance for  $l = \lambda/2$  is equal to [7]:

$$Z_{in} = 73 + j42.5 . \quad (2.9)$$

The antenna must be matched or its length decreased until the reactance is eliminated in order to reduce the imaginary portion of the input impedance to zero. In actual use, half wavelength dipoles most frequently employ the latter.

The dipole's length during the first resonance ranges from roughly  $l = 0.47$  to  $0.48$  depending on the wire's radius; the thinner the wire, the closer the length is to  $0.48$ . In order to generate resonance [32].

The variations of the reactance as a function of the dipole length  $l$ , for different wire radius, are displayed in Figure (2.4):

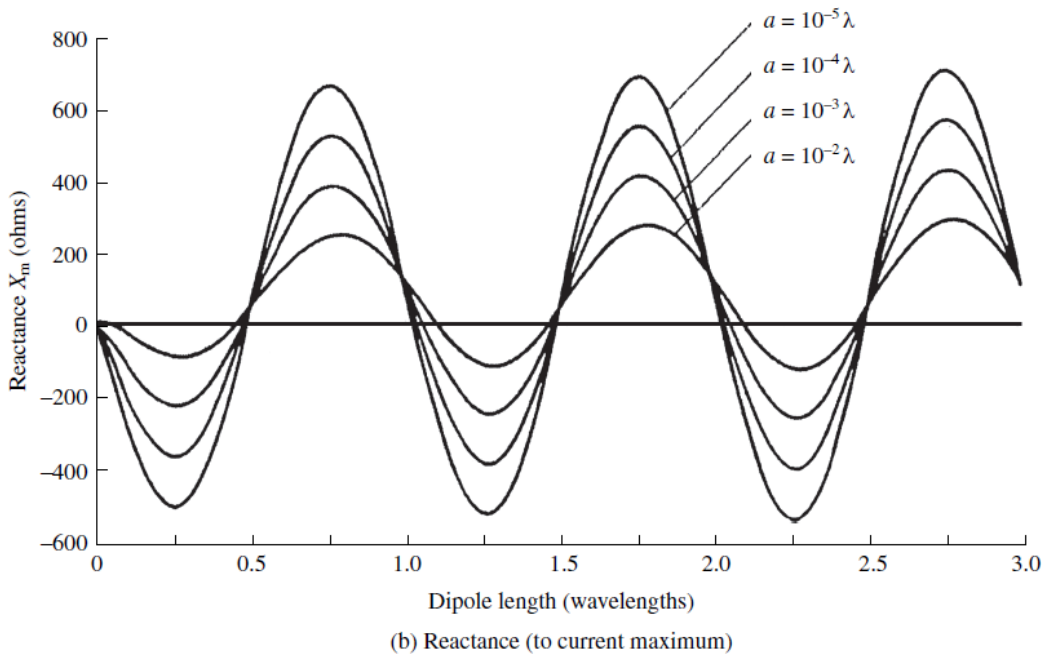
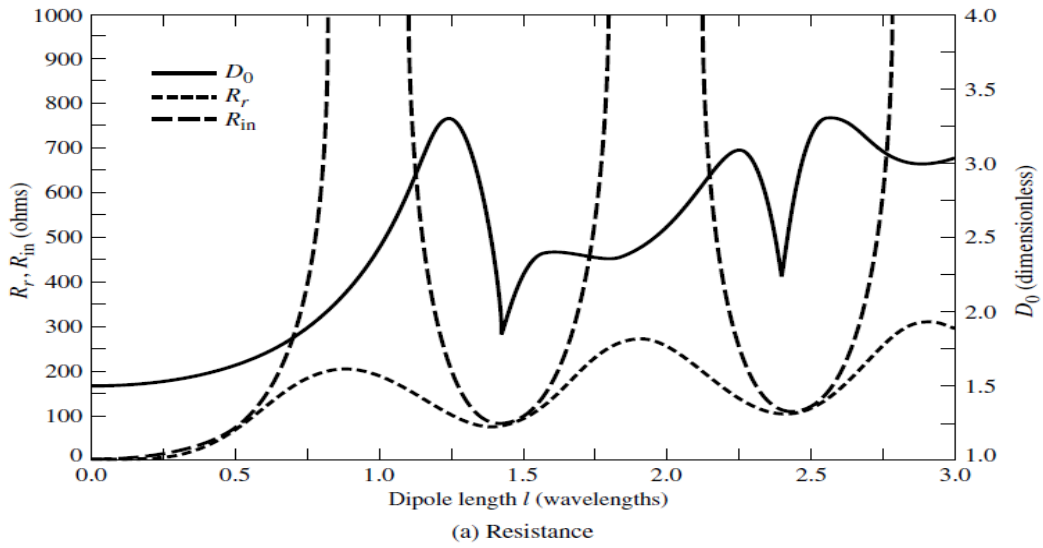


Figure (2.4) Radiation resistance and reactance, input resistance and directivity of a thin dipole with sinusoidal current distribution [32].

Table (2.1) provides a summary of the dipole directivity, gain, and realized gain.

Table (2.1) Summary of Dipole Directivity, Gain and Realized Gain (Resonant  $X_A=0$ ;  $f=100$  MHz;  $\sigma=5.7 \times 10^7$  S/m;  $Z_C=50$ ;  $b=3 \times 10^{-4}\lambda$ ) [32].

	$l = \lambda/50$	$l = \lambda/10$	$l = \lambda/2$	$l = \lambda$
$R_{hf}$	0.0279	0.2792	0.698	1.3692
$R_L$	0.0279	0.1396	0.349	0.6981
$R_r$	0.3158	1.9739	73	199
$R_{in}$	0.3158	1.9739	73	$\infty$
$e_{cd}$	0.9188	0.9339	0.9952	0.9965
	(-0.368 dB)	(-0.296 dB)	(-0.021 dB)	(-0.015 dB)
$D_0$	1.5	1.5	1.6409	2.411
	(1.761 dB)	(1.761 dB)	(2.151 dB)	(3.822 dB)
$G_0$	1.3782	1.4009	1.6331	2.4026
	(1.393 dB)	(1.464 dB)	(2.13 dB)	(3.807 dB)
$\Gamma$	-0.9863	-0.9189	0.18929	1
$e_r$	0.0271	0.1556	0.9642	0
	(-15.67 dB)	(-8.08 dB)	(-0.158 dB)	( $-\infty$ dB)
$G_{re0}$	0.0374	0.2181	1.5746	0
	(-14.27 dB)	(-6.613 dB)	(1.972 dB)	( $-\infty$ dB)

## 2.4.5 Dipole Uses

Half-wave dipole antennas are widely used in various applications, including amateur radio, broadcasting, wireless communication and more application. They are often used as reference antennas for testing and measurement purposes due to their well-known radiation characteristics.

Half-wave dipoles are relatively easy to construct and can be made from simple materials such as copper wire. It provides good efficiency and are well-suited for general-purpose applications. Half-wave length dipoles have omnidirectional patterns in one plane, their patterns can vary in other planes, and they might not be ideal for all directional requirements.

## 2.5 Bowtie antenna

A bowtie antenna is a type of antenna that has a shape resembling a bowtie, as the name suggests. It is a type of dipole antenna that is often used for wideband applications, such as in television reception, where it can cover a range of frequencies effectively. The design consists of two triangular pieces of conducting material (often metal) oriented back-to-back, forming the shape of a bowtie or butterfly as shown in figure (2.5). A triangular metal sheet is used to create a bowtie antenna, and the feed is located at the vertex. Each arm of a bowtie antenna can be printed on a substrate with the antenna's top or bottom surface[33].

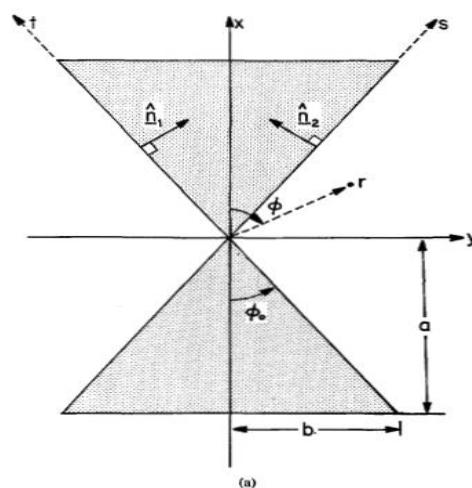


Figure (2.5) Geometry of Bowtie Antenna in Cartesian  $(x, y, z)$  and radial Coordinates  $(r, b)$ , and the corresponding oblique coordinates  $(s, t)$  with unit vectors,  $n_1, n_2$  [34].

Broadband applications due to ability to achieve wider bandwidth are compared to traditional patch antennas. Bowtie antenna offer certain advantages that can help mitigate the narrow bandwidth limitation of patch antennas [35].

Brown and Woodward conducted the first thorough research of the input impedance and radiation from bow-tie antennas in 1952.

**2.5.1 Unipolar Bow-Tie Antennas:** Unipolar bow-tie antennas are a variant of the standard bow-tie antenna design. The "unipolar" term might refer to the way the antenna is fed or to the way the current distribution is structured on the antenna's arms. The flat-top design likely contributes to the broader bandwidth, as it provides additional geometric features that can help improve impedance matching across a wider range of frequencies,[36].Unipolar bow ties are metallic, flat-topped antennas that are fed by a coaxial cable that passes through an image plane. Their parametric analyses demonstrated that the desirable attribute of unipolar bow ties is that they are more broadband than cylindrical monopoles [34].

### **2.5.2 Geometry of The Bow-tie**

The bowtie antenna is created from two triangular pieces of metal, typically made of a conducting material. The two triangles are positioned with their bases or edges touching, and they are mirror images of each other.

### **2.5.3 Feed Point of The Bow-tie**

The feed point of the antenna is located at the vertex where the two triangular elements meet. This is where the radio frequency (RF) signal is introduced into the antenna

**2.5.4 Broadband Performance:** One of the significant advantages of the bowtie antenna is its ability to provide wide bandwidth. This makes it suitable for applications where multiple frequencies need to be received, such as in television reception.

- **Omnidirectional Radiation of Bow-tie:**

The bowtie antenna typically exhibits an omnidirectional radiation pattern in the plane perpendicular to its surface. This means that it can receive signals from various directions without the need for precise alignment.

- **Polarization of Bow-tie:**

The polarization of the bowtie antenna depends on the orientation of the triangular elements. If the triangles are oriented vertically, the antenna will have vertical polarization. Similarly, if they are oriented horizontally, the polarization will be horizontal. The symmetrical design of the bowtie antenna helps reduce unwanted radiation in directions other than the desired one. This can contribute to its relatively clean radiation pattern.

## **2.5.6 Bow-tie Applications**

Bowtie antennas are commonly used for television reception, especially for receiving over-the-air broadcasts in areas with varying signal frequencies. They are also utilized in some radar systems and other wideband communication systems.

## **2.5.7 Types of Bowtie Antenna**

### **A. Triangular and Quadrate Bowtie Antenna**

Oliver Lodge created the triangular bowtie as a UWB antenna in 1898. According to the numerical findings, a wave traveling down the bow's axis at the dielectric wavenumber is the dominating current for wide bows. As the bow narrows, the main current changes to an edge current with a quasistatic wavenumber as the impedances spiral quickly toward a quasistatic value predicted by transmission line theory [34].

## B. Rounded edge/ Corner Bowtie Antenna

Various experts are studying various forms of bow-tie antennas with round corners in depth, Round corners increase return loss, flatten input impedance, and can somewhat simultaneously increase the stability of radiation patterns as shown in Figure (2.6) [33].

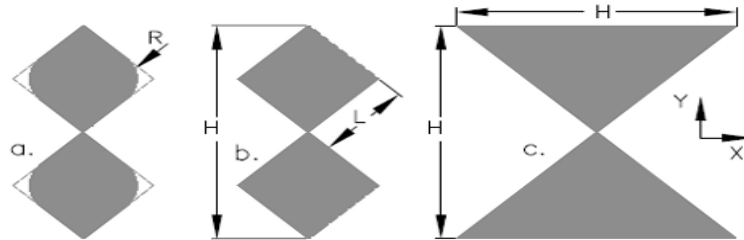


Figure (2.6) Three Types of Bow-tie antenna at the same height [33].

The impedance bandwidth increases with increasing antenna area at the same height, while the pattern bandwidth increases with increasing antenna height [33].

## C. Slot Bowtie Antenna:

One importance of the printed antenna construction is the feed line. CPW-fed slot antennas are one typical form of feed line used with printed antennas. CPW is a type of transmission line that consists of a central conducting strip (the signal line) flanked by two ground planes on either side. CPW offers certain advantages compared to other feed line configurations, such as microstrip lines, due to its balanced structure, which can help reduce common-mode noise and radiation. CPW lines also offer wider bandwidth capabilities and better impedance matching in some cases. is becoming more interesting for current wireless communications. In a CPW-fed slot antenna, a slot is etched or cut into the ground plane of the CPW structure as shown in figure (2.7). The slot serves as the radiating element of the antenna. When the

slot is excited with a signal through the CPW feed line, it generates electromagnetic waves, resulting in antenna radiation [33] .

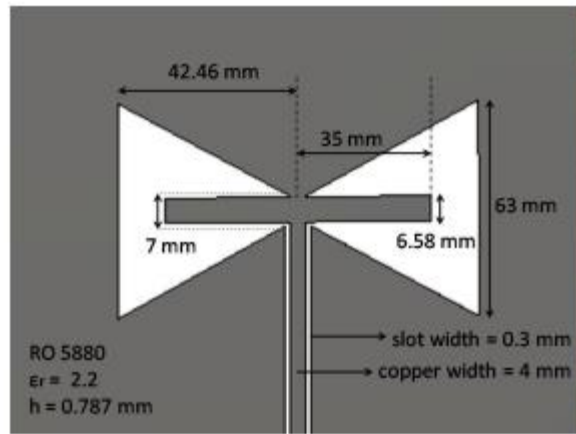


Figure (2.7) The layout of the bow-tie slot antenna and its dimensions [37].

A common broadband design used in many communication applications is the bow-tie slot antenna. Some methods have been proposed to increase the bandwidth of CPW-fed bow-tie slot antennas, including the use of a tapered metal stub to provide impedance matching, the use of inductive coupling, and the adjustment of slot flare angle.

#### **D. Self- Complementary Bow-tie Antenna (SCPB):**

Another type of modified bow-tie antenna is a SCPB antenna, utilizing the self-complementary concept. The design idea comes from modifying the triangle monopole antenna by adding an opposing triangular slot on the ground plane and bending the microstrip feed line [37], as shown in figure (2.8). To enhance the performance of bowtie antenna a new self-complementary bow-tie planar antenna (SCBT-Antenna) is introduced in [38].

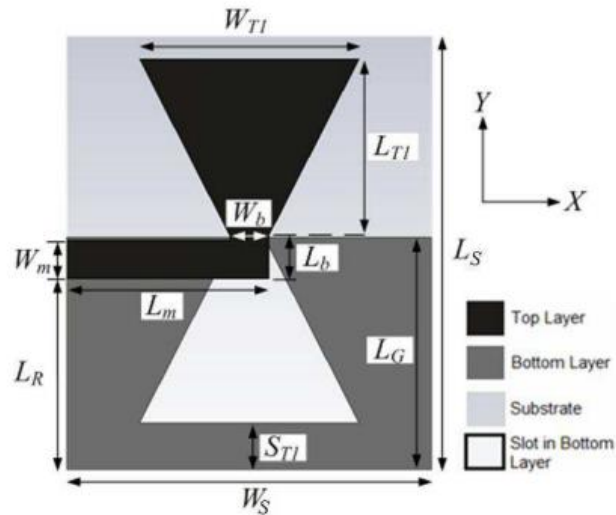


Figure (2.8) Geometry of the self-complementary bow-tie antenna [38].

### E) The Fractal Self-Complementary Bow-tie Antenna (FSCBT-antenna)

The SCBT-antenna was modified using technique of fractal to produce the fractal self-complementary bow-tie antenna (FSCBT-antenna). The fractal repetition has been applied on the triangular radiating patch and its complementary slot. The suggested antenna and its design characteristics are shown in Figure (2.8) and Figure (2.9).

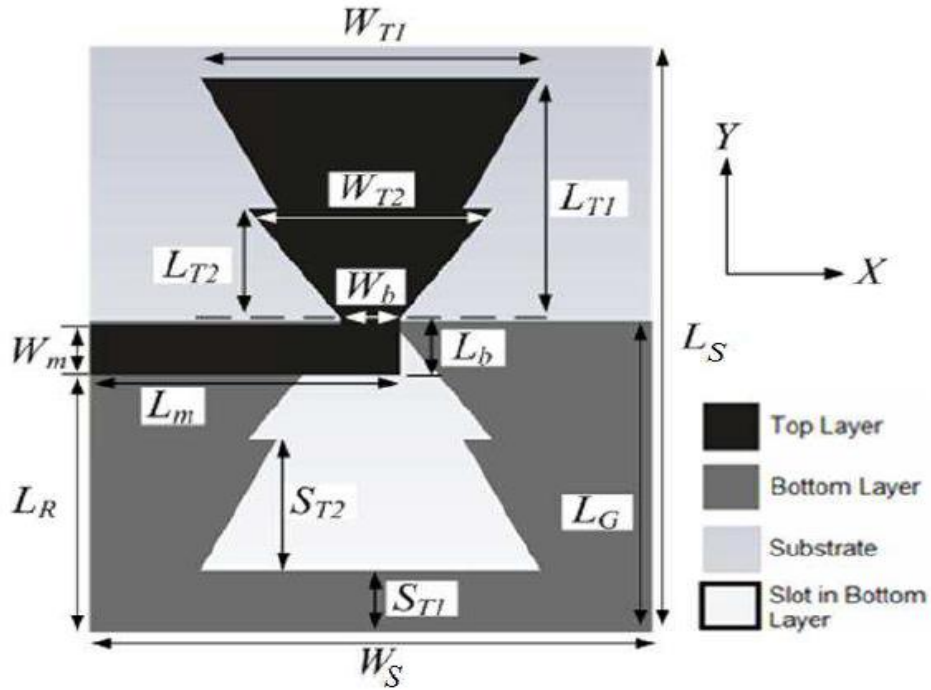


Figure (2.9) Geometry of the fractal self-complementary bow-tie antenna (FSCBT-antenna) [38].

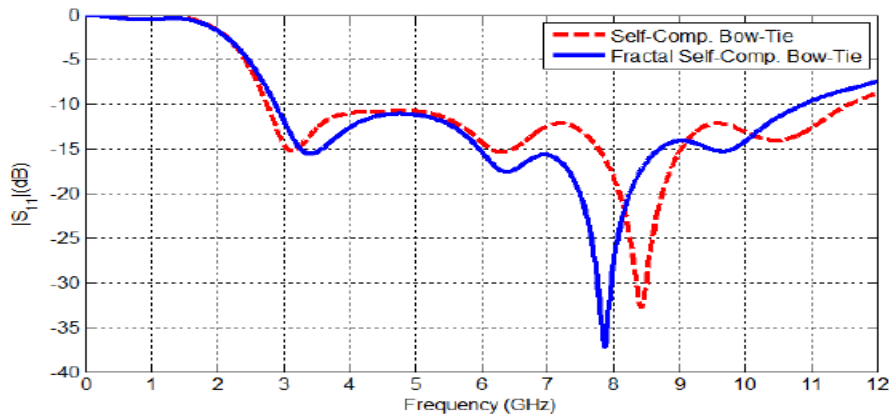


Figure (2.10) Return loss versus frequency simulations for SCBT and FSCBT antennas [38].

## 2.5.8 Different Type of Bowtie Antenna

Rounding the sharp corners of the bow-tie structure and using triangular stubs with extended arms are design techniques that can help achieve compactness in the shape of an antenna. These modifications are often

employed to reduce the physical size of the antenna while maintaining its desired electrical characteristics as shown in figure(2.11) [39].

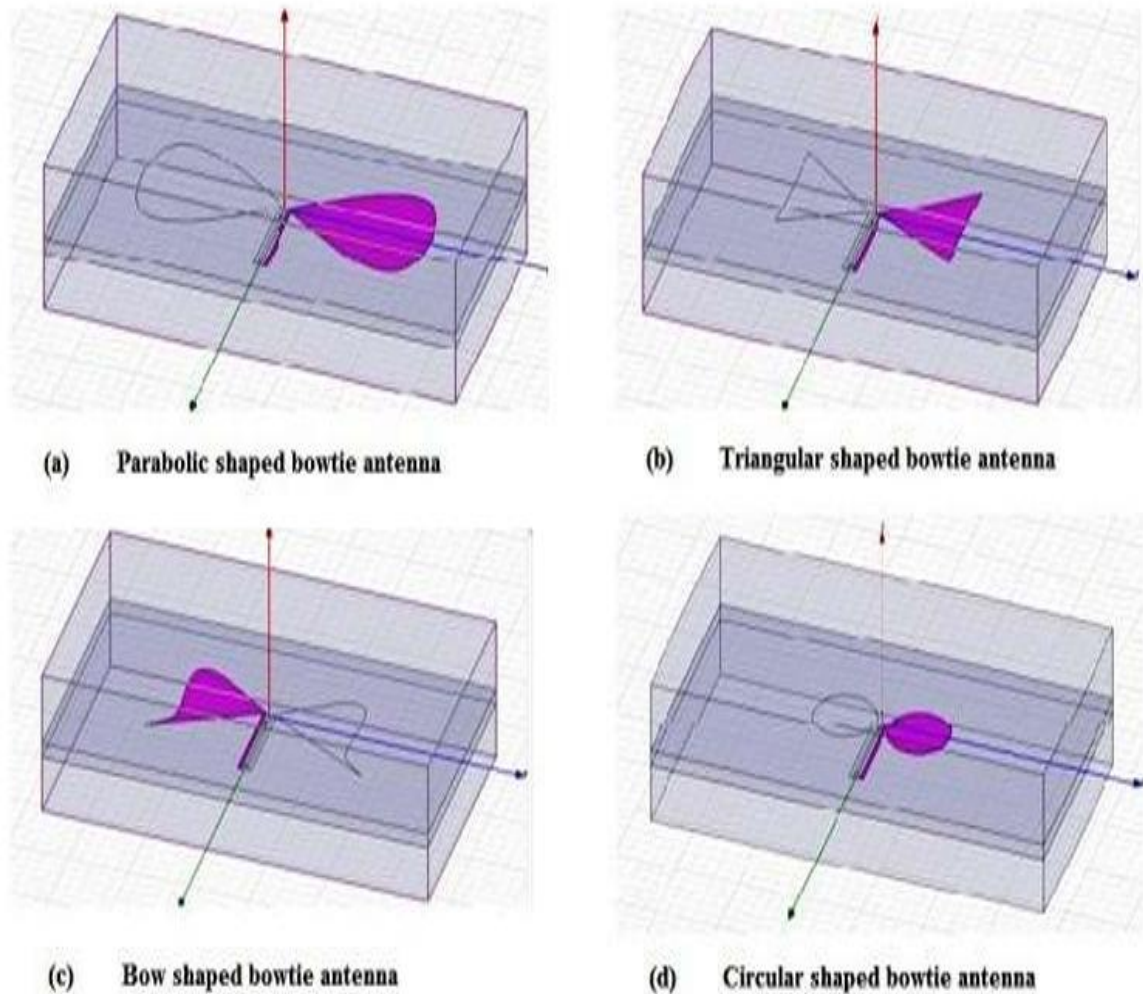


Figure (2.11) Different Design of Bowtie Antenna [14].

### 2.5.9 The Significance of coplanar wave guide( CPW-Fed) Slot Antennas:

**Broadband Performance:** CPW-fed slot antennas are known for their potential to provide relatively wide bandwidths. The combination of CPW's wide bandwidth characteristics and the radiating slot's geometry often results in antennas capable of covering a broad frequency range.

**Low Profile and Compact:** Printed antennas, including CPW-fed slot antennas, are typically planar and compact. This makes them suitable for integration into compact and space-constrained devices such as mobile phones, wireless routers, and other wireless communication systems.

**Ease of Fabrication:** The planar structure of CPW-fed slot antennas lends itself well to modern printed circuit board (PCB) fabrication techniques. This makes manufacturing and prototyping more convenient and cost-effective.

**CPW Benefits:** The use of CPW as the feed line brings advantages such as reduced radiation from feed lines (compared to microstrip feed lines), lower radiation of common-mode noise, and better impedance control. In conclusion, CPW-fed slot antennas are a significant design choice in the realm of printed antennas, particularly due to their broadband capabilities, compactness, ease of fabrication, and impedance matching advantages offered by the CPW feed structure. These antennas are widely used in various wireless communication systems where efficient radiation and wide frequency coverage are crucial.

## 2.6 Fractal Antenna

The construction of wideband, or even multiband, low profile, compact antennas is one of the primary goals of wireless communication systems. Such antennas have many different uses, including but not limited to unmanned aerial vehicles, small satellite communication terminals, and personal communication devices.

Fractal geometry has been used to design novel antenna structures, often referred to as fractal antennas. These antennas exhibit self-similarity at different scales, which can lead to improved performance characteristics. Fractal antennas are known for their multiband capabilities, compact size, and enhanced radiation properties.

Fractal antennas are based on the fractal notion, which is a recursively generated geometry with fractional dimensions pioneered and expanded by Benoit B. Mandelbrot. Mandelbrot first used the term "fractal," which literally translates into "broken or irregular fragments," to refer to a group of complex structures that have a built-in self-similarity or self-affinity in their geometrical structure. Mandelbrot has invented the term fractal and researched the relationship between fractals and nature. Mandelbrot demonstrated that many fractals occur in nature and may be utilized to properly model many processes. Mandelbrot was also able to propose additional fractals to model more complex structures, such as trees and mountains, which have inherent self-similarity and self-affinity in their geometrical design as shown in figure (2.12).



Figure (2.12) Fractals used to represent plants in nature [32]

### **2.6.1 Concept of Fractal**

The term "fractal" comes from the Greek word "Frangere," which meaning "broken or irregular fragments. It was invented in 1975 by mathematician Benoit Mandelbrot. Because of its capabilities and competencies, fractal antennas are multiband, high gain, low profile antennas that are employed for Wi-Fi packages. The practice of subdividing a shape into smaller copies of

itself is referred to as iterative geometry. Traditional antennas operate at a single frequency band, requiring a wider space to couple antennas. Fractal geometry has been applied to a variety of fields, with positive results. Fractal antennas contain the following characteristics:

- a) Self-similarity attribute -Antenna has the same shape but is repeatedly reduced in length.
- b) Because of its space-filling feature, the Hilbert curve is employed to reduce the size of antenna elements. The electrically long, compact, and space-filling properties of space-filling materials enable the downsizing of antenna elements [40].

### **2.6.2 Fractal Antenna Advantages:**

- Wideband/multiband input impedance matching (use one antenna rather than many).
- Frequency neutral (constant efficiency over a wide frequency range)
- Material coupling is reduced in fractal array antennas.
- Better Gains and low Losses.

### **2.6.3 Fractal Antenna Disadvantages:**

- More Complexity
- Numerical Limitations: After the third iteration, the advantages start to fade.

### **2.6.4 Fractal Antennas Applications**

There are many applications of fractal antennas.

1. Fractal antennas have significant effects. The necessity for small, integrated antennas is driven by the recent expansion of wireless communication. The fractals antenna may therefore efficiently fill a small

space. Mobile phones an example of a personal hand-held wireless device in one of the three categories of application.

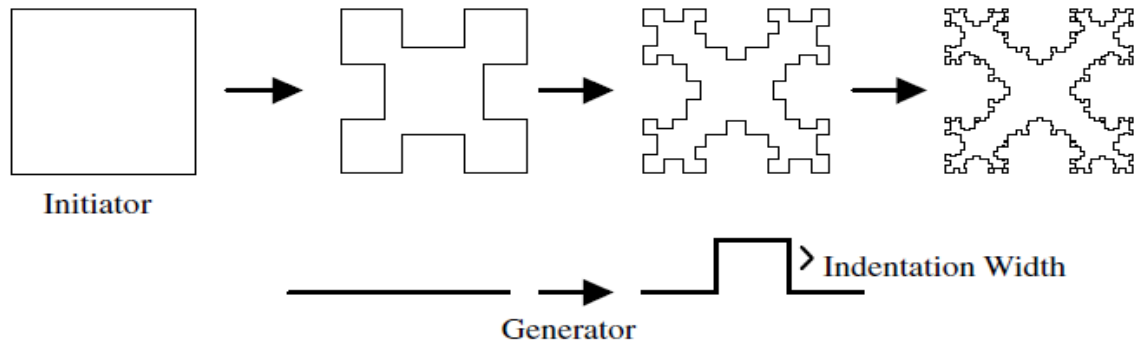
2. Multiband transmission is another application for fractal antennas.

3. Fractal antennas also reduce the resonant antenna's surface area, which may reduce the radar cross section. These advantages can be applied in military contexts.

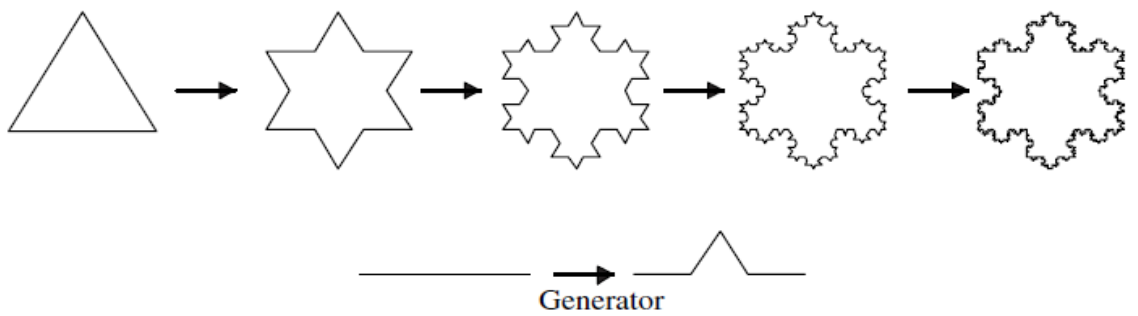
Fractal concepts have found applications in various branches of science and engineering, including the field of fractal electrodynamics. Fractal electrodynamics is a specialized area that applies fractal geometry and related mathematical concepts to the study of electromagnetic radiation, propagation, and scattering phenomena. This approach offers unique insights and tools for understanding complex electromagnetic behaviors that traditional models might not capture effectively [28].

These fractal notions have been applied to antenna theory and design, with several research and implementations of various fractal antenna elements and arrays, among many others.

Fractals are divided into two types: deterministic and random. Deterministic objects, such as the von Koch snowflake and the Sierpinski gaskets, are made up of many scaled-down and rotated copies of themselves. Fractal geometries are best characterized and formed by an iterative process that results in self-similar and self-affinity systems. The process is best shown graphically, as in Figure (2.13) (a, b) for the two different geometries. Figure (2.13) (a) depicts the Minkoski island fractal, whereas Figure (2.13) (b) depicts the Koch fractal loop.



a) Minkowski island



b) Koch loop

Figure( 2.13) Iterative generation process of fractal [32].

A fractal's geometry producing process begins with a basic geometry known as the initiator, which in Figure (2.13) (a) is a Euclidean square and in Figure (2.13) (b) is a Euclidean triangle. Figure (2.13) (a) replaces each of the four straight sides of the square with a generator indicated at the bottom of the picture. The first three iterations created are shown. Figure (2.13) (b) replaces the middle third of each triangle side with its own generator.

The procedure and generator shown in Figure (2.13) (b) can also be utilized to generate the Koch dipole, which will be addressed further below. Observing multiple repetitions of the procedure can reveal the trend of the fractal antenna geometry. The final fractal geometry is a curve with an indefinitely detailed underlying structure such that the fundamental building

pieces cannot be differentiated no matter how closely the structure is studied since they are scaled versions of the initiator.

### 2.6.5 Some Useful Geometries for Fractal Antenna Engineering

The Classification of Fractal Antennas can be explained in Figure (2.14)

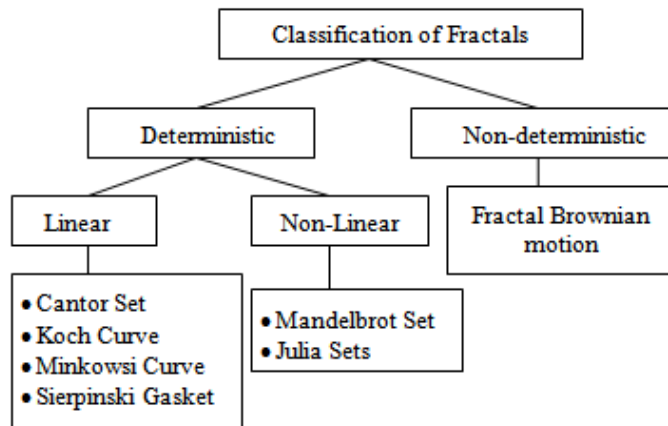


Figure (2.14) Classification of Fractal Antennas [41].

This section will give a brief review of some of the more prevalent fractal geometries that have been proven to be helpful in creating novel and creative antenna designs.

#### 2.6.5.1 Koch Curve:

The Koch curve is a well-known fractal that starts as a simple line segment and progressively adds smaller segments at specific angles. Koch curve-based fractal antennas can achieve multiband operation due to their intricate, self-similar structure.

**2.6.5.2 The Koch snowflake** It is another well-known fractal. As shown in Stage 0 of Figure (2.15), this fractal likewise begins as a solid, equilateral triangle in the plane. The Koch snowflake is created by iteratively adding smaller and smaller triangles to the initial structure, was created by methodically eliminating larger and larger triangles from the original

structure. Figure (2.15) which depicts the initial steps of a Koch snowflake's geoelectrical formation, exemplifies this procedure.

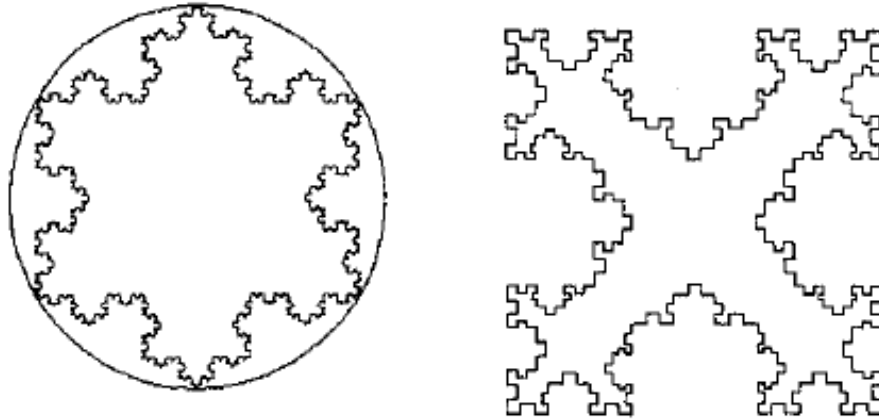


Figure (2.15) Koch snowflakes and Koch islands are popular fractal geometries.

Koch snowflakes and Koch islands are commonly employed in antenna engineering, especially for miniaturized loop antennas and patch antennas. These fractals help achieve compact size and multiband behavior, making them valuable in various wireless communication applications [42].

### 2.6.5.3 Hilbert Curve:

The space-filling features of the Hilbert curve and related curves make them appealing candidates for fractal antenna design. Figure (2.16) depicts the first four steps in the development of the Hilbert curve. The Hilbert curve is an example of a self-avoiding space-filling fractal curve (i.e., it has no intersection points).

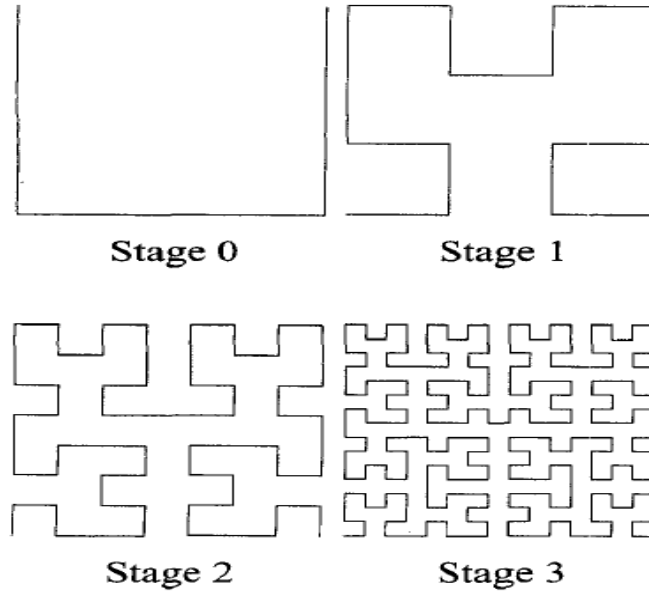


Figure (2.16) a Hilbert curve's initial stages of creation [42].

### 2.6.5.4 Cantor Set:

The Cantor set is a simple yet fundamental fractal pattern formed by iteratively removing middle segments from line segments. Cantor set-based fractal antennas exhibit unique electrical properties and can offer multiband performance. The German mathematician Georg Cantor initially published the Cantor (ternary) set in 1883. In many areas of mathematics, particularly set theory, chaotic dynamical systems, and fractal theory, the Cantor set is crucial.

#### 2.6.5.4.1 The Cantor Ternary Set

The fundamental Cantor (ternary) set, which has a wide variety of definitions and constructions, is a subset of the interval 0–1. Although Cantor initially offered a totally abstract formulation, the "middle-thirds" or ternary set construction is the most approachable. Start by dividing the closed real interval [0,1] into three equal subintervals.

$$I_1 = [0,1] - \left(\frac{1}{3}, \frac{2}{3}\right) = \left[0, \frac{1}{3}\right] \cup \left[\frac{2}{3}, 1\right]. \quad (2.10)$$

Next, divide each of the remaining two intervals into three equal subintervals, remove the center third from each, and proceed as before.

$$\begin{aligned}
 I_2 &= \left( \left[0, \frac{1}{3}\right] - \left(\frac{1}{9}, \frac{2}{9}\right) \right) \cup \left( \left[\frac{2}{3}, \frac{3}{3}\right] - \left(\frac{7}{9}, \frac{8}{9}\right) \right) = \\
 &= \left[0, \frac{1}{9}\right] \cup \left[\frac{2}{9}, \frac{3}{9}\right] \cup \left[\frac{6}{9}, \frac{7}{9}\right] \cup \left[\frac{8}{9}, \frac{9}{9}\right]
 \end{aligned}
 \tag{2.11}$$

In this method, able to produce a series of closed intervals: one in the zero step, two after the first, four after the second, eight after the third, etc.

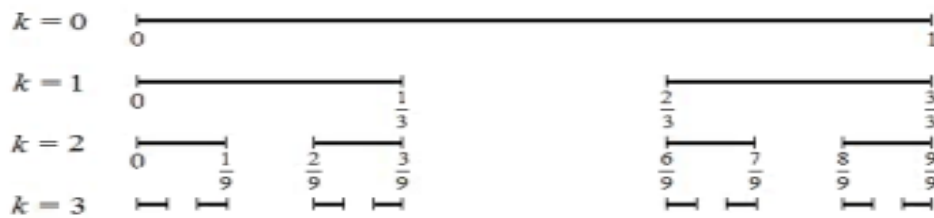


Figure (2.17) the first stages towards creating the Cantor ternary set [43].

Because of the Cantor set's self-similarity, antennas based on this geometry can display multiband behavior. The Cantor set's numerous levels of resonance can result in resonances at different frequencies, allowing coverage over multiple frequency bands. The Cantor set has a non-integer fractal dimension, which can affect the antenna's electrical properties. This can result in unusual impedance matching and radiation patterns. It should be noted that creating and evaluating Cantor set fractal antennas can be difficult, necessitating advanced simulation tools and optimization techniques. Engineers and researchers model and evaluate the electrical activity of these antennas using electromagnetic simulation software [43].

### 2.6.5.5 Sierpinski Carpet:

The rectangular patch is used to obtain the Sierpinski Carpet geometry. To get the desired geometry, a rectangle of 1/3rd size is subtracted from the center of the main rectangle and this process is repeated a number of times. This antenna is designed using the self-similarity property of fractal antennas with variable iteration. Figure (2.17) depicts the Sierpinski Carpet fractal antenna with four iterations [44].

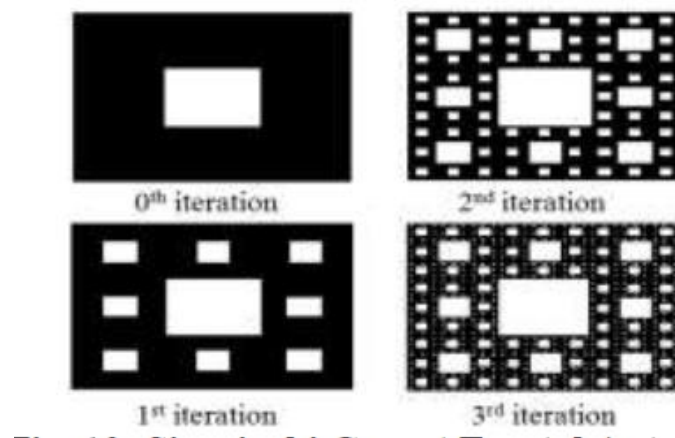


Figure (2.18) Sierpinski carpets, used in multiband antennas [41].

### 2.6.5.6 Hexagonal Fractals:

Hexagonal fractals, such as hexagonal gaskets, exhibit interesting self-similarity as shown in figure (2.19) and are suitable for compact multiband antenna designs

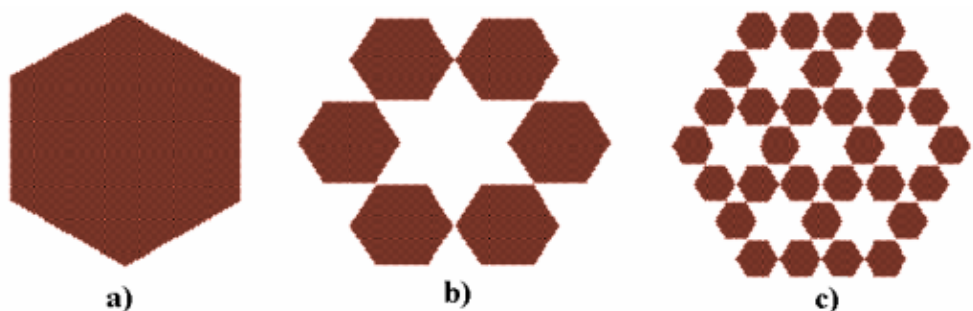


Figure (2.19) The hexagonal fractal's first three iterations [45].

When compared to the Sierpinski Carpet Fractal Antenna, the Hexagonal Fractal Antenna produced a substantial return loss. A hexagonal fractal is created by shrinking a hexagon generator shape to one-third of its original size and combining six smaller hexagons together. The matrix describes this technique, which is known as the iterated function system (IFS) [46].

### 2.6.5.7 Minkowski Geometry

Minkowski geometry was named after Hermann Minkowski, a German mathematician in 1907. The Minkowski curve's geometric shape is designed by taking the straight line (initiator) as shown in Figure (2.20) (a), and the generator structure as shown in Figure (2.20) (b). As seen in Figure (2.20) (c), this recursive procedure is continued up to the second iteration. To obtain the needed Minkowski fractal shape, the Iterated Function System (IFS) can alternatively be employed. It is similar to Koch curves in that equilateral triangles are utilized, but rectangles are used in Minkowski geometry. The rectangle's length is  $L$  and its height is  $rL$ , where  $L$  signifies the length of the original antenna and  $r$  specifies the ratio coefficient, [44].

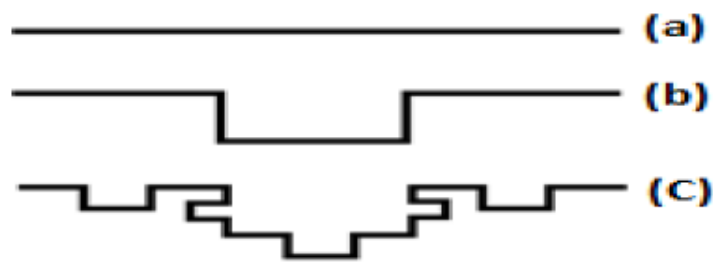


Figure (2.20) (a) Initiator geometry, (b) Generator geometry and (c) Proposed Minkowski curve [44].

### 2.6.5.8 Sierpinski Gasket

Sierpinski geometry was proposed in 1961 by the mathematician Sierpinski. Sierpinski Gasket is an extensively studied and used fractal

geometry for antenna applications. This antenna's self-similar current distribution demonstrates multi-band features. The multi-band nature of this antenna may be adjusted by modifying the antenna geometry, and the band characteristics of such antennas can be modified by varying the flare angle. As illustrated in Figure (2.21) (a), two alternative approaches, multiple-copy and decomposition, can be employed to produce the Sierpinski Gasket antenna using self-similarity and space-filling features. The Sierpinski Gasket shape is obtained by extracting the central part of the main triangle with an inverted equilateral triangle from the main triangle, as shown in Figure (2.21) (b) [44].

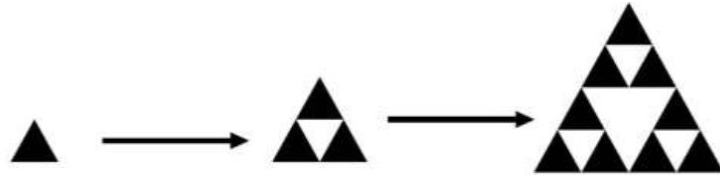


Figure (2.21) a) Sierpinski Gasket - Approach to Multiple Copy Generation [44].

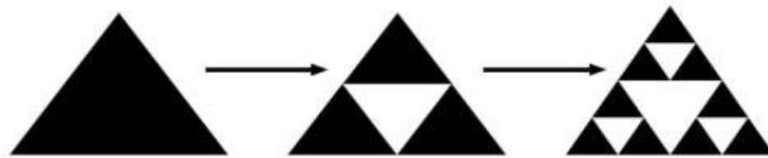


Figure (2.21) b) Sierpinski Gasket - Decomposition Generation Approach [19].

### 2.6.5.9 Antenna Hybrid Fractal

To improve the performance of a fractal antenna, it is occasionally recommended to construct a fractal antenna by merging two or more geometries. A hybrid fractal antenna is one that is created by mixing at least two fractal shapes. The following hybrid fractal antenna configurations are possible [44]. Koch-Koch, for example, is a fractal shape with itself as shown in figure (2.22) .

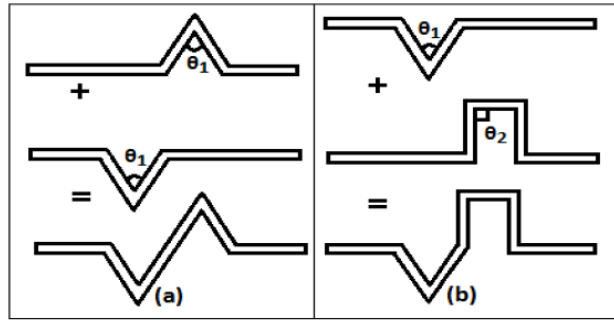


Figure (2.22) Hybrid fractal slot - (a) Koch- Koch and (b) Koch- Minkowski [41].

Figure (2.22) (c) shown another type of hybrid fractal structure combined Minkowski Curve and Sierpinski Carpet.

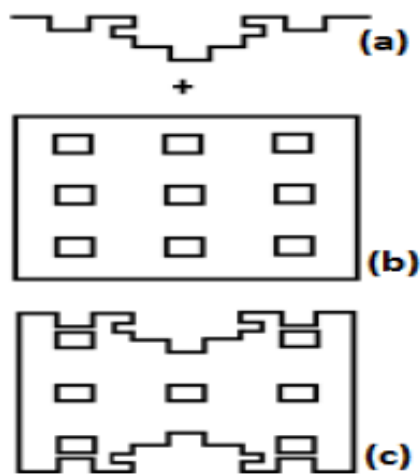


Figure (2.23) (a) Minkowski Curve, (b) Sierpinski Carpet geometry and (c) Hybrid fractal structure [44].

## **CHAPTER THREE**

# **Design and Simulation of Narrowband Dipole and Wideband Bow-tie Antennas**

### **Introduction**

Antennas play an important role in wireless communication because they allow electromagnetic waves to be transmitted and received. Bowtie and dipole antennas stand out among the numerous types of antennas due to their extensive use and unique properties. Dipole antennas are among the simplest and most fundamental types of antennas. A basic dipole antenna consists of two conductive elements, usually metal rods, oriented end-to-end with a small gap between them. This configuration creates an antenna that is typically half a wavelength long at its operating frequency; hence, it is often called a half-wave dipole. In this chapter, two types of antennas are designed narrowband dipole and wideband bow-tie and their performance is evaluated using MATLAB and CST software.

### **3.1 Software Tools:**

#### **3.1.1 MATLAB Simulation**

This software tool is used for antenna simulation and analysis. It likely provides a user-friendly interface for designing and evaluating antennas. The simulation results from MATLAB can help assess antenna performance.

#### **3.1.2 CST Full-Wave Modeling Software**

is a well-known full-wave electromagnetic simulation software suite. It allows for detailed modeling and analysis of electromagnetic fields, which is critical for understanding antenna behavior.

### **3.2 Antenna Design and Simulation:**

### 3.2.1 Half Wave Length Dipole:

To connect the two wires, a transmission line feeds through the opening. The term "center fed dipole" is used when the length of the two wires is equal. A dipole antenna that is half the wavelength long at its operating frequency is known as a half wave dipole antenna. A half-wave dipole is a resonant antenna with nodes at the ends and the current maxima in the middle. The radius of the wire, the spacing between the ends, and the change in length all affect the antenna's characteristics [30]. Half-wavelength dipole antennas are used in a wide range of applications, including AM and FM radio transmission, television broadcasting, amateur radio, and wireless communication systems. They are frequently used as benchmarking and testing antennas for other antenna designs.

### 3.2.2 DESIGNING ANTENNA PARAMETERS

The following are the fundamental formulas for building a wired dipole antenna] 29]

$$L = 143/f \quad (3.1)$$

$$D = 0.002\lambda \quad (3.2)$$

$$g = L / 200 \quad (3.3)$$

Where  $f$  is the resonance frequency in GHz , and  $\lambda$  is the wavelength in mm,  $L$  is the antenna's length in mm,  $D$  is the wired antenna's diameter in mm, and  $g$  is the space between a half-wave dipole antenna's two arms [30]. To produce resonance in an antenna, the actual part of the input impedance (resistance) must match the characteristic impedance of the transmission line to which it is attached (e.g., 50 ohms for standard coaxial cables). Antennas, on the other hand, frequently have a reactive component to their impedance known as reactance, which can be capacitive (negative reactance) or

inductive (positive reactance). As a result of this reactance, the impedance deviates from the required real value, resulting in poor impedance matching.

Adjustments to the antenna's physical dimensions are performed to match it and reduce the reactance to zero.

The dipole's length during the first resonance ranges from  $L = 0.47\lambda$  to  $0.48\lambda$ , depending on the wire's radius; the thinner the wire, the closer the length is to  $0.48\lambda$ . In order to generate resonance, a larger piece of the wire must be removed from  $\lambda/2$  for thicker wires [30].

### **3.2.3 The discrepancy between the half wavelength dipole's physical and electrical lengths**

The physical length of an antenna is not always exactly equal to the free-space wavelength of the signal it is designed to transmit or receive. The discrepancy is primarily due to the "end effect," which arises from the interaction between the electromagnetic wave and the finite length of the antenna conductor in the context of its immediate surroundings. The "end effect" refers to the additional electrical length introduced by the antenna's finite physical length and its proximity to dielectric materials (usually air). This extra electrical length is necessary for the antenna to operate at its resonant frequency, and it can cause the antenna to be slightly shorter than what would be expected based on free-space calculations.

The antenna end effect is caused by a drop in inductance and a rise in capacitance at the antenna conductor's end. This effectively lengthens the antenna. It has been discovered that the antenna end effect grows with frequency and varies with placement. The diameter of the wire also has a significant impact on this. The length of a wave traveling in free space is computed for a half wave dipole and multiplied by "A" factor. It is often between 0.96 and 0.98 and is mostly determined by the length of the antenna

to the thickness of the wire or tube used as the element. Its value can be estimated using the graph in Figure (3.1).

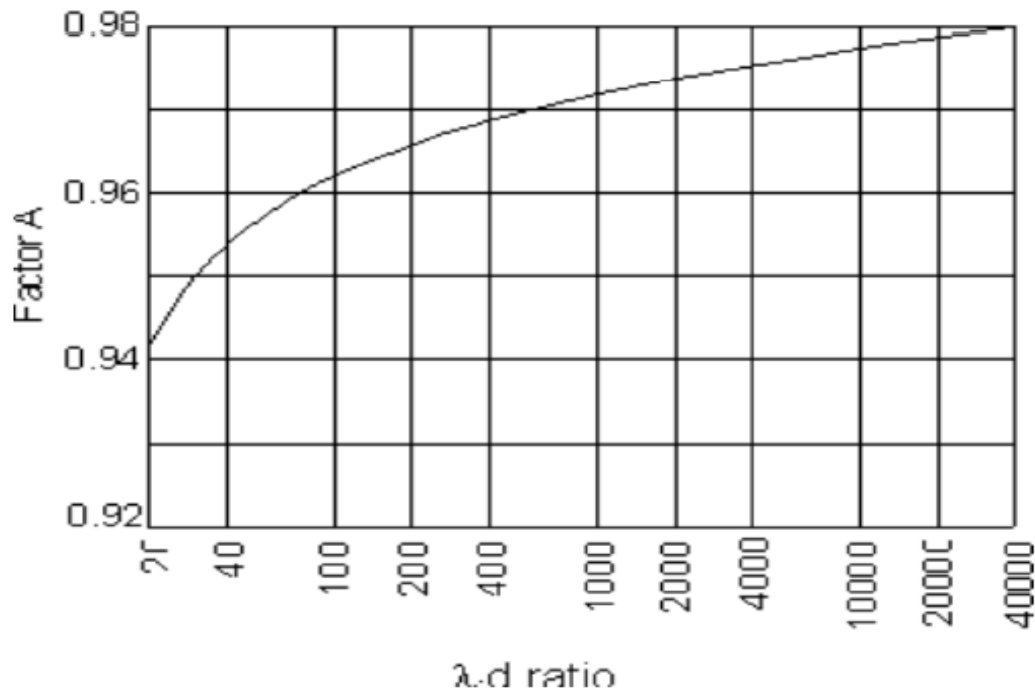


Figure (3.1) Factor "A" of multiplication is used to determine the length of a dipole [44].

Figure 3,1 shows the multiplicative factor "A" used to determine a dipole's length. However, a factor "A" or end factor, must be added to the length of a wave traveling in free space for a half wave dipole. The new length (physical length) ( $L_n$ ) is thus equal to  $A \times L$

Dipole radius:  $R = 0.001 \times \lambda$  [27]. The diameter then equals  $2 \times R$ . Feeding gap ( $g$ ) is equal to length ( $L_n$ ) / 200 [27]. The parameters listed below are utilized to design the proposed antenna.

Table 3.1 Design parameters of half wave length dipole at ( $f=2.4$  GHz) using CST.

Parameter	Value
Wavelength ( $\lambda$ )= $c/f$	125 mm
Length (L)= $\lambda/2$	62.5mm
Radius of the dipole = $0.001 \times \lambda$	0.125mm
Diameter D= $2 \times R$	0.25mm
$\lambda/D$	500
A (found from figure 3.1)	0.97
The new length (Ln) = $A \times L$	60.625mm
Feeding gap (g) = length (Ln) / 200	0.303mm

The feeding point is located at the center of the dipole. The designed dipole antenna's performance in terms of reflection coefficient, radiated power, and gain will be evaluated. Figure (3.2) shown the design structure of half-wave length dipole at 2.4 GHz.

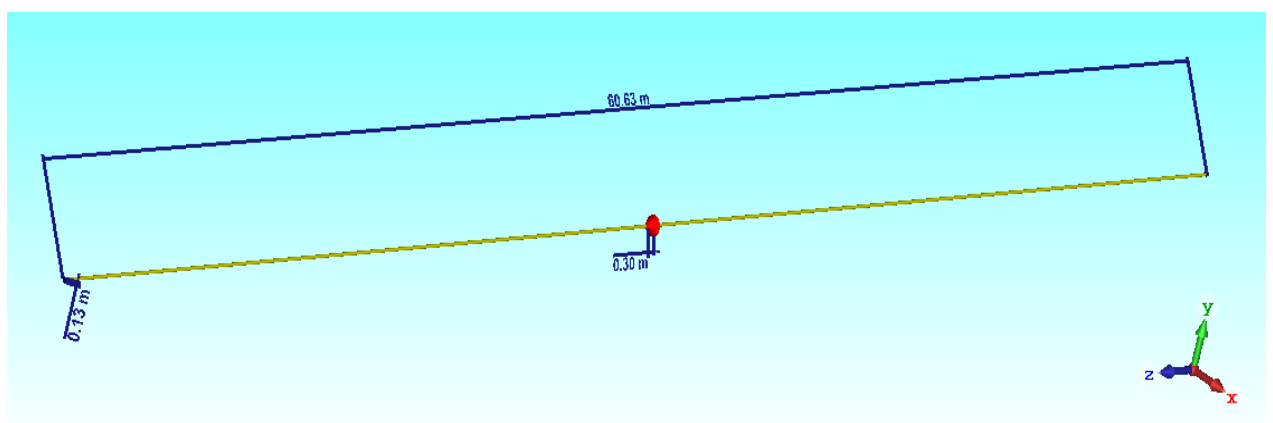


Figure 3.2 narrow band dipole antenna at 2.4 GHz using CST software.

The front view geometry and structure of the half wave dipole antenna designed on CST Microwave Studio software are shown in Figure (3.2). The dimensions and specifications of the proposed antenna have been tuned to

achieve the best feasible impedance match. As antenna copper (annealed) has been used. Figure (3.3) shown the reflection coefficient in (dB) with frequency in (GHz) of dipole at 2.4 GHz using CST.

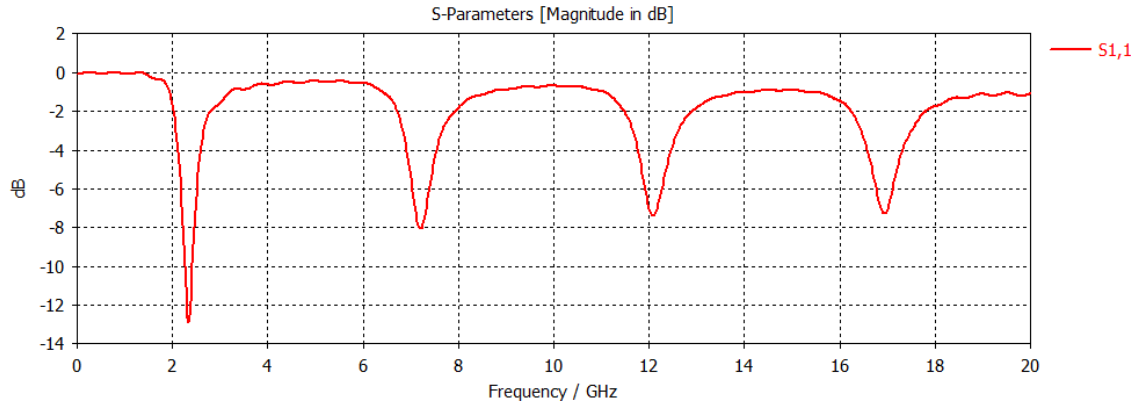


Figure (3.3) Dipole reflection coefficient with frequency.

Form figure (3.3) observed the proposed dipole tuned at 2.4 GHz, the reflection coefficient will reach about -13 dB and other notch at multiple integers of frequencies less than

Figure (3.4) shown the radiated power in (w) with frequency in (GHz) of dipole using CST will be reached to 0.45 W.

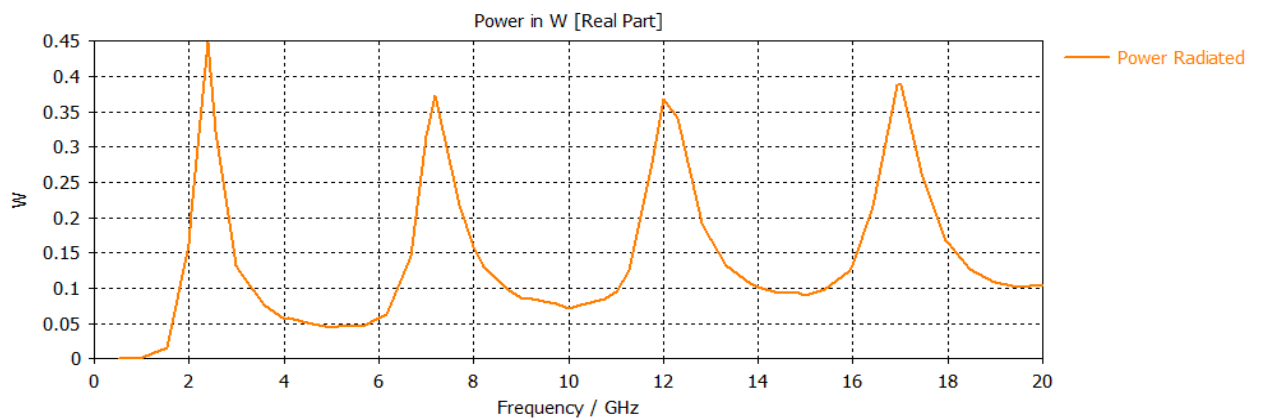


Figure (3.4) Dipole radiated power.

From Figure (3.5) can observed the B.W of the proposed dipole antenna equal to 0.1534 GHz,

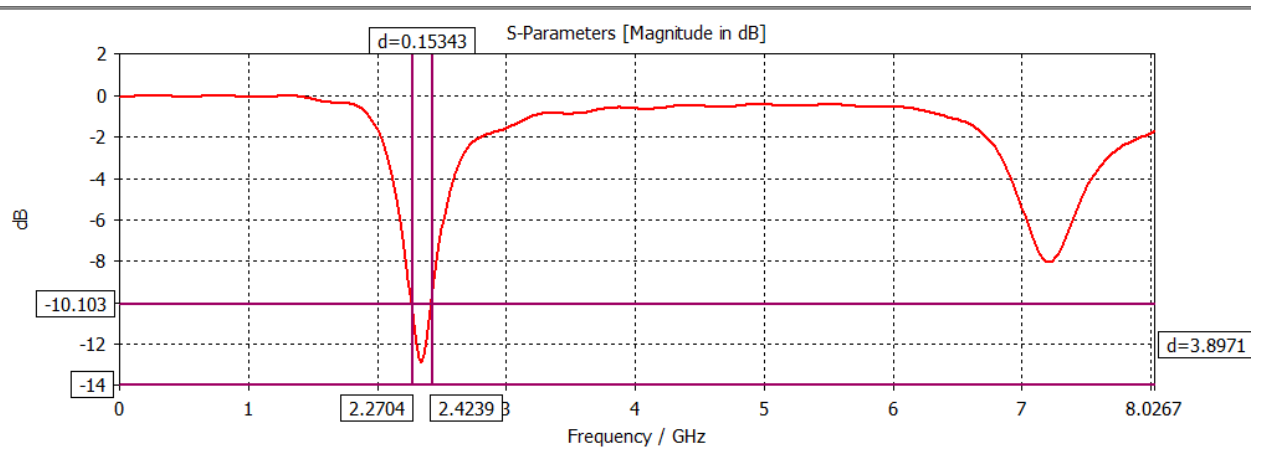


Figure (3.5) Bandwidth curve for the half-wavelength dipole antenna.

### 3.2.4 Simulated Performance of Narrowband Dipole Antenna Using MATLAB

The simulated performance of the designed narrowband dipole antenna in terms of the reflection coefficient, radiated power, and the antenna gain as a function of the frequency are shown in Figure 3.6. The MATLAB constructed half-wavelength dipole operates at the resonance frequency which is at 2.4 GHz. It is also observed that there is other two resonance frequencies appearing which are at 6.9 GHz and 11.6 GHz respectively. The method of moment is used to design these antennas in MATLAB which involves dividing the antenna's surface into a number of small triangular segments. For each segment, the electric and magnetic fields have been solved. Figure (3.6) shown the general construction of half wavelength dipole using MATLAB.

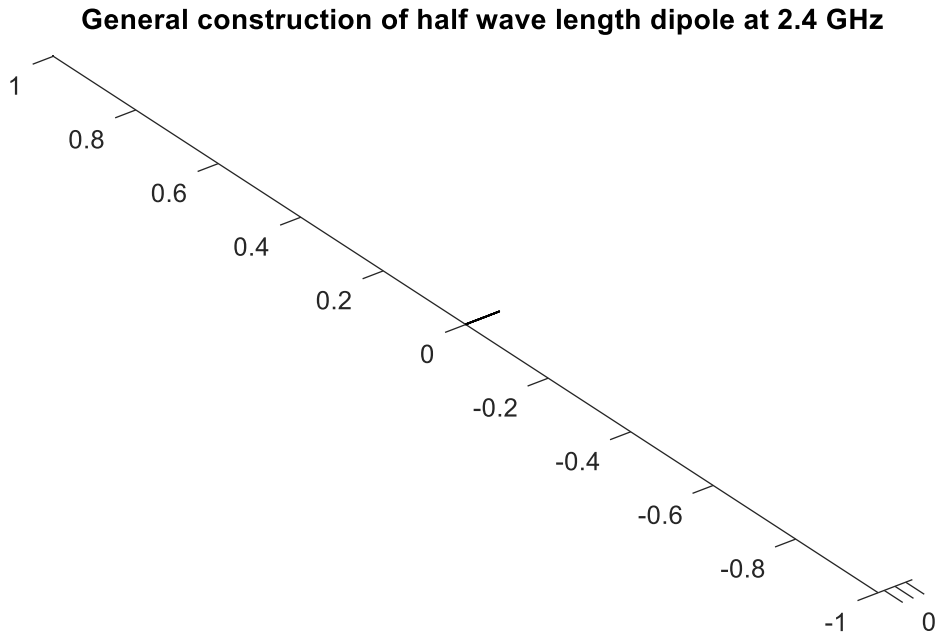
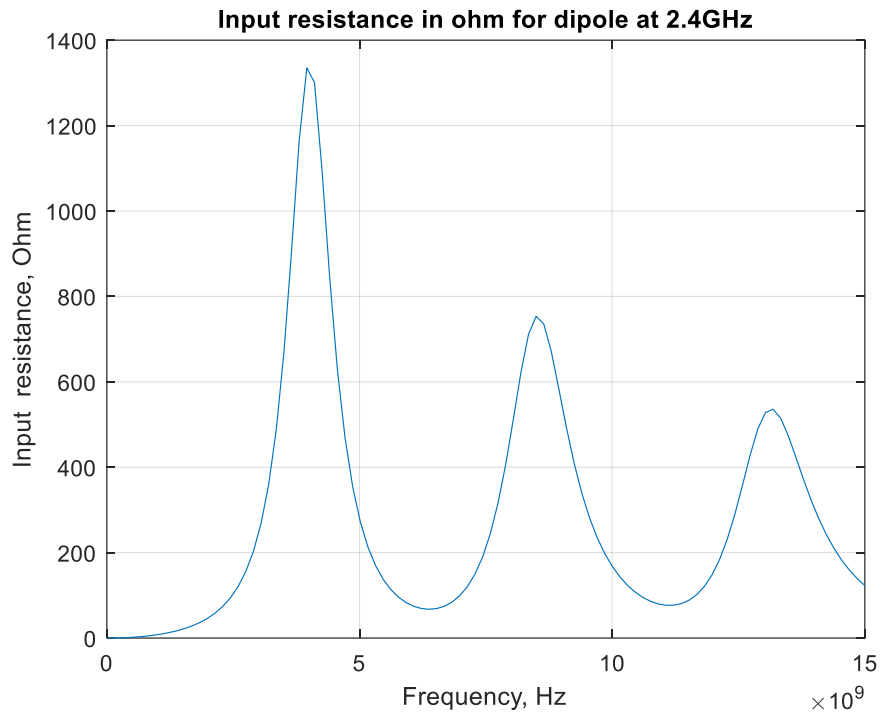


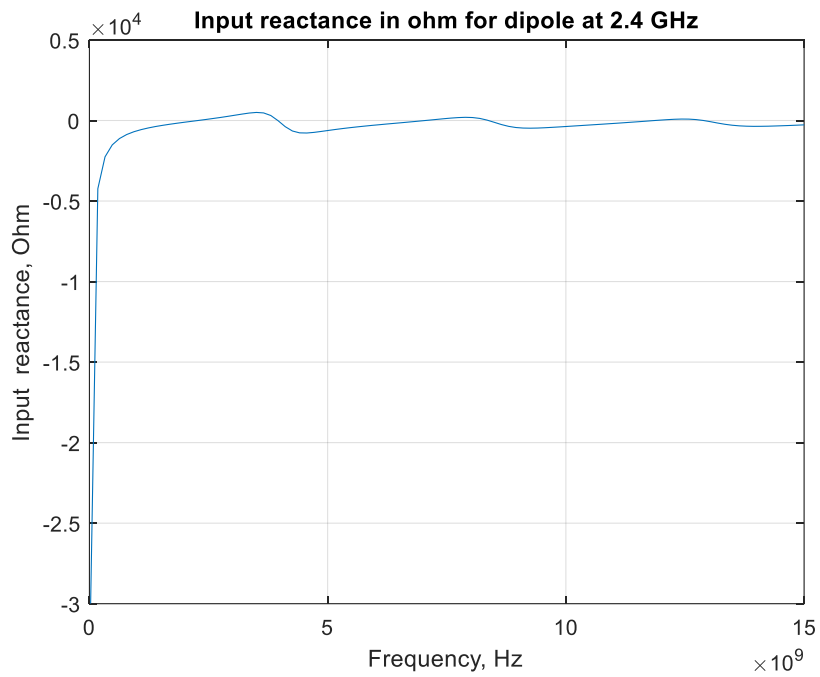
Figure (3.6) Genral construction of half-wavelength dipole  
(A 62.5mm length).

### **3.2.5 Dipole Input Impedance and Power Resonance.**

The mesh file name is specified as strip2.mat at the top of script rwg1.m, and then scripts rwg1.m and rwg2.m are executed to retrieve the frequency characteristics of the dipole. For the current dipole with a total length of 62.5mm the frequency loop parameters are chosen from F1= 25 MHz to fh= 15 GHz in script rwg3. m. Figure (3.7), which displays the ultimate outcome, was observed using the script sweepplot.m.



a)



b)

Figure (3.7) Dipole input impedance as a function of frequency. A 62.5mm length and 0.625mm diameter of wire.

Figure (3.7) shows that when the frequency of the feed voltage increases, the input impedance of the dipole is subject to significant real and imaginary oscillations. For some frequencies known as resonant lengths, the center-fed dipole's input impedance is exclusively resistive. One of the lowest resonances for the dipole might be used.

### 3.2.6 Dipole Radiated Power, Reflection Coefficient and Gain.

The script `efield2.m` should be run after the script `rwg3.m` to acquire the total radiated power and gain as a function of frequency. Figure 3.8 shows the outcome as it was observed using the script `sweepplot.m.2`.

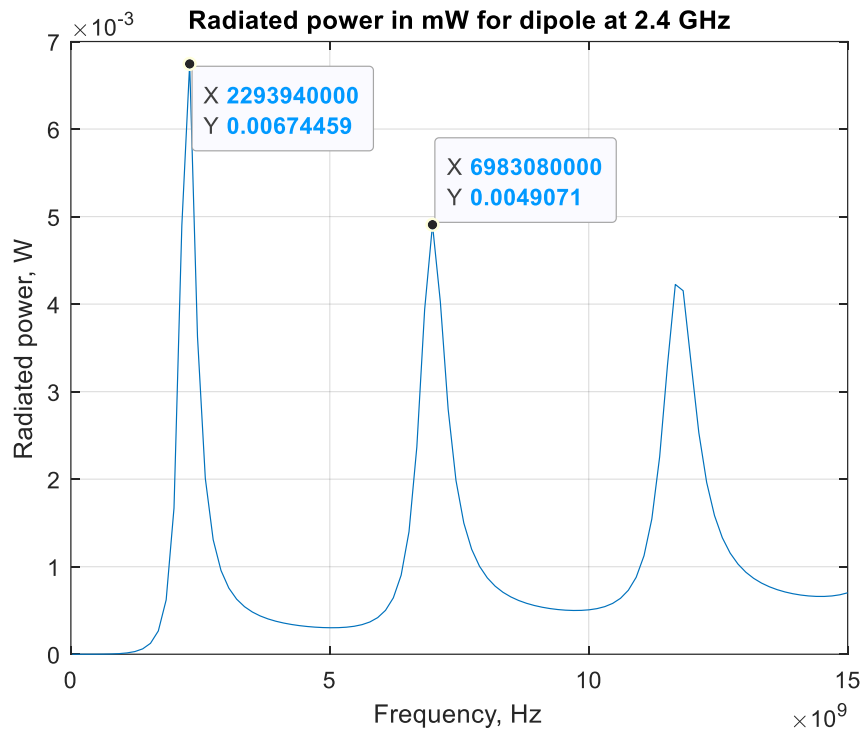
It is clear that the power being radiated has high peaks that match the resonant frequency; at the lower frequency, the dipole will emit up to 6.8mW. Based on the reflection coefficient in the antenna feed vs the 50-transmission line, The return loss is calculated [31]:

$$\Gamma = \frac{Z_A - 50 \Omega}{Z_A + 50 \Omega} \quad (3.4)$$

Where  $Z_A$  is the antenna input impedance. The reflection coefficient's magnitude in dB

$$R_L = 20 \log \Gamma \quad (3.5)$$

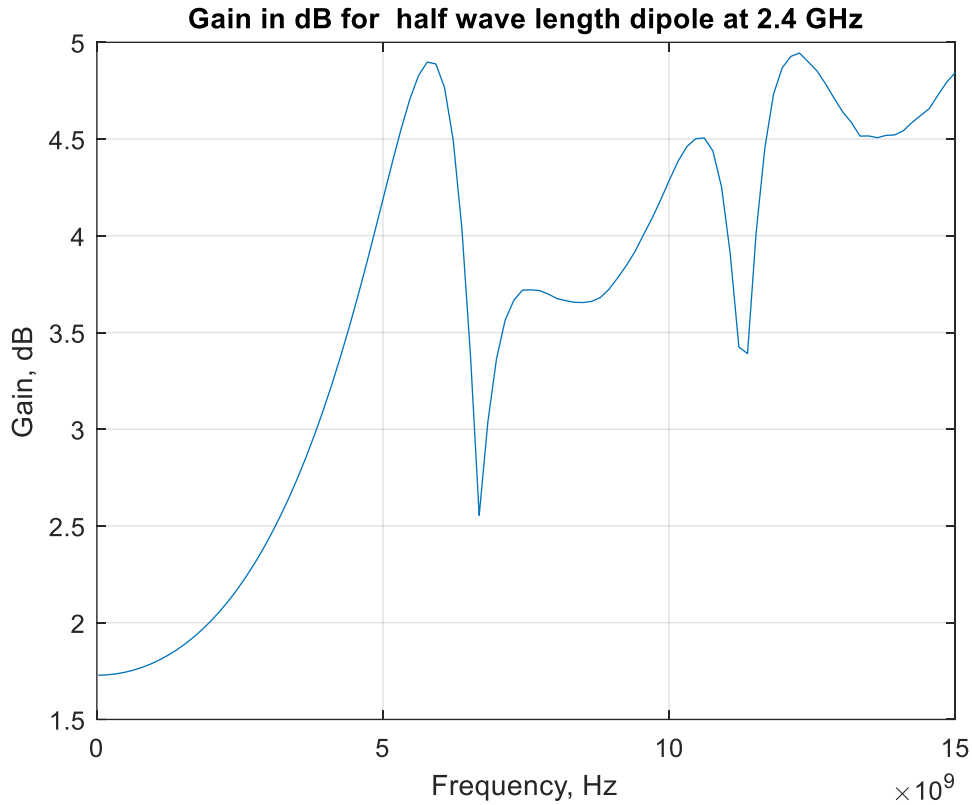
Figure (3.8) shown Performance of the constructed dipole antenna using MATLAB (a) Reflection coefficient, (b) Radiated power and (c) Gain



a)



b)



c)

Figure (3.8) (a) Dipole radiated power, (b) Reflection coefficient and (c) Gain as a function of frequency

When one increases the dipole thickness (or the width of a wire), the slope of the power curve and RL curve in Figure (3.8) (a) smooths out. There is no relationship between the gain and the antenna's input impedance or radiated power, as seen in Figure (3.8) (c), which plots the dipole gain as a function of frequency. In conclusion, it is best to treat the ordinary dipole like an unusual resonant antenna. It cannot be used as a broadband antenna due to its significantly oscillating input impedance and gain.

### 3.3 Wideband Bowtie Antenna

In recent years, a lot of energy has been spent on planar antennas supported by a dielectric substrate the bow-tie is one such antenna.

### 3.3.1 Planar Bowtie Antenna with Thick Dielectric Substrate:

Considerations for Design: Several aspects must be considered while building a planar bowtie antenna on a thick dielectric substrate:

- **Substrate Material:** The dielectric substrate material selected is critical. Fiberglass, ceramic, and other high-permittivity dielectrics are common materials. The dielectric constant of the material influences the electrical properties of the antenna.
- **Thickness of the substrate:** A thick substrate can provide mechanical support and aid improve the bandwidth of the antenna. The thickness should be selected to match the intended operating frequency and performance objectives.
- **Bowtie Geometry:** The length, width, and spacing of the bowtie elements will be changed dependent on the substrate thickness and operating frequency. These dimensions can be optimized using simulation and modeling techniques.
- **Feed Mechanism:** Microstrip or coplanar waveguide feed structures on the substrate are commonly used in planar antennas. For impedance matching and effective power transfer, the feed mechanism and placement should be properly planned [34].

Planar bowtie antennas supported by a thick dielectric substrate are an appealing alternative for obtaining wideband performance while remaining small in a variety of RF and microwave applications. The material and dimensions of the substrate are critical in producing the appropriate antenna properties. In applications where wideband performance is required. As it is mentioned, it consists of two bowtie-shaped elements facing each other, and it offers several advantages for wideband radio frequency (RF) and microwave applications. It is made up of two triangular or trapezoidal conductive pieces

arranged in the shape of an open V or bowtie. The feedline is normally connected at the center point where the two parts meet. The bowtie antenna's broad bandwidth is one of its main features. It can function effectively over a wide range of frequencies thanks to its distinctive design, making it useful for situations where signal frequencies may change greatly.

Bowtie antennas are often designed to be relatively low profile, which means they don't require a lot of physical space. This makes them suitable for applications where space is limited or where aesthetic considerations are important.

Bowtie antennas can produce directed or omnidirectional radiation patterns, depending on the individual design. Engineers can customize the radiation properties of the antenna to match the needs of a specific application by varying the size and spacing of the bowtie elements.

### **3.3.2 Wideband Bowtie Antenna Design Using CST software.**

Bow-tie is a second style of this dissertation. A dipole antenna of this kind has two bowtie-shaped components facing one another. It is a well-liked design for wideband RF and microwave applications, which are frequently employed in radars, wireless communication systems, and television reception. Additionally, this antenna is made for 2.4 GHz. As shown in Figure (3.9) it had the following dimensions: height = 22.06 mm, width = 34.91 mm, flare angle =  $67.380^\circ$  and distance between two triangles = 1.82 mm. According to the specified frequency or wavelength, this antenna can generally be configured as follows using CST software.

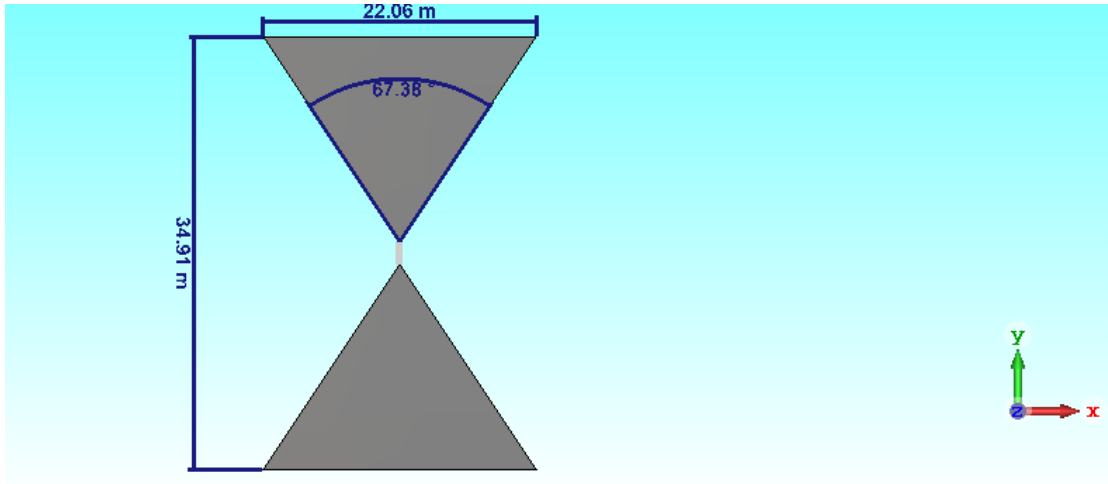
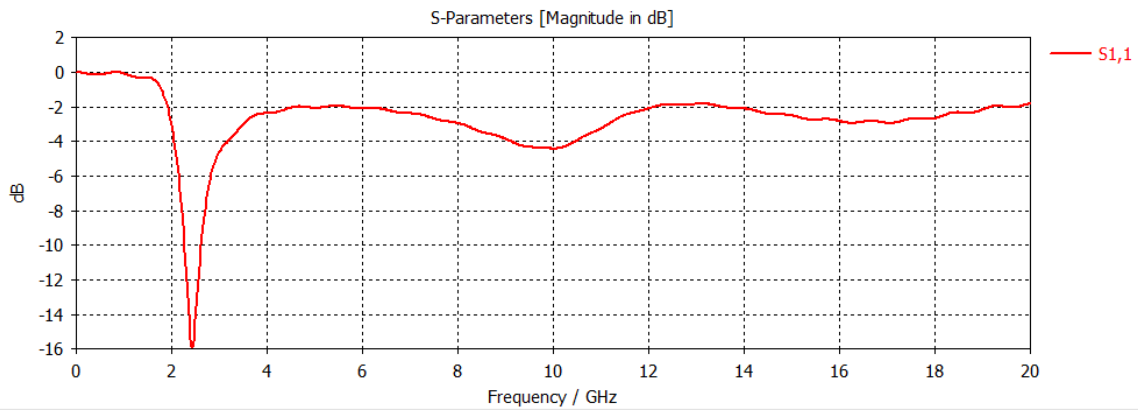
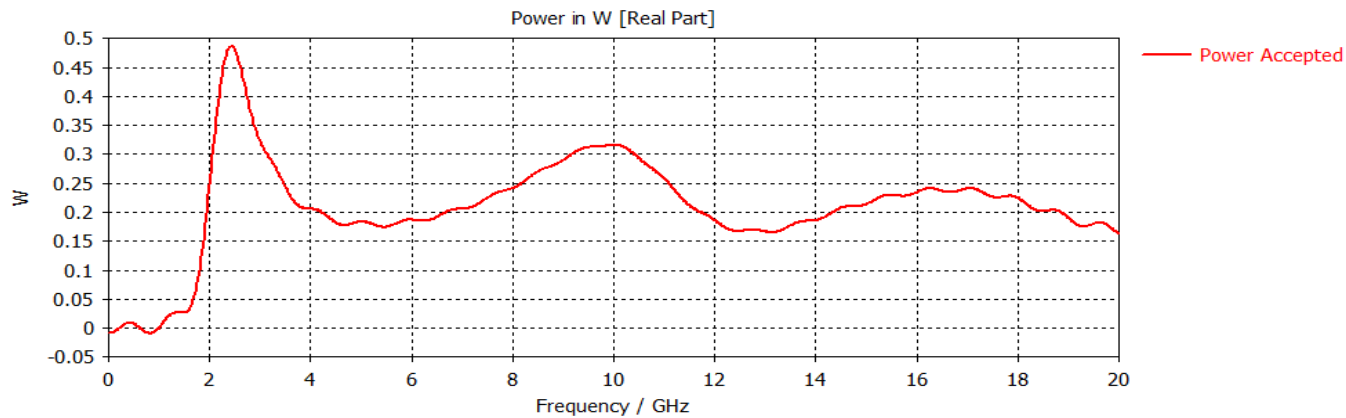


Figure (3.9) Front view Wide- Band Bow-tie Antenna at 2.4GHz using CST Software.

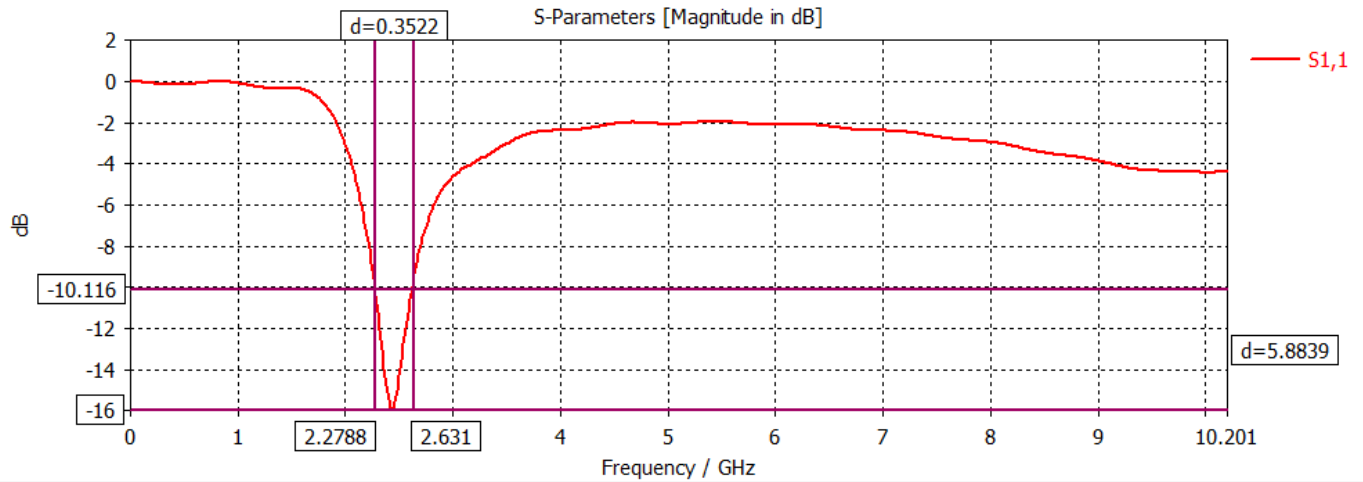
### 3.3.3 Simulation Result for Wideband Bow-tie using CST



a)



b)



c)

Figure (3.10) (a) Reflection coefficient 2.4GHz. (b) Radiated power with respect to frequency at 2.4GHz. (c) Bandwidth curve for bowtie antenna.

The B.W from last figure will equal to 0.3522 GHz

From figures (3.5) and (3.10) (c) the B.W frequency has doubled.

### 3.3.4 Wide-Band Bow-tie Antenna Design and Simulation Using MATLAB.

The MATLAB script bowtie.m was utilized to produce a bowtie shaped at 2.4 GHz as seen in figure (3.11). The feeding edge is always at the origin, with 34.91mm total width with flare angle  $67.38^\circ$ .

**General construction for bowtie antenna with flare angle(67.38)at 2.4 GHZ using MATLAB.**

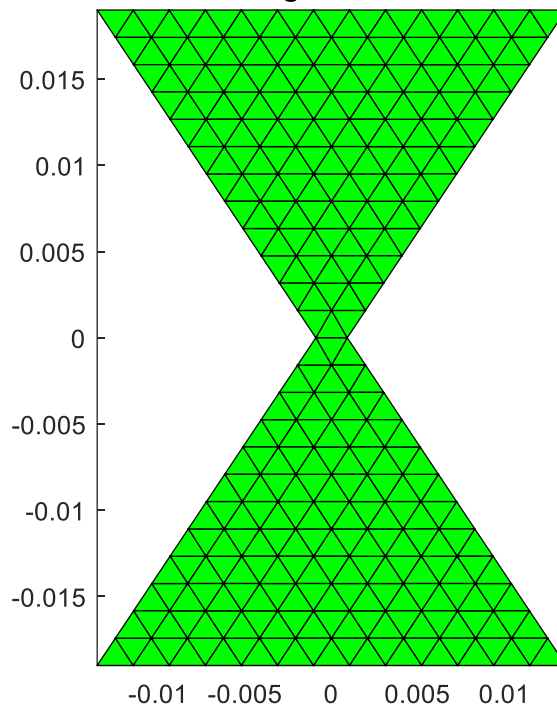


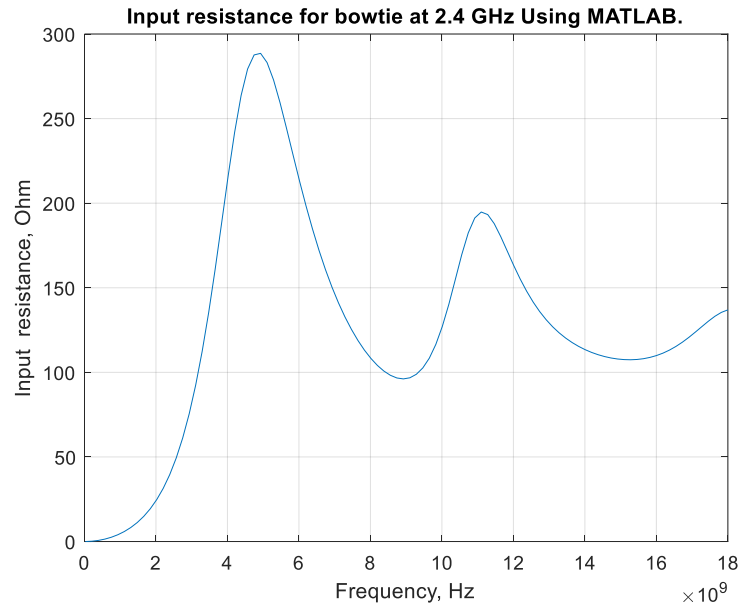
Figure (3.11) Broadband Bow-tie design using MATLAB in XY-plane.

### **3.3.5 MATLAB MESH FOR BOWTIE ANTENNA**

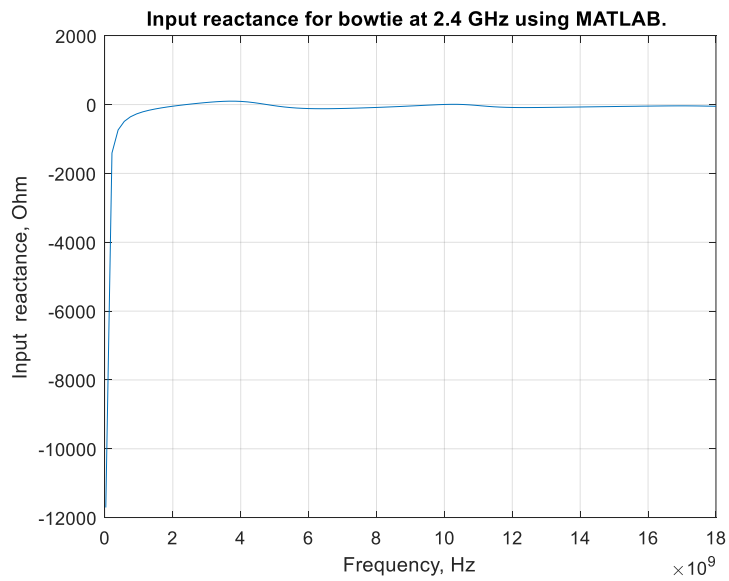
At the top of the script `rwg1.m`, the study gives the mesh file name as `bowtie` in order to acquire the frequency characteristics of the bowtie antenna. Additionally, the calculations are the same as those for a dipole antenna.

#### **Input Impedance**

First, the scripts `rwg1.m` and `rwg2.m` are executed. In the script `rwg3.m`, the frequency range of 25 MHz to 18 GHz is selected. The script `sweepplot.m` outputs the data for the input impedance of the bowtie as illustrated in figure (3.12) after the script `rwg3.m` has been executed.



a)



b)

Figure (3.12) Bowtie input impedance as a function of frequency. The flare angle is  $67.38^\circ$ .

It is clear that the bowtie's impedance characteristics are far smoother than those of the dipole. The behavior of the reactance, which has a nearly constant negative value

(capacitive reactance) in the range of 1.5 to 5 GHz, is very attractive.

The bowtie antenna is known for its wideband characteristics and relatively smooth

impedance behavior. The bowtie shape, with its open geometry and wide aperture,

lends itself to wideband operation. The smooth impedance characteristics observed in the bowtie antenna's impedance curve make it an attractive choice for broadband applications, including many wireless communication systems.

In antenna design, a smoother impedance curve is often desirable because it indicates that the antenna's impedance (both resistance and reactance) remains relatively consistent across a frequency range. Smooth impedance characteristics are essential for impedance matching, which ensures that the antenna efficiently transfers power to and from the transmission line or feed system. The observation of nearly constant negative reactance (capacitive reactance) in the frequency band of 1.5 to 5 GHz is significant. Capacitive reactance means that the antenna's impedance appears as though it has a capacitive component, which can be thought of as a virtual capacitor in parallel with the antenna. This behavior can have specific advantages:

### **Impedance Matching**

A capacitive reactance in the impedance curve can be counteracted with an inductive component to achieve better impedance matching. This helps improve the antenna's performance by ensuring that the impedance seen by the feed system closely matches the characteristic impedance of the transmission line (e.g., 50 ohms).

### **Wideband Operation:**

The presence of a nearly constant capacitive reactance in a specific frequency band, as observed in the 1.5 to 5 GHz range, can contribute to the antenna's wideband characteristics. Wideband antennas can operate

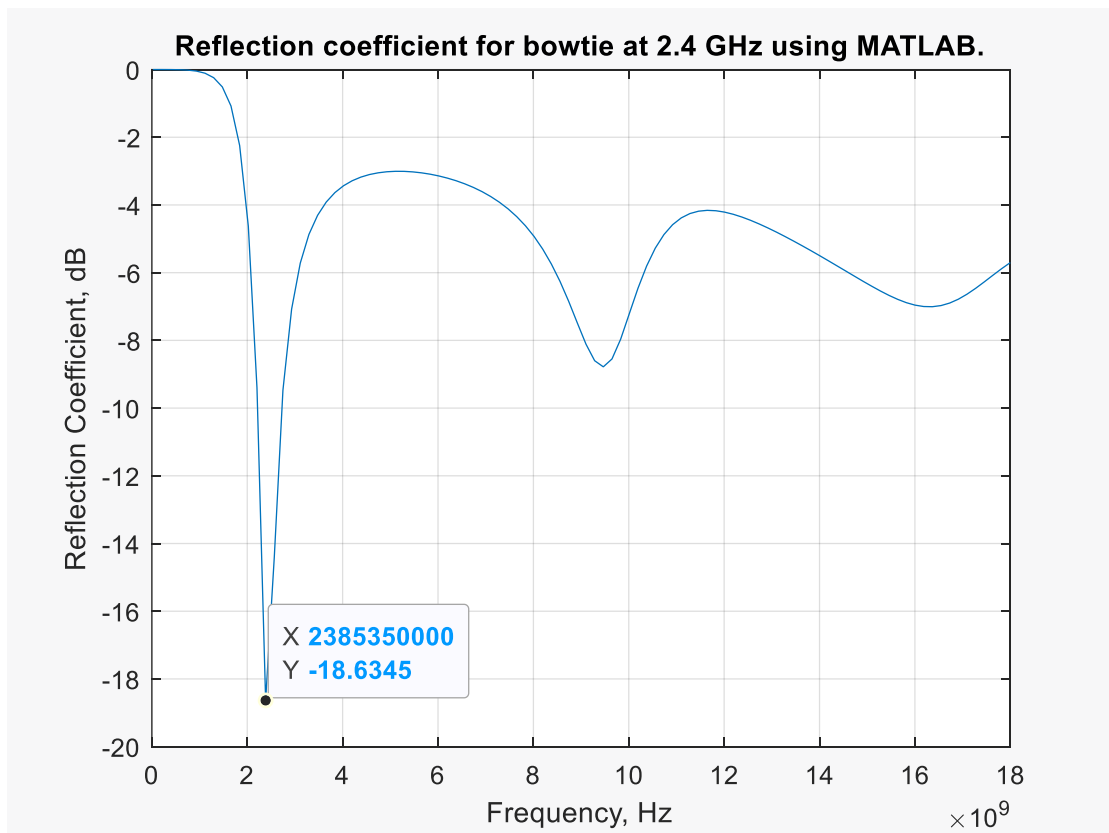
effectively over a broad range of frequencies, making them versatile for various communication standards and frequency bands.

The flare angle plays a crucial role in determining the impedance, behavior and radiation characteristics of a bowtie antenna. The flare angle refers to the angle at which the arms of the bowtie open up from their central axis. The flare angle can impact the behavior of the antenna's reactance component (capacitive or inductive). Depending on the specific design and flare angle, the reactance may vary across the frequency band of interest. Careful selection of the flare angle can help achieve desired reactance characteristics, such as capacitive or inductive reactance in specific frequency ranges. Also, the flare angle affects the physical size of the bowtie antenna. A wider flare angle generally results in a larger antenna, while a narrower flare angle can lead to a more compact design. The choice of flare angle should align with the available space and application requirements. In conclusion, the flare angle is an important design parameter for bowtie antennas. It affects impedance matching, resonance frequency, bandwidth, radiation pattern, reactance behavior, physical size, and overall antenna performance significantly. The proper flare angle must be chosen in order to optimize the antenna for its intended purpose and frequency range.

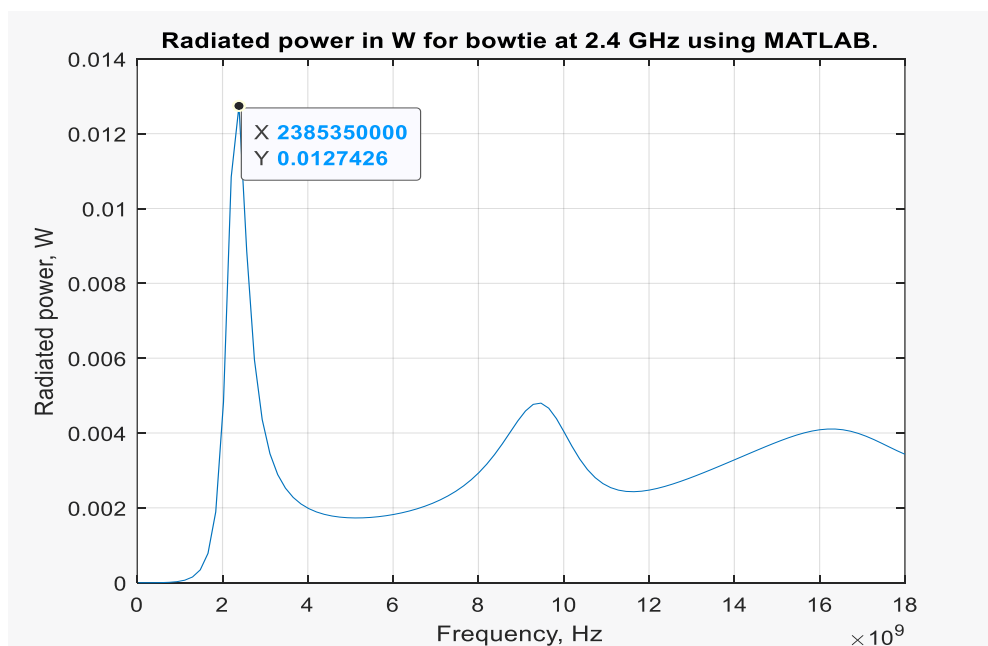
### **3.3.6 Bowtie Radiated Power, Reflection Coefficient and Gain**

The script `efield2.m` should be conducted following the script `rwg3.m` to acquire the total radiated power and gain as a function of frequency, and the result is viewed using the script `sweepplot.m`, as illustrated in Figure 3.13. For the current bowtie antenna with flare angle 90, only one power resonance can be identified. When the antenna length/wavelength ratio is slightly less than 1:3, this resonance occurs. The initial resonance is highly developed, with a high output power of around 0.0127 W recorded at the resonance. The bowtie

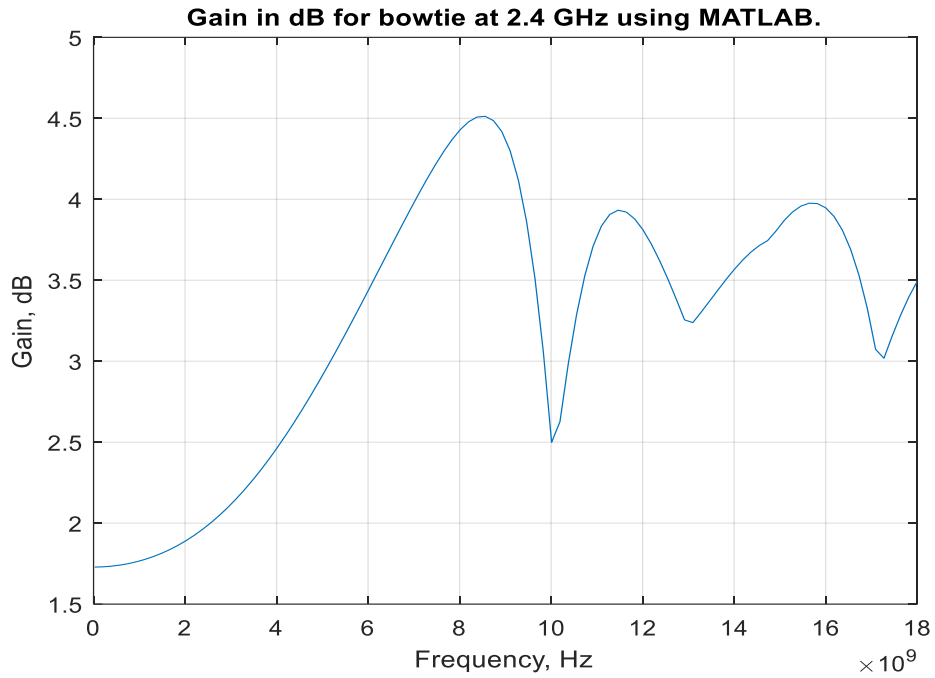
gain ranges from 2 to 4.5 dB. When the frequency is increased, the output power exhibits moderate fluctuations and increases in general.



a)



b)



c)

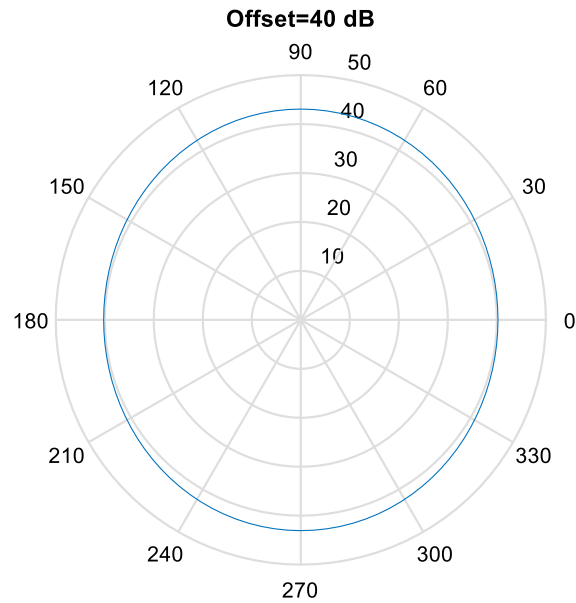
Figure (3.13) Performance of the constructed bowtie antenna using MATLAB (a) Reflection coefficient, (b) Radiated power, (c) Gain.

The harmonic current is reflected back and forth from the dipole ends in the case of the dipole antenna. The current in a bowtie antenna is dispersed over a vast area and finally dissipates into the radiated field before reaching the antenna's end. The same holds true for a thick cylindrical dipole or a sheet dipole. As a result, reflections at the antenna's end are significantly decreased, making the bowtie antenna an appealing virtually no resonant shape attractive for both broadband and UWB applications.

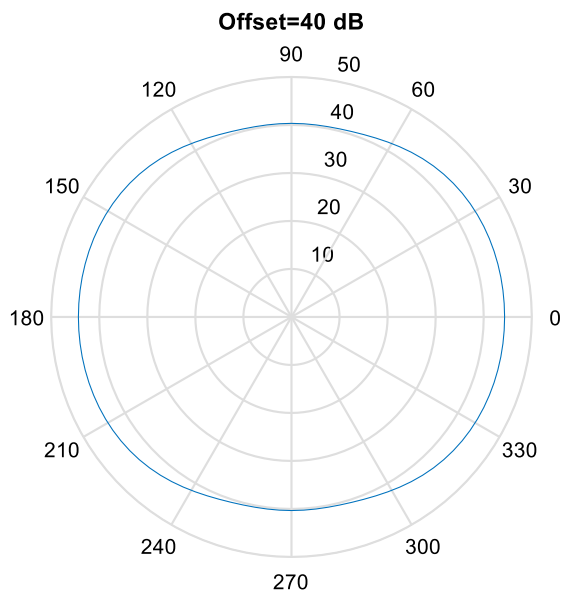
### 3.3.7 Bowtie Radiation Pattern

Following the completion of the two frequency loops (rwg3.m and efield2.m), the scripts rwg5single.m, efield2single.m, and efield3single.m display the antenna parameters at any frequency within the bandwidth. At the start of each code, the desired frequency should be set.

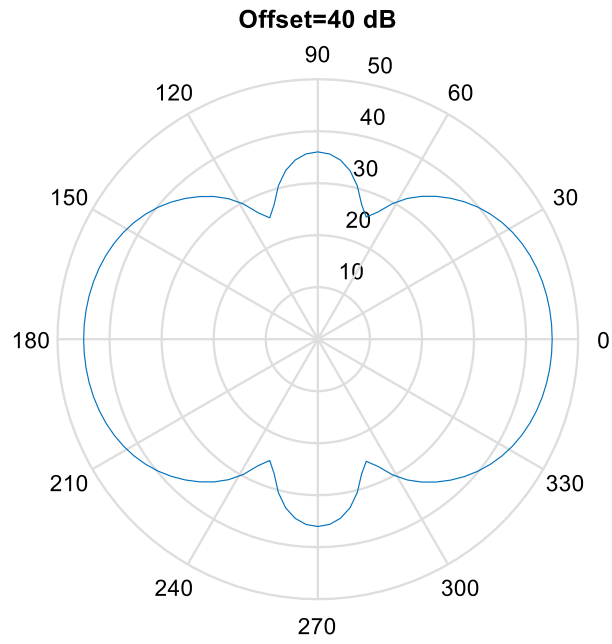
This is seen in Figure (3.14) that the result at 1 and 2 GHz implies a nearly omnidirectional radiation pattern with very little directivity variation. However, the results at 3 and 4 GHz are far from satisfactory.



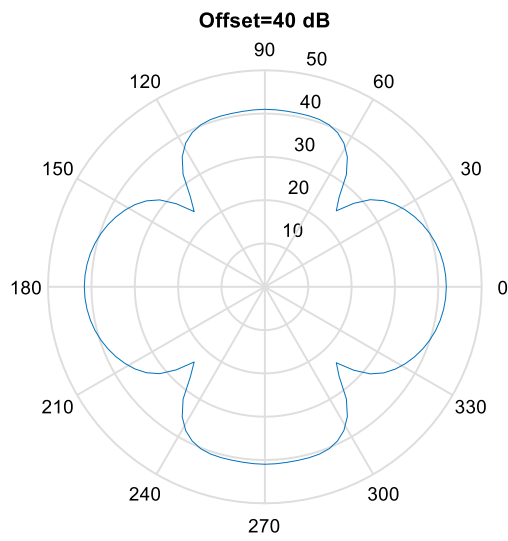
a) At 1 GHz



b) at 2 GHz



c) at 3 GHz



d) at 4GHz

Figure (3.14) Radiation Pattern of the Bowtie Antenna at four different frequencies in the xz-plane.

It is worth noting that the bowtie geometry explored here easily stretched to one of the simplest fractal antennas: the Sierpiniski fractal antenna or Sierpiniski gasket. The Sierpiniski fractal is essentially a bowtie with a carefully designed hole structure as seen in the next chapter.

### **3.3.8 Bow-tie Applications**

Bowtie antennas are used in various applications, including:

- Because of their wideband features, they are often employed for receiving over-the-air TV transmissions.
- Bowtie antennas are commonly employed in Wi-Fi routers, cell phone base stations, and other wireless communication devices.
- Radar systems: They are employed in radar applications including weather radar and military radar.
- EMC (Electromagnetic Compatibility) testing: Due to its broad performance, bowtie antennas are frequently used as reference antennas for EMC testing.
- Multiple bowtie pieces can be combined to form arrays, which can improve their performance in specialized applications like phased array radar systems.

Bowtie antennas have indeed found applications in various high-frequency and millimeter-wave systems, including superconducting tunnel junctions, Schottky diode mixers, linear imaging arrays, and these systems have been applied in fields such as plasma diagnostics and radio astronomy [34].

In conclusion, the bowtie antenna is an adaptable and popular solution for wideband RF and microwave applications. Its distinct bowtie-shaped form enables it to work efficiently across long distances.

## Chapter Four

### **Design and Analysis of Bowtie Fractal Antenna by Sierpiniski.**

#### **4.1 Bowtie Fractal Antenna by Sierpiniski.**

The Sierpiniski bowtie fractal antenna is the third developed antenna in this dissertation. The Sierpiński fractal bowtie is created by starting with a triangle. The primary construction rule is to divide the triangle into smaller triangles and then remove the middle triangle from each group of three. The height, width, and distance are all equal to the bowtie dimension. This method is performed indefinitely on the remaining smaller triangles.

#### **4.2 Sierpinski Triangle/Gasket:**

Using Sierpinski fractal shapes in the design of a bowtie antenna can indeed be a fascinating and innovative approach to regulate its multifrequency response. Sierpinski fractals are self-replicating geometric patterns that can be used in antenna design to achieve various objectives [47].

The interaction of electromagnetic waves with fractal objects has indeed been a subject of interest in recent research, and it has led to various intriguing findings and applications. Fractal objects, characterized by their self-similar and self-replicating geometric properties, introduce unique electromagnetic behaviors that differ from those of traditional Euclidean shapes [48].

The Sierpinski gasket is named after the mathematician Sierpinski who described some of the most important characteristics of this fractal structure in 1916, three equal triangles remain on the construction, each of these half size of the original. It is possible to execute the same subtraction method on the remaining triangles an endless number of times to create the ideal fractal Sierpinski gasket.

Each of the three gaskets that comprise any of the three main components in

such an ideal construction is exactly equal to the total thing, but scaled by a factor of two, because of these resemblance qualities, which are shared by many other fractal designs, the Sierpinski gasket is said to be a self-similar structure as shown in Figure (4.1).

The Sierpinski gasket exhibits several intriguing fractal properties, including self-similarity, which means that smaller parts of the pattern resemble the entire pattern. It also has a non-integer fractal dimension, which quantifies its space-filling properties and complexity.

The Sierpinski gasket is not only a fascinating mathematical concept but also has practical applications in various fields. It is often used in mathematics education to introduce the concept of fractals and self-similarity. Additionally, it has found applications in signal processing, image compression, and even antenna design, where it can be used to create fractal antennas with unique electromagnetic properties [48].

The scaling factor in the Sierpinski gasket is  $1/2$ . This means that at each iteration, the size of the remaining triangles is halved compared to the previous iteration.

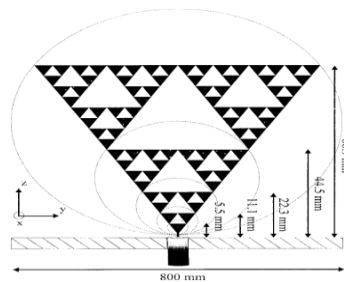


Figure (4.1) Sierpinski's monopole. A scaled-down representation of the entire structure may be seen in each sub gasket (circled) [48].

### **4.3 Affine Transformations**

Affine transformations are a type of transformation that includes translation, rotation, scaling, and shearing. These changes are expressed as mathematical equations in the context of IFS. Each transformation is specified by a set of parameters that govern how the position and size of points in space are altered.

### **4.4 Collection of Transformations:**

A set of these affine transformations defines an IFS. An IFS often contains numerous such transformations, each with its own set of parameters. These transformations represent various methods for changing the position of points in space.

### **4.5 Iterative Process:**

The process of constructing a fractal using an IFS entails beginning with a single point or set of points and continually applying transformations from the collection. Every point in the collection is transformed by each transformation in the collection at each iteration, resulting in a new set of points.

### **4.6 Weights:**

Each transformation in the IFS collection may have a weight associated with it that determines the likelihood of that transformation being selected throughout the iteration. The weights are used to influence the look and distribution of points in the fractal.

### **4.7 Contraction Property:**

The transformations in the IFS collection must satisfy a contraction property in order to build fractal structures. This means that the transformations, on

average, shrink the size of the points with each repetition, resulting in self-similarity and the production of fractal patterns.

These iterated function systems are built using a series of affine transformations,  $w$ , described by

$$w \begin{pmatrix} x \\ y \end{pmatrix} = \begin{pmatrix} a & b \\ c & d \end{pmatrix} \begin{pmatrix} x \\ y \end{pmatrix} + \begin{pmatrix} e \\ f \end{pmatrix}, \quad (3.18)$$

or, equivalently, by:

$$w(x, y) = (ax + by + e, cx + dy + f), \quad (3.19)$$

where  $a$ ,  $b$ ,  $c$ ,  $d$ ,  $e$ , and  $f$  are all real numbers. As a result, the affine transformation,  $w$ , has six parameters.

$$\left( \begin{array}{cc|c} a & b & e \\ c & d & f \end{array} \right),$$

Rotation and scaling are controlled by  $a$ ,  $b$ ,  $c$ , and  $d$ , whereas linear translation is controlled by  $e$  and  $f$ .

Assume that  $w_1, w_2, \dots, w_N$  are a collection of affine linear transformations, and that  $A$  is the original geometry. Then, a new geometry can be represented by applying the set of transformations on the old geometry,  $A$ , and collecting the results from  $w_1(A), w_2(A), \dots, w_N(A)$  can be represented by

$$W(A) = \bigcup_{n=1}^N w_n(A), \quad (3.20)$$

W stands for the Hutchinson operator. By continually applying W to the prior geometry, a fractal geometry can be generated. For instance, if set 4 represents the initial geometry, we will have

$$A_1 = W(A_0), A_2 = W(A_1), \dots, A_{k+1} = W(A_k). \quad (3.21)$$

For fractal antenna designers, iterated function systems have shown to be a highly powerful design tool. This is partly due to the fact that they provide a general framework for fractal description, classification, and manipulation. Figure (4.2) shows the iterated function system code for such different objects as a Sierpinski gasket.

<b>a</b>	<b>b</b>	<b>c</b>	<b>d</b>		<b>e</b>	<b>f</b>
<b>0.500</b>	<b>0.000</b>	<b>0.000</b>	<b>0.500</b>		<b>0.000</b>	<b>0.000</b>
<b>0.500</b>	<b>0.000</b>	<b>0.000</b>	<b>0.500</b>		<b>0.500</b>	<b>0.000</b>
<b>0.500</b>	<b>0.000</b>	<b>0.000</b>	<b>0.500</b>		<b>0.000</b>	<b>0.500</b>

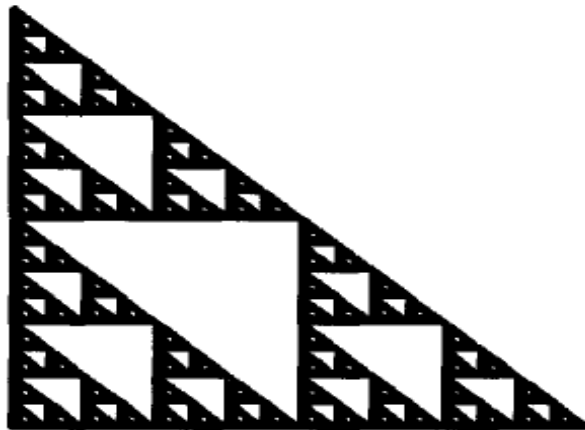


Figure (4.2) The code for an iterated function system for a Sierpinski gasket [42].

At the end of IFS can said Iterated Function Systems offer a powerful and adaptable foundation for creating fractal structures that are not only mathematically interesting but also have practical uses in computer graphics,

art, data compression, and simulating complicated natural processes. They are a key topic in the study of fractal geometry.

#### **4.8 Flare Angle and its effected-on Antenna Performance**

The band characteristics of antennas, including bowtie antennas, can be changed by varying the flare angle of their radiating elements. The flare angle refers to the angle at which the antenna's radiating elements open or spread apart from their central axis.

Varying the flare angle can influence the bandwidth of the antenna. A wider flare angle can lead to a broader bandwidth, allowing the antenna to operate effectively over a range of frequencies. This can be advantageous for applications that require frequency agility or wideband operation.

The flare angle can also impact the impedance characteristics of the antenna. It may affect the input impedance and the antenna's ability to match the impedance of the transmission line or the connected equipment. Adjusting the flare angle can help achieve better impedance matching for optimal power transfer.

The flare angle can influence the resonant frequency of the antenna. By modifying the angle, one can shift the antenna's resonant frequency higher or lower. This can be useful for tuning the antenna to a particular frequency of interest [49].

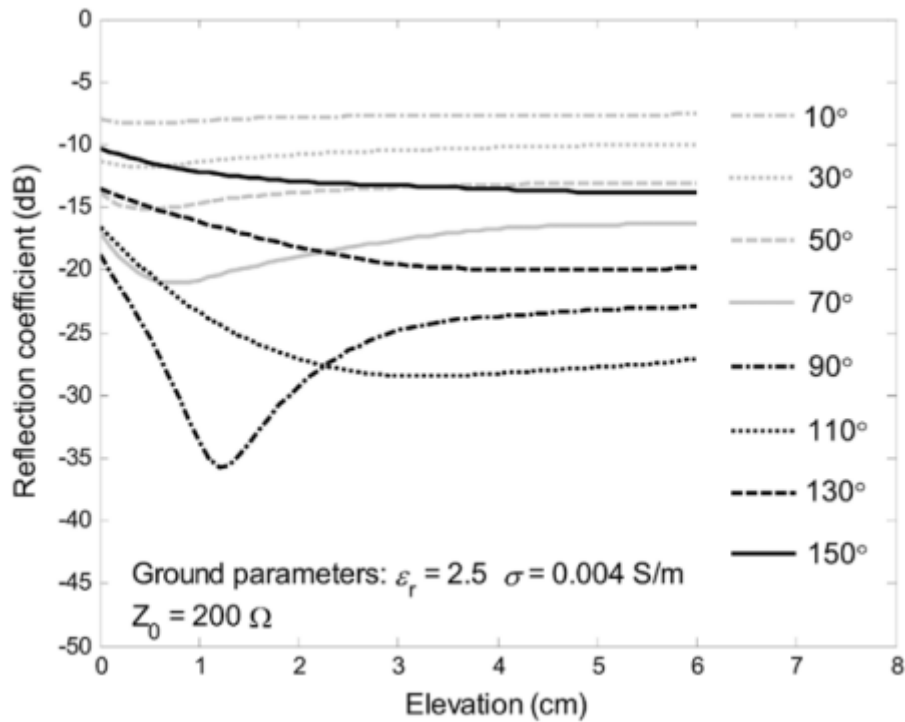


Figure (4.3) Computed reflection coefficients of the adaptive wire bow-tie antenna as functions of antenna elevation for the eight possible effective flare angles [49].

The polarization of the antenna's radiation can be controlled by adjusting the flare angle. Different flare angles can result in either linear or circular polarization, allowing the antenna to match the polarization requirements of a communication system [50]

The directivity or radiation pattern of the antenna can be affected by the flare angle. A narrower flare angle tends to produce a more focused and directional radiation pattern, while a wider flare angle can result in a more omnidirectional pattern. Designers can choose the flare angle to suit the specific radiation pattern requirements of their application [51]

The gain of the antenna, which quantifies its ability to focus radiation in a particular direction, can be controlled by altering the flare angle. A well-

designed antenna can achieve the desired gain by choosing an appropriate flare angle.

The overall size and form factor of the antenna can be affected by the flare angle. A wide flare angle may lead to a physically larger antenna, while a narrow flare angle can result in a more compact design.

When designing an antenna and adjusting its flare angle, it is essential to consider the specific requirements of the application, including the desired frequency range, radiation pattern, and impedance matching. Antenna simulation tools and modeling software can be helpful in predicting how changes in the flare angle will impact the antenna's performance, allowing for more precise design and optimization [44].

#### **4.9 Fractal Sierpiniski Antenna Design and Simulation Using MATLAB.**

This type of antennas will be designed using MATLAB software at 2.4 GHz as shown in Figure (4.4). The feeding edge is always at the origin.

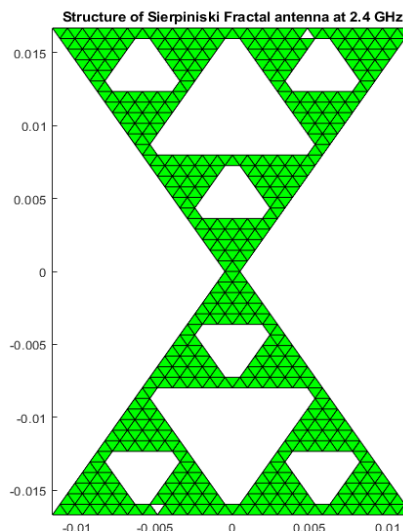


Figure (4.4) Designed Fractal multiband bowtie at second iterations.

antennas using MATLAB simulation.

The MATLAB script fractal .m was utilized to produce a bowtie-shaped Sierpinski gasket as seen in figure (4.5). The script was evaluated using the fractal growth stages  $S=1,2,3$ .

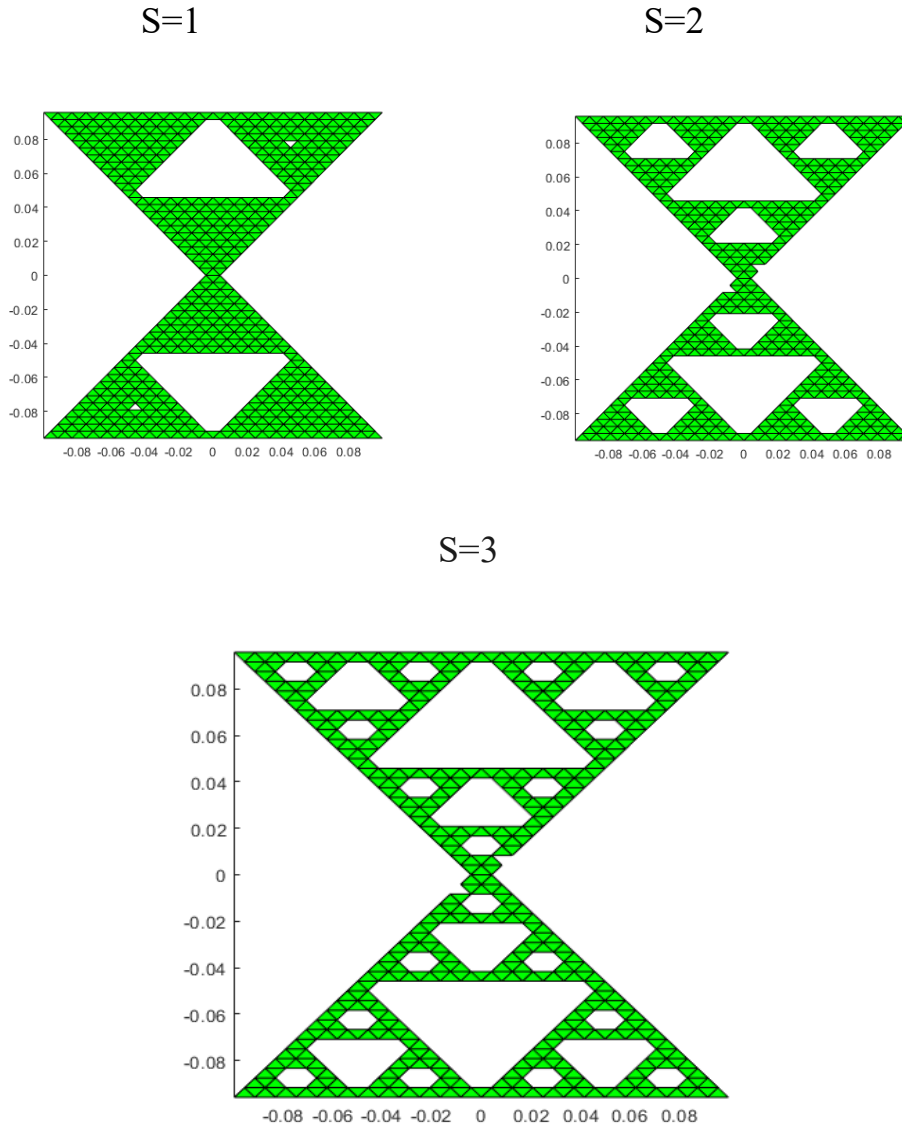


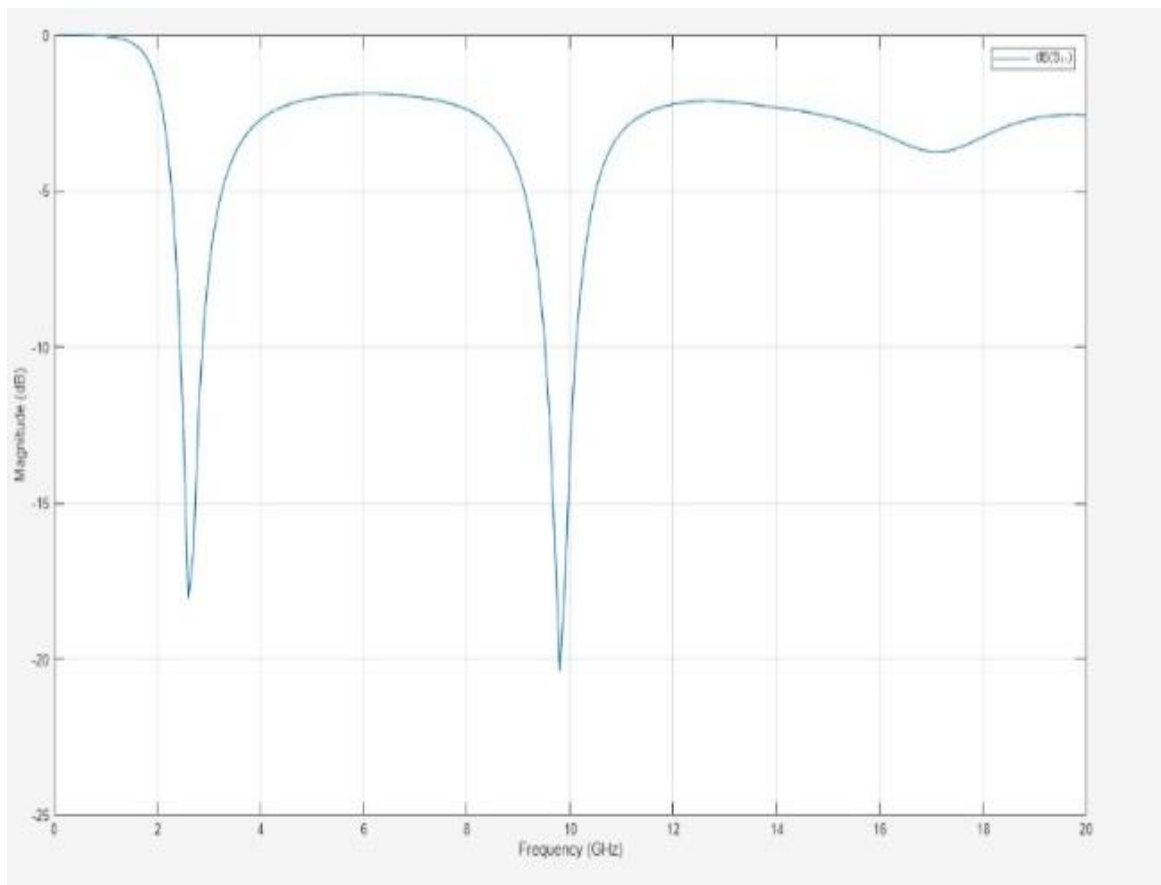
Figure (4.5) Geometry of the Bowtie Fractal Antenna.

#### 4.9.1 Sierpinski Fractal's Reflection Coefficient and radiated Power.

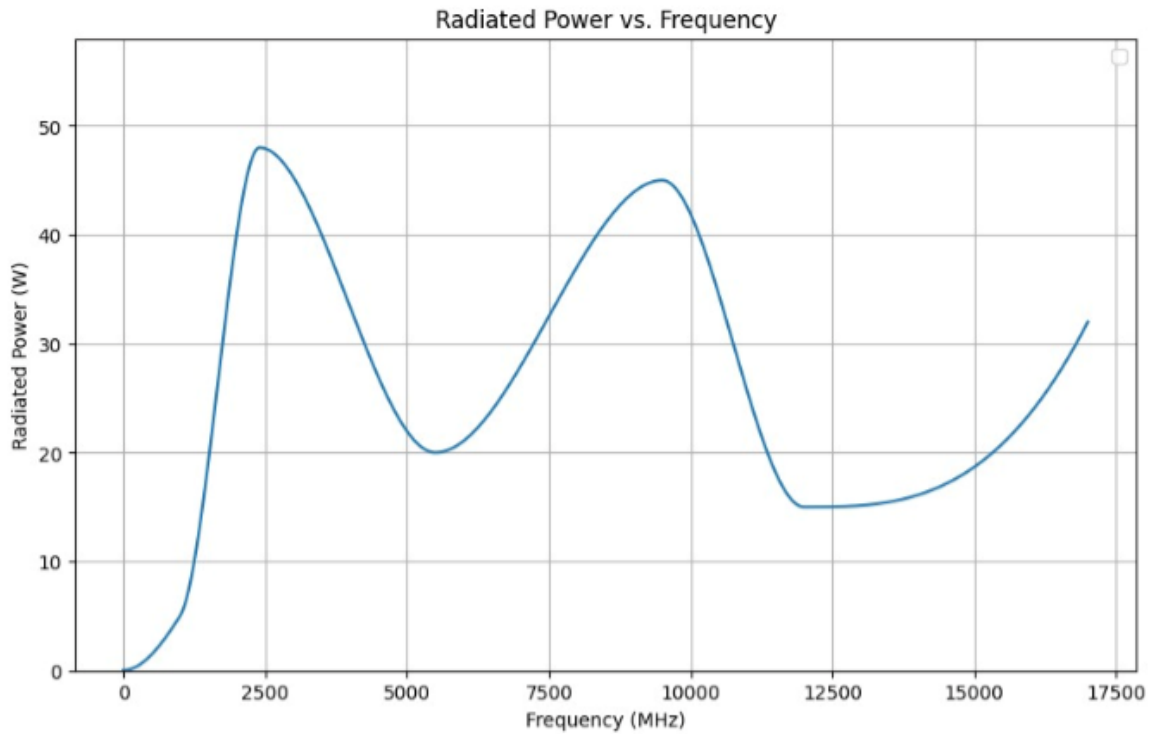
At the top of script rwg1.m, the study specifies the mesh file name as fractal in order to acquire the frequency characteristics of the fractal antenna.

Then, the scripts `rwg1.m` and `rwg2.m` are run. The antenna is around the same size as a bowtie antenna.

The frequency range from 0.025 to 20 GHz is covered by the frequency band in the `rwg3.m` script. The data from the reflection coefficient, radiated power of the fractal antenna are output by the script `sweelot.m` as depicted in Figure (4.6) (a) and (b).



a) Reflection Coefficient of Sierpiniski Fractal Antenna Using MATLAB.



b) Radiated power of Sierpinski Fractal Antenna Using MATLAB.

Figure (4.6) Reflection Coefficient and Radiated Power of multiband fractal antenna.

The multi-band behavior of the fractal is not yet characterized in the analysis of impedances. We are particularly interested in resonances where the antenna radiates at its maximum power with zero input reactance. Additionally, the multi-band behavior will be established if the input resistance at these resonances is adequately matched to a 50-ohm load.

Therefore, the number of resonances is equal to the fractal stage number ( $S = 2$ ) plus one. The initial resonance, which corresponds to  $f_1$ , is that of the pure bow-tie equal to 2.4 GHz. Whether the fractal structure is present or not, this resonance takes place. The first fractal iteration corresponds to the second resonance at  $f_2 = 9.2$  GHz, and the third resonance is at  $f_3$ . The second iteration of the fractal is at  $= 17.4$  GHz. The ratios of frequencies.

Since the scale factor relating triangle size at each step of expansion is 2, the resonant bands are consequently log-periodically spaced apart by a factor of 2. The magnitude of the reflection coefficient to a logarithmic scale is displayed versus in Figure (4.6)(a).

The study can construct a well-matched antenna at these power resonances because the study has observed that the coefficient minima are strongly related to the power resonances.

#### 4.10 Fractal Sierpiniski Antenna Design and Simulation Using CST Software.

In this dissertation, the fragmentation process is repeated two times which corresponds to the second iteration fractal antenna as shown in Figure (4.7), where the first one represents the original bowtie antenna without fractal structure while the second one represents the fractal bowtie at first iteration and the third one represents the fractal bowtie at the second iteration.

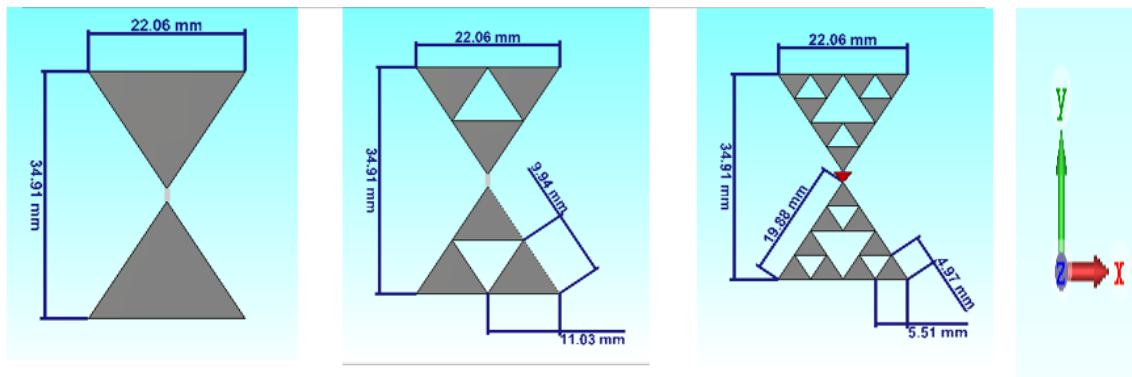
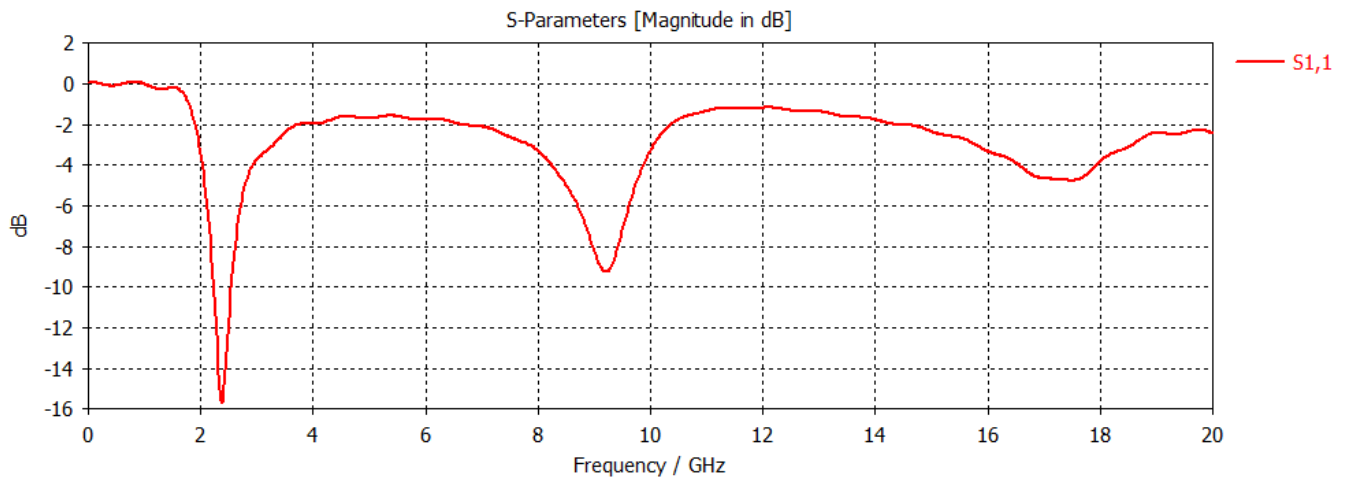


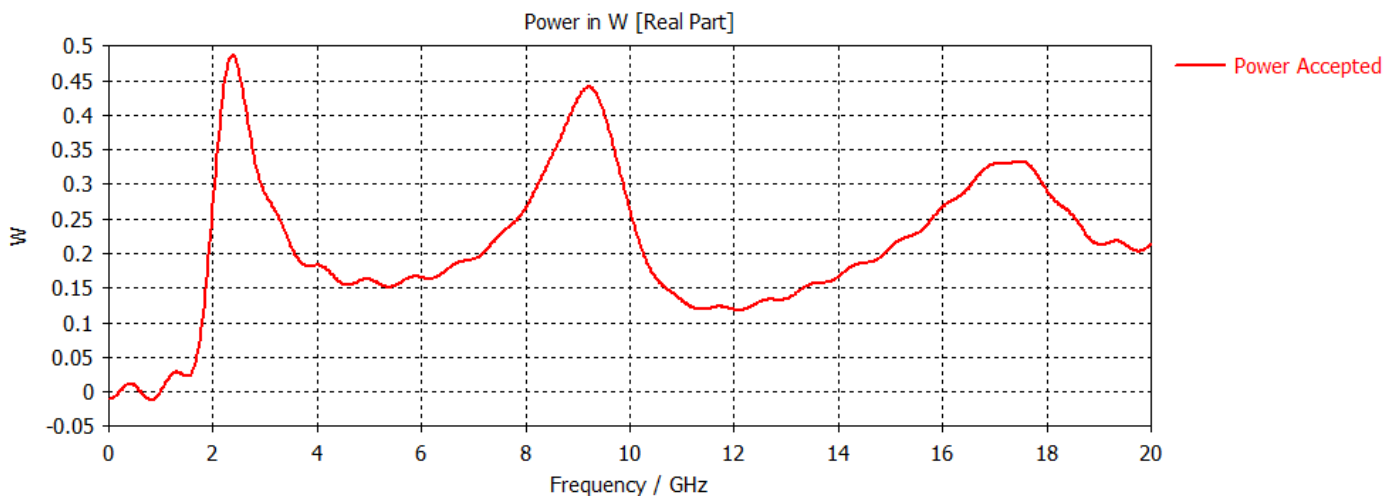
Figure (4.7) Fractal Multiband Bowtie at various iteration using CST software in xy-plane.

It can be seen from Figure (4.7) that the Sierpiński triangle exhibits self-similarity because each smaller copy of itself is similar to the overall structure. Also, the feeding edge is always at the origin.

The CST full-wave modeling is used to construct these three antennas at the designed frequency of 2.4 GHz. The reflection coefficient, radiated power as a function of frequency for the fractal bowtie antennas are shown in Figure (4.8).



a) Reflection coefficient for Sierpiniski fractal antenna (s11)



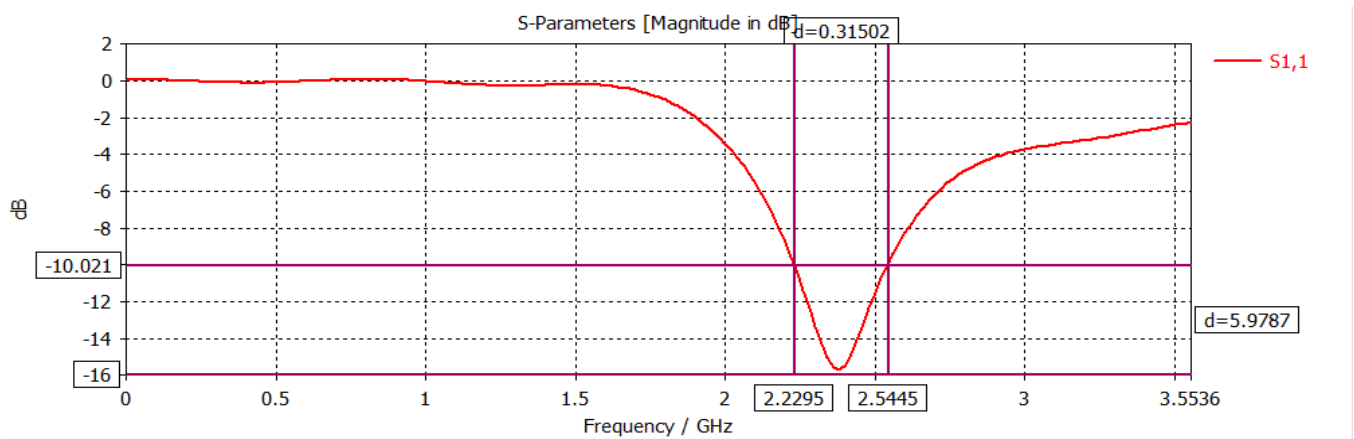
b) Radiated power in Watt for Sierpiniski Fractal antenna with frequency.

Figure (4.8) Performance of designed Sierpiniski Fractal Antenna.

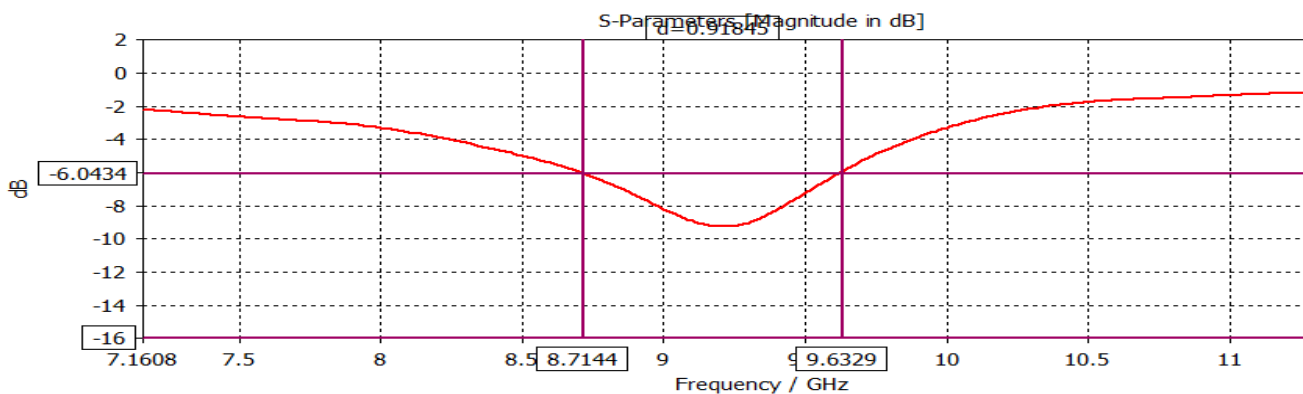
From above figure (4.8) a) observed three resonant frequencies at 2.4 GHz the reflection coefficient reached to -15 dB, at 9.2 GHz the reflection coefficient reached to -9.2 dB, at 17.4 GHz reached to -4.2GHz.

From figure (4.8) b) the power reached to 0.5 W at 2.4 GHz and reached to 0.45 W at 9.2 GHz, at 17.4 GHz the power reached to 0.3 W.

The beamwidth of a fractal antenna is 0.3 GHz at first iteration, the beamwidth (-6 dB) at second iteration equal to 0.9 GHz.



a) The B.W curve at first iteration of Sierpinski fractal antenna.



b) The B.W curve at second iteration of Sierpinski fractal antenna.

Figure (4.9) The B.W curve at first and second iteration of Sierpinski fractal antenna.

From figure (4.9) it seems that B. W of the second null is about three times of first null at -6dB (some authors compute B.W at this value). Next, the reflection coefficient of three antennas will be compared in the same figure.

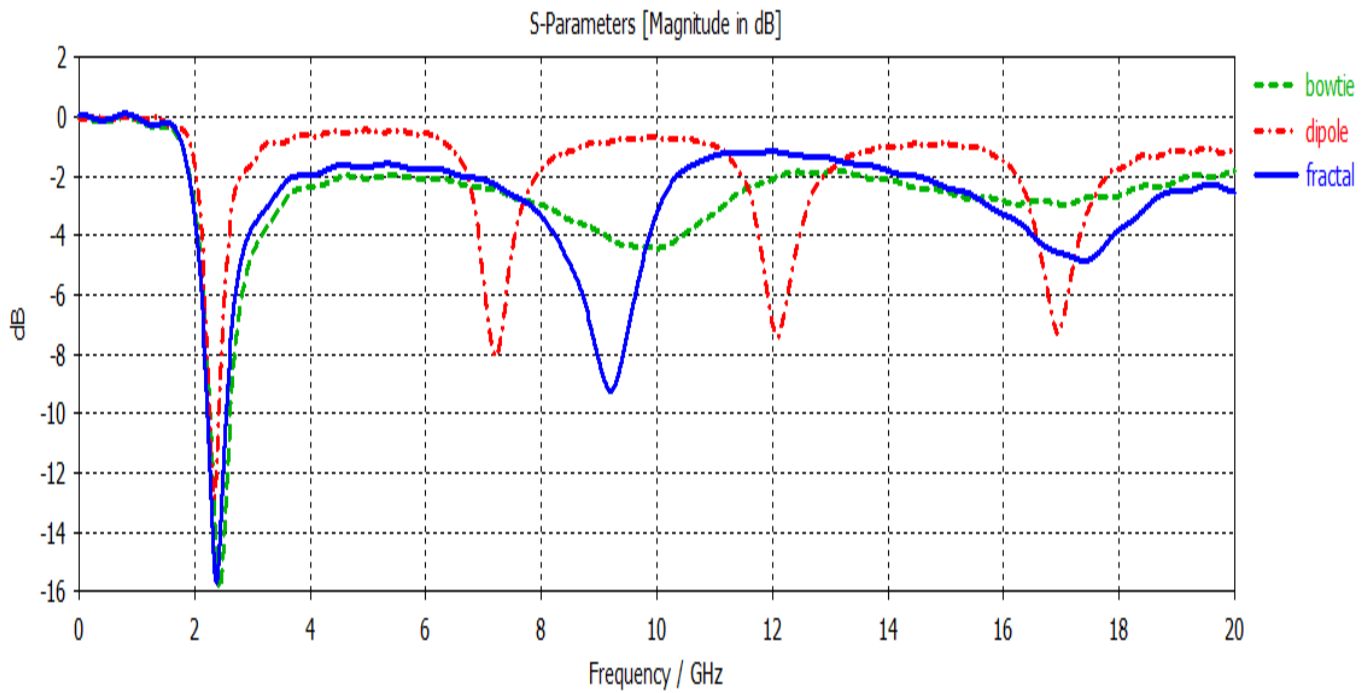


Figure (4.10) Reflection Coefficient of Three Designed Antennas under study using CST.

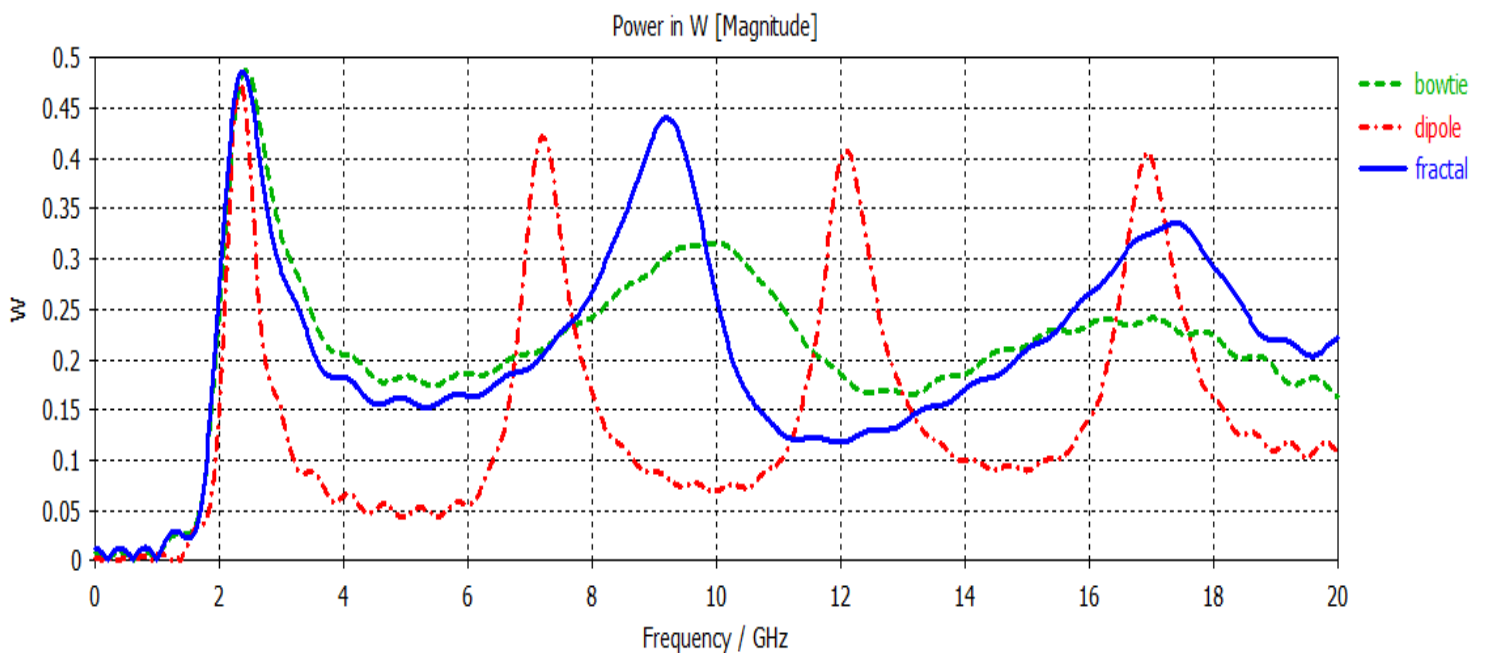


Figure (4.11) Radiated powers of the designed three antennas using CST.

From the results of Figures (4.10) and (4.11), it can be observed that the dipole antenna is a narrow band antenna and it has a fine tune at the resonance frequency of 2.4 GHz. To be noted that there are other resonance frequencies

at 7.3 GHz, 12.0 GHz and 17.0 GHz due to the dipole behavior repeating at the multiple integers. The slope of the power curve becomes smoother when one increases the dipole thickness. Thus, the dipole is treated as a typical resonant antenna. It has strongly oscillated gain that exhibit peak at each multiple integers of the resonance frequency and it cannot be treated as a broadband antenna. From figure (4.11), it can be observed that only one power resonance can be identified for the constructed bowtie antenna with flare angle  $=67.38^\circ$ . This resonance occurs when the antenna length/wavelength ratio is slightly smaller than 1:3. As expected, the first resonance of the fractal bowtie antenna is fine-tuned at 2.4 GHz which is strongly coincidence with that of the original bowtie antenna and its output power peak of about 0.48W is observed at the resonance. The antenna size at the second iteration of the fractal bowtie antenna is approximately equal to the size of the original bowtie antenna where the width is same 34.91 mm whereas the height is 22.06 mm. The frequency band is chosen to cover the range from 0 to 20 GHz. The radiated power of the fractal bowtie antenna (blue color) clearly shows its effectiveness in radiating the wanted powers at the three multiband frequencies. The designed fractal bowtie antenna at the growth stage of 2 has three resonance bands at 2.4 GHz, 9.2 GHz, and 17.4 GHz respectively. The first resonance corresponds to that of the original bowtie antenna which is  $f_1=2.4$  GHz. This resonance always occurs whether or not the fractal structure is present. The second resonance at  $f_2=9.2$  GHz corresponds to the first fractal iteration, and the third resonance at  $f_3=17.4$  GHz corresponds to the second fractal iteration.

From table (4.1) below it can be seen that the reflection coefficient is equal for three antennas with very slight offsets, the reflection coefficient of the bowtie antenna is more than the reflection coefficient of the dipole antenna by an amount 3 dB, but it is similar for the fractal antenna because calculated it at the first iteration, at the same triangle and the same

dimensions. The same applies to radiated power. A half-wave dipole in free space has a theoretical maximum gain of approximately 2.15 dBi [32]. The gain of the dipole antenna in this dissertation by using CST equal to 1.778 dBi and about 1.639 dBi for bowtie and fractal.

Despite their structural differences, both dipole and bowtie antennas can attain identical radiation patterns, directivity, and efficiency and gain when tuned for the same operating frequency. The bandwidth of the bowtie antenna is twice the bandwidth of the dipole antenna, the bowtie's main benefit is its larger bandwidth but equal to the fractal at first iteration. The fractal bowtie antenna is also not a broadband but rather a multiband antenna.

Table 4.1 summarizes and compares between the performances of the three investigated antennas under study.

<b>Performance Measurement</b>	<b>At Resonance Frequency Band</b>		
	<b>Dipole</b>	<b>Bowtie</b>	<b>Fractal</b>
<b>Reflection Coefficient (dB)</b>	-12.865	-15.77	-15.23
<b>Gain (dBi)</b>	1.778	1.639	1.6
<b>Radiated power (Watt)</b>	0.44	0.486	0.48
<b>Bandwidth (GHz)</b>	0.1534	0.3522	0.3 at 1 <sup>st</sup> iteration

## Chapter Five

### CONCLUSIONS AND FUTURE WORK

#### 5.1 CONCLUSIONS

Three different antennas namely narrowband, wideband and multiband have been constructed and analyzed using both the method of moment in MATLAB and the full-wave modelling in CST to verify their performances

The investigations have revealed the following conclusions:

- 1- Bowtie shape has been used and is recognized for having a wider bandwidth in antenna applications when compared to thin dipole antennas.
- 2-In both simulation methods, an original bowtie antenna was designed and then efficiently and simply modified to obtain multiband fractal bowtie properties, by applying the fractal structures on the original broadband bowtie antenna.
- 3-multiband behavior can be obtained and the total number of the tuned frequency depends directly on the number of the formed fractal structures. Thus, the proposed fractal bowtie can be considered as a reconfigurable antenna according to the desired multiband operation.
- 4- second iteration stage of growth was applied; thus, two extra resonance frequencies were obtained as well as the original tuned frequency. Results of the constructed fractal bowtie showed that it has three frequency bands at 2.4 GHz, 9.2 GHz and 17.4 GHz.
- 5- The use of the fractal structures with the bowtie antenna provides the ability to precisely control the spacing of operating frequencies, achieving repeated resonances between bands. Thus, the proposed fractal antenna offers many advantages in terms of bandwidth utilization, multiband Operation.

- 6- The proposed fractal antenna can be effectively used in the applications that span different frequency ranges in which stable performance characteristics are needed.

## **5.2 Future Works**

This research work can be further investigated the following:

1. It is possible to investigate and study other antenna shapes that have some common geometrical features that can be exploited in constructing the initial and the successive fractal stages. One promising shape can be circular or sierpiniski carpet.
2. For higher frequencies, there will be rising some difficulties in the implementation issues of the fractal antennas. This can be further investigated by employing these antennas in the mm wave applications.
3. Incorporating both wideband and multiband operations in a single antenna design.
4. Using fractal antenna arrays instead of a single antenna element to increase the overall directivity and many other radiation characteristics.

## References

- [1] Sharma, Nitika, Simranjit Kaur, and Balwinder S. Dhaliwal. "A new triple band hybrid fractal boundary antenna." 2016 IEEE International Conference on Recent Trends in Electronics, Information & Communication Technology (RTEICT). IEEE, 2016.
- [2] Weng, Wei-Chung, and Chia-Liang Hung. "An H-fractal antenna for multiband applications." *IEEE Antennas and Wireless Propagation Letters* 13 (2014): 1705-1708.
- [3] Jena, Manas Ranjan, B. B. Mangaraj, and Rajiv Pathak. "Design of a novel sierpinski fractal antenna arrays based on circular shapes with low side lobes for 3G applications." *American Journal of Electrical and Electronic Engineering* 2.4 (2014): 137-140.
- [4] Song, C. T. P., Peter S. Hall, and Hooshang Ghafouri-Shiraz. "Perturbed Sierpinski multiband fractal antenna with improved feeding technique." *IEEE Transactions on Antennas and Propagation* 51.5 (2003): 1011-1017.
- [5] Shu, Lin, et al. "A novel semi-circle fractal multi-band antenna." 2008 2nd International Symposium on Systems and Control in Aerospace and Astronautics. IEEE, 2008.
- [6] Sayidmarie, Khalil H., and Yasser A. Fadhel. "UWB fractal monopoles of rectangular and triangular shapes." 2011 4th IEEE International Symposium on Microwave, Antenna, Propagation and EMC Technologies for Wireless Communications. IEEE, 2011.
- [7] Fadhel, Yasser A., and Haval N. Alsofi. "A planar self-complementary fractal triangular antenna for uwb applications." 2019 International Conference on Advanced Science and Engineering (ICOASE). IEEE,

- 2019.
- [8] Li, Daotie, and Jun-fa Mao. "A Koch-like sided fractal bow-tie dipole antenna." *IEEE Transactions on antennas and propagation* 60.5 (2012): 2242-2251.
- [9] Dorostkar, M. Ali, R. Azim, and M. T. Islam. "A novel  $\Gamma$ -shape fractal antenna for wideband communications." *Procedia Technology* 11 (2013): 1285-1291.
- [10] T. Tamilnadu, "Design of koch fractal bow tie antenna for wireless applications," *Int. J. Mob. Comput. Appl.*, vol. 1, no. 2, pp. 4–7, 2014, doi: 10.14445/23939141/ijmca-v1i2p102.
- [11] Kumar, N. Naresh, et al. "Compact modified Sierpinski fractal monopole antenna for multiband wireless applications." 2014 International Conference on Communication and Signal Processing. IEEE, 2014.
- [12] Srivastava, Sonam, Pooja Mishra, and Rajat Kumar Singh. "Design of a reconfigurable antenna with fractal geometry." 2015 IEEE UP Section Conference on Electrical Computer and Electronics (UPCON). IEEE, 2015.
- [13] Bhatia, Sumeet Singh, and Jagtar Singh Sivia. "A novel design of wearable fractal antenna for wideband applications." 2016 International Conference on Advances in Human Machine Interaction (HMI). IEEE, 2016.
- [14] Yu, Zhen, et al. "A novel ancient coin-like fractal multiband antenna for wireless applications." *International Journal of Antennas and Propagation* 2017 (2017).
- [15] Mishra, Guru Prasad, et al. "Study of Sierpinski fractal antenna and its

- array with different patch geometries for short wave Ka band wireless applications." *Procedia computer science* 115 (2017): 123-134.
- [16] Madhav, B. T. P., et al. "Compact metamaterial inspired periwinkle shaped fractal antenna for multiband applications." *International Journal of Engineering and Technology* 7.1.1 (2018): 507-512.
- [17] Kumar, Devesh, et al. "Performance analysis of meta-material based bow-tie shaped fractal antenna for THz application." 2017 7th International Conference on Cloud Computing, Data Science & Engineering-Confluence. IEEE, 2017.
- [18] Mondal, Tapas, et al. "Compact circularly polarized wide-beamwidth fern-fractal-shaped microstrip antenna for vehicular communication." *IEEE Transactions on Vehicular Technology* 67.6 (2018): 5126-5134.
- [19] Saharsh, S. B., and Sanoj Viswasom. "Design and Analysis of Koch Snowflake Fractal Antenna Array." 2020 Fourth International Conference on I-SMAC (IoT in Social, Mobile, Analytics and Cloud)(I-SMAC). IEEE, 2020.
- [20] Yu, Zhen, et al. "A Cloud-Structured Fractal Multiband Antenna for 4G/5G/WLAN/Bluetooth Applications." *International Journal of Antennas and Propagation* 2022 (2022).
- [21] Sultan, Qusai H., and Ahmed MA Sabaawi. "Design and implementation of improved fractal loop antennas for passive UHF RFID tags based on expanding the enclosed area." *Progress In Electromagnetics Research C* 111 (2021): 135-145.
- [22] Sabaawi, Ahmed MA, Qusai H. Sultan, and Tareq A. Najm. "Design and Implementation of Multi-Band Fractal Slot Antennas for Energy Harvesting Applications." *Periodica Polytechnica Electrical Engineering and Computer Science* 66.3 (2022): 253-264.

- [23] El-Khamy, Said E., Huda F. El-Sayed, and Ahmed S. Eltrass. "Synthesis of Wideband Thinned Eisenstein Fractile Antenna Arrays with Adaptive Beamforming Capability and Reduced Side-Lobes." *IEEE Access* 10 (2022): 122486-122500.
- [24] Rahim, Abdul, Praveen Kumar Malik, and Rajesh Singh. "Fractal geometry-based chakra-shaped microstrip patch antenna array for vehicular communications under 5G environments." *Journal of Information and Telecommunication* 6.4 (2022): 482-500.
- [25] Benkhadda, Omaima, et al. "A Miniaturized Tri-Wideband Sierpinski Hexagonal-Shaped Fractal Antenna for Wireless Communication Applications." *Fractal and Fractional* 7.2 (2024): 115.
- [26] Falconer, Kenneth. *Fractal geometry: mathematical foundations and applications*. John Wiley & Sons, 2004..
- [27] Gao, Fei, et al. "Low-profile dipole antenna with enhanced impedance and gain performance for wideband wireless applications." *IEEE Antennas and Wireless Propagation Letters* 12 (2013): 372-375.
- [28] Kuo, Fang-Yao, et al. "A novel dipole antenna design with an over 100% operational bandwidth." *IEEE Transactions on Antennas and Propagation* 58.8 (2010): 2737-2741.
- [29] Kaur, Baljinder, and Lakhvinder Singh Solanki. "A brief review on bowtie antenna." *NCCN-12, Sant Longowal Institute of Engineering and Technology* (2012).
- [30] Kiminami, Hirata, and Shiozawa. "Double-sided printed bow-tie antenna for UWB communications." *IEEE antennas and wireless propagation letters* 3 (2004): 152-153.
- [31] Shlager, Kurt L., Glenn S. Smith, and James G. Maloney. "Optimization of bow-tie antennas for pulse radiation." *IEEE*

- Transactions on Antennas and Propagation 42.7 (1994): 975-982.
- [32] Balanis, Constantine A., "Antenna Theory Analysis and Design", John Wiley & Sons, 3rd Edition, USA (2005),
- [33] Compton, R. I. C. H. A. R. D. C., et al. "Bow-tie antennas on a dielectric half-space: Theory and experiment." *IEEE transactions on antennas and propagation* 35.6 (1987): 622-631.
- [33] S. W. Qu and C. L. Ruan, "ANTENNAS," pp. 179–195, 2006.
- [34] Khanna, Ghriti, and Narinder Sharma. "Fractal antenna geometries: A review." *International Journal of Computer Applications* 153.7 (2016): 29-32.
- [35] Vignesh, LK Balaji, and K. Kavitha. "A survey on fractal antenna design." *International Journal of Pure and Applied Mathematics* 120.6 (2018): 10941-10959.
- [36] Werner, Douglas H., and Suman Ganguly. "An overview of fractal antenna engineering research." *IEEE Antennas and propagation Magazine* 45.1 (2003): 38-57.
- [37] F. Chovanec, "Cantor sets," no. March 2010, 2014.
- [38] Sharma, Narinder, and Vipul Sharma. "A journey of antenna from dipole to fractal: A review." *J. Eng. Technol* 6.2 (2017): 317-351.
- [39] Saidatul, N. A., A. A. H. Azremi, and P. J. Soh. "A hexagonal fractal antenna for multiband application." *2007 International Conference on Intelligent and Advanced Systems*. IEEE, 2007.
- [40] Tang, and Wahid. "Hexagonal fractal multiband antenna." *IEEE antennas and wireless propagation letters* 3 (2004): 111-112.
- [41] Low, Xue Ni, Zhi Ning Chen, and Terence SP See. "A UWB dipole antenna with enhanced impedance and gain performance." *IEEE Transactions on Antennas and Propagation* 57.10 (2009): 2959-2966.

- [42] Ali, Jawad, et al. "Ultra-wideband antenna design for GPR applications: A review." *International Journal of Advanced Computer Science and Applications* 8.7 (2017).
- [43] K. Kiminami, A. Hirata, and T. Shiozawa, "Double-sided printed bow-tie antenna for UWB communications," *IEEE Antennas Wireless Propag. Lett.*, vol. 3, pp. 152–153, 2004.
- [44] Puente-Baliarda, Carles, et al. "On the behavior of the Sierpinski multiband fractal antenna." *IEEE Transactions on Antennas and propagation* 46.4 (1998): 517-524.
- [45] Jayarenjini, Jayarenjini N. "Meandered CPW-fed Hexagonal Ring fractal Multi-band antenna loaded with Labyrinth Resonator." (2022).